INFLUENCE OF NONTRADITIONAL AND NATURAL POZZOLANS (NNPS) ON THE MECHANICAL AND DURABILITY PROPERTIES OF MORTARS AND CONCRETES

by

Alberto Castillo

A Thesis

Submitted to the Faculty of Purdue University

In Partial Fulfillment of the Requirements for the degree of

Master of Science in Civil Engineering

Lyles School of Civil Engineering

West Lafayette, Indiana

May 2022

THE PURDUE UNIVERSITY GRADUATE SCHOOL

STATEMENT OF COMMITTEE APPROVAL

Dr. Jan Olek, Chair

School of Civil Engineering

Dr. Mirian Velay-Lizancos

School of Civil Engineering

Dr. Robert Spragg

Federal Highway Administration

Approved by:

Dr. Dulcy Abraham

Dedicated to my mom, dad, siblings, and girlfriend – thanks for being there at all times

ACKNOWLEDGMENTS

First and foremost, I would like to thank my advisor, Professor Jan Olek, for his continuous support over the past two years. Your wisdom, encouragement, and infinite patience are kindly appreciated. I would also like to thank Professor Mirian Velay-Lizancos for believing in me and always helping me out, regardless of the circumstance. I can confidently say that I would not be in this position without your guidance. I would also like to thank my other committee member, Robert Spragg for his valuable input. It has been an enormous pleasure to work with you.

I would also like to acknowledge the financial support of the Federal Highway Administration under the FHWA EAR-693JJ31950019 project and for being able to perform some experiments at the TFHRC. I am also grateful for the work performed in collaboration with Penn State University (Dr. Farshad Rajabipour and his team) and Clarkson University (Dr. Sulapha Peethamparan and her team). I am also thankful to our lab manager, Robert Hershberger. Without him, much of my experimental work could not have been done.

I would also like to thank my colleagues and friends: Vito Francioso, Carlos Moro, Raikhan Tokpatayeva, Dan Huang, Fabian Rodríguez, Marina Lopez-Arias, Miguel Montoya, Jonah Roberts, and Andrés Aguilar. Thanks for receiving me with open arms and for all the support throughout these past few years. I appreciate all the help and enjoyable time together.

TABLE OF CONTENTS

LIST OF TABLES

LIST OF FIGURES

NOMENCLATURE

AEA – Air entraining agent

ASR – Alkali-silica reaction

CC – Calcined clay

CMD – Concrete mix design

CO_2 – Carbon dioxide

FA/tot. agg. – Fine aggregate to total aggregate ratio

FBC – Fluidized bed combustion

GBA – Ground bottom ash

INDOT – Indiana Department of Transportation

MTO – Ontario Ministry of Transportation

NNP – Nontraditional and natural pozzolan

NP – Natural pozzolan

OPC – Ordinary portland cement

PSD – Particle size distribution

QXRD – Qualitative x-ray diffraction

SCM – Supplementary cementitious material

SSD – Saturated surface-dry

SEM – Scanning electron microscope

SP - Superplasticizer

VA – Volcanic ash

w/cm – water-to-cementitious ratio

WRA – Water reducing agent

ABSTRACT

Concrete is the second most consumed material in the world after water and is an essential element of constructed infrastructure. Over 14 billion m^3 of concrete are being produced annually, resulting in a serious impact on the environment. The production of cement, which is the main component of concrete, is responsible for 5 – 8 % of global CO_2 emissions. As a result, several global initiatives have been undertaken to achieve carbon neutrality by 2050. This carbon neutrality target coincides with the Paris Agreement's goal to limit global warming to 1.5 °C. A well-known, and successful strategy to reduce CO_2 emissions in the concrete industry is to use supplementary cementitious materials (SCMs) as a partial replacement for cement. However, it is projected that in 2030 the demand for two of the most commonly used SCMs, fly ash and slag cement, will exceed their supply. Using nontraditional and natural pozzolans (NNPs) can help to close this supply gap, but there is a lack of knowledge regarding the reactivity and long-term performance of these materials.

The purpose of this research was to perform experiments on several NNPs, some of which can be supplied in commercially viable quantities with the objective of evaluating their performance in cementitious systems (mortars and concretes) with the goal of accurately assessing their potential for use as alternative SCMs. The mortar study was performed using a total of 11 different NNPs, belonging to 4 distinctive groups and distributed as follows: 3 from the group of calcined clays (CCs) - CC1, CC2, and CC3, 3 from the group of natural pozzolans (NPs) - NP1, NP2 and NP3, 2 from the group of fluidized bed combustion (FBCs) ashes - FBC1 and FBC2, and 3 from the group of bottom ashes (GBAs) - GBA1, GBA2, and GBA3.

The concrete study was performed on 4 different materials, one from each of the previously mentioned groups. The materials selected for concrete study were the worst-performing members of each group, as determined by the analysis of the test results obtained from mortars. These included CC2, NP3, FBC1, and GBA3 materials. This approach was adopted under the assumption that achieving adequate concrete characteristics with lowest-quality materials will all but assure satisfactory performance of concretes with higher-quality materials.

The findings generated from this research indicate that several of the NNPs used in this study present a viable alternative to traditional SCMs. As an example, out of the 11 NNPS, 9

were found to conform to the requirements of the ASTM C618-19, the standard specification currently used to assess the suitability of coal fly ash and raw or calcined natural pozzolans for use in concrete. Results obtained from tests performed on mortars demonstrated that, when used at the replacement level of 25%, all 11 NNPs produced mixtures with characteristics similar to those obtained from the plain cement (OPC) mortar. For that reason, this level of replacement was selected to prepare concrete specimens. The results collected from concrete specimens showed that, when compared to plain concrete, mixtures with all 4 NNPs attained comparable (or improved) mechanical (compressive and flexural strength), durability (freeze-thaw resistance), and transport (formation factor and rate of water absorption) properties. As in the case of traditional SCMs, the mixtures with NNPs were found to require extended curing times to fully realize their property-enhancing potential associated with pozzolanic reactions. Overall, the best performing materials were those from the CCs group, followed by those belonging to, respectively, NPs, GBAs, and FBCs groups.

1. INTRODUCTION

Parts of this chapter has been submitted for the following publication:
Tokpatayeva, R., Castillo, A., Yoon, J., Kaladharan, G., Arachchige, R.M., Rajabiour, F., Peethamparan, S., and Olek, J., "Comparative study of the reactivity and performance of different non-traditional and natural pozzolans in cementitious system", submitted to *Advances in Civil Engineering Materials*, 2022.

1.1 Background

Concrete is one of the most widely used materials in the world due to its strength, durability, and low cost of production. While the usage of concrete certainly provides benefits to society, it also negatively affects the environment (in the form of CO_2 emissions). As of 2020, about 4.1 – 4.3 billion tons of cement, which is the main component of concrete, were produced annually [1], [2]. This production was responsible for 5 – 8 % of global CO_2 emissions [3], [4]. These emissions are caused by three different factors: (i) the burning of fossil fuel to heat the cement kiln, which is responsible for 40% of the total emissions; (ii) the decarbonization of limestone ($CaCO_3$) which contributes to 50% of the total emissions; (iii) the transportation of the finished product, which accounts for the remaining 10% of the total emissions [5]. If this trend continues, the production of cement will reach the level of about 4.7 – 5.1 billion tons in the year 2050 [6].

One of the principal approaches to increasing the sustainability in cementitious systems is by using supplementary cementitious materials (SCMs). The use of SCMs is important as they directly help to reduce the carbon footprint of concrete (by replacing part of the cement) while also improving the durability (and thus sustainability) of constructed infrastructure. The improvement of sustainability by SCMs, when used as a partial replacement for cement, has been extensively researched over the years, with some of the more recent works focusing on such aspects as environmental and economic benefits, functional improvements [7], reduction in CO_2 emissions [8], and decrease in greenhouse gas emissions [9].

To reduce global CO_2 emissions, and to achieve carbon neutrality of concrete by 2050, several initiatives, such as the Global Cement and Concrete Association (GCCA) roadmap for net zero concrete [10], and the Portland Cement Association (PCA) roadmap to carbon neutrality [11] have taken place. The net zero pathway of these initiatives has several steps, each geared

toward achieving specific milestones in the upcoming years. One of the focal points in the process of achieving net zero CO_2 is by promoting new cementitious binders and novel concrete mixtures. These new concrete mixes can be based on existing SCMs (used at higher replacement levels) or on alternative SCMs, like the ones used in this study.

1.2 Motivation

Due to the diminishing availability of the traditional SCMs (such as fly ash and slag cement), there is some degree of uncertainty with respect to their ability to cost-effectively meet the future needs of the construction sector. It is expected that, by the year 2030, the demand for fly ash complying with ASTM C618-19 [12] specification will surpass the supply for this material by more than 50% [13]. The supply shortage is primarily attributed to power plants shifting from coal to natural gas as a source of fuel [14]. On the other hand, slag cement supplies are also declining, as the number of blast furnaces that produce this material continues to decline [14]. Finding alternative, cost competitive SCMs that are abundant and readily available is therefore critical with respect to closing the supply shortage of traditional SCMs.

This study aims to characterize the performance of cementitious systems containing eleven non-traditional and natural pozzolans (NNPs), with the objective of determining their suitability for use in concrete. While currently not sold on a commercial scale, several of these NNPs can certainly be supplied in commercially viable quantities, providing there is an interest from the construction industry [15]. The NNPs used in this research belong to four different groups of materials: calcined clays (CCs), natural pozzolans (NPs, also known as volcanic ashes (VAs)), fluidized bed combustion (FBCs) ashes, and ground bottom ashes (GBAs). Each of the CC, NP, and GBA groups contained three different materials while there were only two materials that belonged to the FBC ash group. These materials were selected since, based on their properties and availability, they seemed to have a high potential to replace some of the traditional SCMs in the future. Currently, some of them (e.g. FBCs and GBAs), are primarily landfilled.

1.3 Organization of Thesis

The thesis contains 7 individual chapters and 1 Appendix. The content of these sections is as follows:

Chapter 1 is the introductory section that covers the background and motivation for this research and presents the organization of the thesis.

Chapter 2 presents a literature review pertaining to NNPs and summarizes the effects of traditional SCMs on cementitious systems.

Chapter 3 describes the research objectives, scope, and hypothesis.

Chapter 4 presents the physical and chemical characteristics of CCs, NPs, FBCs, GBAs, cement, and aggregates used in this study.

Chapter 5 describes the investigation of the mechanical and durability characteristics of mortars containing NNPs.

Chapter 6 analyzes the mechanical and durability characteristics of concretes containing NNPs.

Chapter 7 presents the overall conclusions from the study.

Appendix A contains sample calculations for some of the results.

2. LITERATURE REVIEW

Parts of this chapter has been submitted for the following publication:
Tokpatayeva, R., Castillo, A., Yoon, J., Kaladharan, G., Arachchige, R.M., Rajabiour, F., Peethamparan, S., and Olek, J., "Comparative study of the reactivity and performance of different non-traditional and natural pozzolans in cementitious system", submitted to *Advances in Civil Engineering Materials*, 2022.

2.1 Effects of Traditional SCMs on the Different Properties of Cementitious Systems

Fresh, mechanical, and durability properties are some of the characteristics used to assess the performance of concrete. Understanding the effect of traditional SCMs (like fly ash, slag cement, silica fume, etc.,) on these properties is critical to developing an understanding of the possible influence of the NNPs used in this study on cementitious systems. Furthermore, the methods used to assess different properties of cementitious systems containing traditional SCMs provided a framework for the methods used in this study.

The plastic state of concrete is referred to as its fresh state. Properties of concrete in its fresh state allow it to be transported, placed, and compacted as needed. Additionally, these properties directly influence the quality of concrete once it hardens. Some of the important properties associated with a fresh state include workability, fresh air content, bleeding, and setting time. The use of both, admixtures and SCMs in concrete mixtures is fairly common, as they help to provide desirable fresh and hardened properties. It has been reported that fly ash and silica fume improve workability at low replacement levels (0-15%) [16]–[19], whereas mixtures with slag cement had comparable (or in some cases lower) workability [19] than the plain (i.e. based on the ordinary portland cement - OPC) concrete. As for the fresh air content, it has been shown that fly ash, slag cement, and silica fume tend to lower the fresh air content of concrete at every replacement level [19]–[22]. Lastly, the use of these SCMs has been reported to either retard, or lead to setting times comparable to setting times to control mixtures [19], [23]–[25].

Mechanical properties of concrete represent physical response of concrete to the externally applied forces. These properties are crucial when concrete is used to create structural components to safely carry all of the applied loads. Some of the most important mechanical properties include: compressive, tensile, and flexural strengths, creep, and modulus of elasticity.

Concretes containing some of the SCMs, such as fly ash and slag cement, tend to have lower (or sometimes comparable) compressive strengths than specimens prepared with OPC alone, but only at an early age (before 28 days) [26]–[28]. However, at later ages (after 28 days), the SCMs-containing concretes develop compressive strengths comparable to, or higher, than the OPC concretes [26]–[28]. As for tensile and flexural strengths, these were either comparable or lower when compared to specimens containing OPC only at 28 days [29]–[32]. In other words, there is an increased property-enhancing potential resulting from pozzolanic reactions with a longer curing time. The optimum replacement percentage for these SCMs appeared to be anywhere between 10 - 25%, depending on the mechanical property investigated [27]–[29], [31].

The ability to resist weathering action, chemical attack, abrasion, or any other process of deterioration is defined as the durability of concrete [33]. The physical causes of concrete deterioration can be assigned to two different categories: (i) surface wear or loss of mass due to abrasion, erosion, and cavitation; (ii) cracking due to normal temperature and humidity gradients, structural loads, and exposure to temperature extremes such as freezing or fire [34]. To assess the chemical aspects of the durability of concrete, the resistance against alkali-silica reaction (ASR), chloride ion penetration, and steel corrosion, are typically evaluated. Fly ash, silica fume, and slag cement, when used as a partial replacement for cement, can effectively mitigate ASR [35]–[38], and increase the resistance against chloride ion penetration [39]–[42] On the other hand, these SCMs can be comparable or more susceptible to scaling than mixtures containing OPC only [42], [43].

2.2 Insight on NNPs and their Effect on Cementitious Systems

As previously mentioned, the NNPs utilized in this study cover CCs, NPs (in the form of VAs), FBC ashes, and GBAs. Currently, there is limited knowledge on the reactivity and performance of these pozzolanic materials as SCMs. Furthermore, the lack of guidance or test methods prevents the widespread usage of these NNPs. The unfamiliarity and end-user concerns with how to proportion or evaluate these NNPs also play a role in preventing the more widespread usage of these materials.

Clays, especially those containing kaolinite, are available in large deposits throughout the world and can be relatively easily processed to become effective SCMs. In fact, suitable clays are so abundant that in some countries they are currently stockpiled as waste [15]. Clay minerals

are primarily composed of silica (SiO_2), alumina (Al_2O_3) or magnesia (MgO), and water (H_2O), and are generally classified into nine groups (See Table 2.1), depending on their chemical composition and atomic structure [44]. From these nine clay minerals groups, the clays containing kaolinite are most commonly calcined to produce the SCMs with pozzolanic properties. To a lesser extent, clays containing illite and smectite can also be used for these purposes [45]–[47]. Unlike the illite and smectite, the kaolinite dihydroxylation process is able, for the most part, to break down the clay structure by removing the chemically bound water, thus changing crystalline clay into an amorphous material [48], [49].

Table 2.1. Clay mineral groups.

Clay mineral groups
Kaolin
Pyrophyllite
Mica
Vermiculite
Smectite
Chlorite
Sepiolite-palygorskite
Interstratified clay minerals
Allophane-imogolite

CCs containing different kaolinite content (low to high purities) with additional limestone (calcined clay limestone cement or LC^3) on cementitious systems have been subjected to multiple studies [50]–[53]. Since calcined kaolinitic clays have an elevated alumina content, the co-substitution with limestone appears to be suitable [50]. These studies have reported results indicating an increase in mechanical properties at 7 and 28 days [50], comparable carbonation to other blends [51], and refinement of the pores [51], [53] in LC^3 systems. However, the maximum replacement of low purity kaolinitic CCs in concrete containing OPC only has been reported to be about 30-35% by weight [49], [54]. This is because the use of CCs can lead to issues with workability, especially at higher replacement levels, and mixtures containing this material require the use of high dosages of high range water reducing agents (HRWRA) [55], [56]. Furthermore, most studies involving CCs in concrete containing OPC only have been performed on metakaolin (MK), which is derived from a high purity calcined kaolinite clay. Nonetheless,

studies have found that CCs can enhance mechanical and durability properties of concrete such as compressive strength [57]–[59], flexural strength [57], resistance to chloride ion penetration [58], and resistance to sulfate attack [59]. Currently, there is only limited knowledge of how low-purity kaolin clays, such as these used in this study, may perform in concrete and mortar as a partial replacement of OPC only.

Natural pozzolans such as VAs are plentiful available globally, but localized [15] as the majority of VAs deposits are located in areas of Cenozoic volcanic activity [60]. The most common VAs used as an SCM are pyroclastic ashes (pumice, scoria, ashes, and tuff) resulting from explosive eruptions since they show higher pozzolanic activity due to their high glass and high porous content [60]–[62]. The sources of volcanic deposits are generally readily accessible. The material from these deposits can be naturally mined and deposited as ash layers [61], [62]. The VAs used in this study are differentiated by the type of their mineralogical composition (obsidian, pumice, and tuff).

VAs are classified (per ASTM C618-19) as class N natural pozzolans. Studies show that at replacement levels greater than 30% the VAs increase porosity of the cementitious matrix system [63]. The effect of VAs on the mechanical properties, such as compressive strength, and drying shrinkage shows that they perform similarly to, or at a slightly lower level, than mixtures containing OPC only [64], [65]. In terms of durability properties, such as resistance to chloride ion penetration and sulfate resistance, mixtures with VAs also show similar behavior to that of the control mixtures containing OPC only [65], [66]. At the moment, there is limited research data available on how VAs may further impact other mechanical and durability properties of concrete.

FBC ashes are produced at levels similar to fly ash and are widely available. In the majority of instances, FBC ashes are disposed of in landfills [67]. In conventional coal-fired electric plants, coal is pulverized and then combusted at high temperatures (1400 - 1700 °C). At these high temperatures, molten mineral residue (impurities) is produced and subsequently solidified in the flue gas to form fly ashes. During this process, high sulfur, and nitrogen is emitted. The process of FBC was developed as a measure to eliminate external emissions control units, reduce costs, and fulfill environmental restrictions while being able to use coals with high sulfur content [68]. FBC boilers operate at lower temperatures (800 - 900 °C) where sulfur-absorbing materials in powder form are added with an inert material to the fuel. This produces

gaseous sulfur which is captured in situ by injecting limestone and calcium-based sorbents [69]–[71]. FBC ashes are a byproduct of this process.

FBC ashes have very similar chemistry but different mineralogy than conventional fly ashes [68], [71]; yet their properties and performance are not well researched. FBC ashes are currently landfilled although they may potentially represent a viable source of pozzolanic material since they generally meet the requirements of ASTM C618-19, except for elevated levels of LOI [68], [71]. The available research shows that, when used at the levels of around 20% replacement by weight, fresh properties of FBC concretes, such as slump, and air content, are similar (or improved), compared to mixtures containing cement only [68]. Furthermore, acceptable (or improved) performances were observed concerning the mechanical and durability properties of cementitious systems in tests such as strength activity index [71], compressive strength [71], [72], drying shrinkage, resistivity, and resistance to chloride ion penetration [71].

Bottom ashes are abundantly available as 10-30% of the ashes collected from pulverized coal furnaces are bottom ashes [73]. An elevated tonnage of bottom ashes has been disposed of in landfills globally [74]. During the process of pulverized coal combustion, which has been described previously, the heavier ashes that do not get carried away by the flue glasses, fall at the bottom of the hopper of the furnace. These are considered bottom ashes.

The chemical composition of the bottom ashes is similar to that of the fly ashes from the same coal power plants [75] meaning that they could potentially conform to the requirements of the ASTM C618-19. Bottom ashes can be used as a suitable fine aggregate replacement [76], however, limited research shows that when ground to a fineness comparable to that of the fly ash, these materials can perform at a level similar (and in some cases better) than traditional SCMs [77]–[81]. After adequate grinding bottom ashes display an improvement in pozzolanic activity [77]. Adding to this, concretes with low replacement percentages of cement by GBAs have been found to have a similar slump and water absorption to mixtures containing cement only [78]. They also had similar strength activity index [77], [80], compressive and flexural strength [78], and resistance to chloride ion penetration [81]. Currently, there is insufficient knowledge of the long-term performance of GBAs when used as SCMs.

3. RESEARCH OBJECTIVE

3.1 Research Objective and Scope

This research aims to bridge the knowledge gap of four groups of unconventional NNPs (CCs, NPs, FBC ashes, GBAs) and their effect on cementitious materials to facilitate their usage. The main objectives of this investigation are:

i. To perform a state-of-the-art review about the influence of the NNPs used in this study on cementitious materials.

ii. To characterize the chemical, mineralogical, and physical composition of the NNPs.

iii. To evaluate the NNPs effect on the fresh, durability, and mechanical performance of mortar.

iv. To study the NNPs effect on the fresh, durability, and mechanical performance of concrete.

3.2 Research Hypothesis

Several hypotheses were formulated based on the relevant literature found about CCs, VAs, FBC ashes, and GBAs. These are:

- NNP specimens used in selected studies will perform similarly, or better than OPC-only specimens, regardless if they meet (or do not meet) the requirements of the ASTM C 618 standard.
- Similar to traditional SCMs, the concrete properties-enhancing potential will depend on the extent of pozzolanic reaction developing over time.
- The impact of NNPs on the performance of concrete will depend on the type of material and its replacement level.

4. MATERIALS CHARACTERISTICS

Parts of this chapter has been submitted for the following publication:
Tokpatayeva, R., Castillo, A., Yoon, J., Kaladharan, G., Arachchige, R.M., Rajabiour, F., Peethamparan, S., and Olek, J., "Comparative study of the reactivity and performance of different non-traditional and natural pozzolans in cementitious system", submitted to *Advances in Civil Engineering Materials*, 2022.

4.1 Methods

4.1.1 Particle Size Distribution

The particle size distribution (PSD) of the eleven NNPs was measured using the PSA 1090 machine (Figure 4.1). This machine measures the particle size or the PSD by having the powders in a dispersed state of either air ("dry") or liquid ("wet") via laser diffraction ultrasonication. The PSD can be approximated by using the Fraunhofer diffraction theory or Mie scattering theory.

The PSD of the NNPs was measured by liquid dispersion and approximated using the Mie scattering theory. Liquid dispersion by isopropanol was used since an improved dispersion of finer particles can be achieved by using a liquid medium. The Mie scattering theory was selected as this method describes the complete scattering by homogeneous spherical particles of all sizes. Not only is this method considered to be the most rigorous method available [82], but it also is more accurate for particles under 10 μm. The refractive index used in the Mie method for the NNPs was the same as the one given by the machine for cement.

Figure 4.1. PSA 1090 (Anton Paar, Austria).

4.1.2 Scanning Electron Microscope

To observe the grains of all eleven NNPs, imaging of the dry powder in the scanning electron microscope (SEM) was performed by using backscattered electrons. The SEM analysis was performed using the ASPEX Personal SEM.

The dry powders were impregnated under vacuum with a hardening epoxy resin to fill the voids and maintain the microstructure. After impregnating under vacuum, the dry powders were placed in an oven at 70 °C until the epoxy resin hardened. The samples were then ground by lapping and subsequently polished (to 0.25 μm) to expose the grain of the NNPs. The polished surfaces were then coated with a thin layer of conductive material in the form of palladium. The SEM images provided in this study were obtained by Nicholas Christ, an undergraduate assistant of the project.

4.1.3 Quantitative X-Ray Powder Diffraction

To estimate the crystalline and amorphous phases of the NNPs, Quantitative X-Ray Diffraction (QXRD) was performed. The Siemens D500 Diffractometer (Figure 4.2) with a 45-kV voltage and a 40-mA current was used to perform the analysis at a 0.02°/sec scanning rate. The 2θ-range of the scan to collect the diffraction patterns was 5-70°.

The NNP powders were ground to a d_{50} value close to 5 μm and 15% wt. ZnO powder was added as an internal standard to then place the sample on the holder to be tested. The quantification was performed using Jade V 7.5.0 software and the ICDD database (PDF-4+2021)

to perform Rietveld refinement analysis. The QXRD used in this study was performed by Raikhan Tokpatayeva, the postdoc associated with the project.

Figure 4.2. Siemens D500 Diffractometer.

4.2 Materials

4.2.1 Calcined Clays

Three different CCs were used in this study and labeled as CC1, CC2, and CC3. These CCs were obtained based on low, intermediate, and high purity kaolinite with a potentially low cost. CC1 was obtained from the Northeastern United States (0% kaolinite). CC2 was obtained from the Midwestern United States (0% kaolinite). CC3 was obtained from the Western United States (~29% kaolinite). The chemical composition of the CCs is given in Table 4.1 while the physical properties can be seen in Table 4.2. The data was provided by Penn State University as part of the FHWA EAR-693JJ31950019 project.

Table 4.1. Chemical composition of CCs.

Common name	Chemical Abbreviation	CC1	CC2	CC3
		Wt., %		
Total Carbon		0.04	0.05	0.05
Sodium Oxide	Na_2O or N	0.17	0.0	0.0
Magnesium Oxide	MgO or M	0.41	0.34	0.0
Aluminum Oxide	Al_2O_3 or A	25.02	34.89	36.83
Silicon Dioxide	SiO_2 or S	56.00	56.33	54.44
Phosphorus Oxide	P_2O_5	0.19	0.21	0.05
Sulfur Trioxide	SO_3 or $	0.04	0.05	0.09
Potassium Oxide	K_2O or K	1.28	1.19	0.3
Calcium Oxide	CaO or C	0.06	0.32	0.08
Titanium Oxide	TiO_2	1.10	2.06	3.1
Iron Oxide	Fe_2O_3 or F	14.55	2.68	0.74
Equivalent Alkalis	Na_2O_{eq}	1.01	0.78	0.20
Loss on Ignition	LOI	0.63	1.71	4.17
Moisture Content		0.64	0.42	0.16

Table 4.2. Physical properties of CCs.

Properties	CC1	CC2	CC3
Fineness (%)	15	12	13
7-Day Strength Activity Index (%)	96	94	103
28-Day Strength Activity Index (%)	89	94	95
Water requirement (%)	115.7	105.4	113.6
Autoclave expansion or contraction	-0.05	-0.01	-0.05
Specific Gravity (g/cc)	2.89	2.75	2.66

Based on the chemical composition and physical properties provided in Table 4.1 and Table 4.2, CC2 and CC3 conform to the requirements given in ASTM C618-19 for Class N Raw or calcined natural pozzolans. While CC1 meets most of the chemical and physical requirements, its elevated water requirement is higher than what the specification demands (< 115%).

The kaolinite content was one of the main factors when selecting the materials. This is because impure calcined clays (a mixture of kaolinite and other impurities) are abundant and at a lower price than pure calcined clays, as previously mentioned. It can be noted that all three calcined clays had comparable amounts of Al_2O_3 and SiO_2, making them mostly aluminosilicate

materials. CC1 was the only CC to show an elevated presence of Fe_2O_3. Additionally, the sum of SiO_2, Al_2O_3, and Fe_2O_3 for CC1, CC2, and CC3 was over 70% (81.02%, 91.22%, and 91.27% respectively) as ASMT C618-19 requires for class N calcined clays. Furthermore, both CC1 and CC2 had a high presence of equivalent alkalis. The moisture content and total carbon content found in CCs were relatively low. The LOI was relatively low for CC1 and CC2 but elevated for CC3. CC3 high LOI could be due to uncalcined clay present in the material.

Table 4.2 shows that CCs had an intermediate fineness value as well as a high water requirement. This may potentially increase the water demand and water reducing agent needed to obtain a workable mixture. All CCs had comparable SAI at 7 and 28 days and varying specific gravities.

Table 4.3. Mineralogical composition of CCs.

NNP	Crystalline phases, %	Amorphous phase, %
CC1	Muscovite ($Al_2H_2KO_{12}Si_4$) – 12.9, quartz (SiO_2) – 29.1, hematite (Fe_2O_3) – 7.5, anatase (TiO_2) – 1	49.5
CC2	Muscovite ($Al_6H_4K_2O_{24}Si_6$) – 29.5, quartz (SiO_2) – 12.1, hematite (Fe_2O_3) – 1.2, anatase (TiO_2) – 1,	56.2
CC3	Muscovite ($Al_2H_2KO_{12}Si_4$) – 2.7, kaolinite ($Al_2H_4O_9Si_2$) – 29, quartz (SiO_2) – 9.3, anatase (TiO_2) – 3.4	55.6

The crystalline phases provided in Table 4.3 show that all CCs have the same crystalline phases at different percentages (except for kaolinite found in CC3). The muscovite and kaolinite crystalline phases found in CCs were a product of the leftover remains of uncalcined clay. On the other hand, the amorphous phase found in CCs were comparable to one another. CC2 had the highest amorphous phase (56.2%), followed by CC3 (55.6%), and then CC1 (49.5%).

The particle size distribution for CC1 and CC3, as seen in Figure 4.3, was similar to one another. CC2 particle size distribution appeared to shift to the right, implying a coarser particle size than CC1 and CC3. This is corroborated when evaluating the d_{50} of each CC since CC3 had the highest (20.76 μm), followed by CC3 (9.66 μm) and then by CC1 (9.35 μm). Adding to this, all materials had a broad peak, suggesting a non-uniform gradation, which correlates to the SEM images of the materials (See Figure 4.4). Not only that but the figures for CC1 and CC3 showed the grains to be formed into clusters, whereas CC2 grains showed no sign of agglomeration. The

size of the grains for CC2 and the agglomeration found for CC1 and CC3 may directly impact the water requirement of the materials. As seen in Table 4.2, the water requirement was close to the maximum limit, which could be explained by the previously mentioned agglomeration and coarse size of the particles.

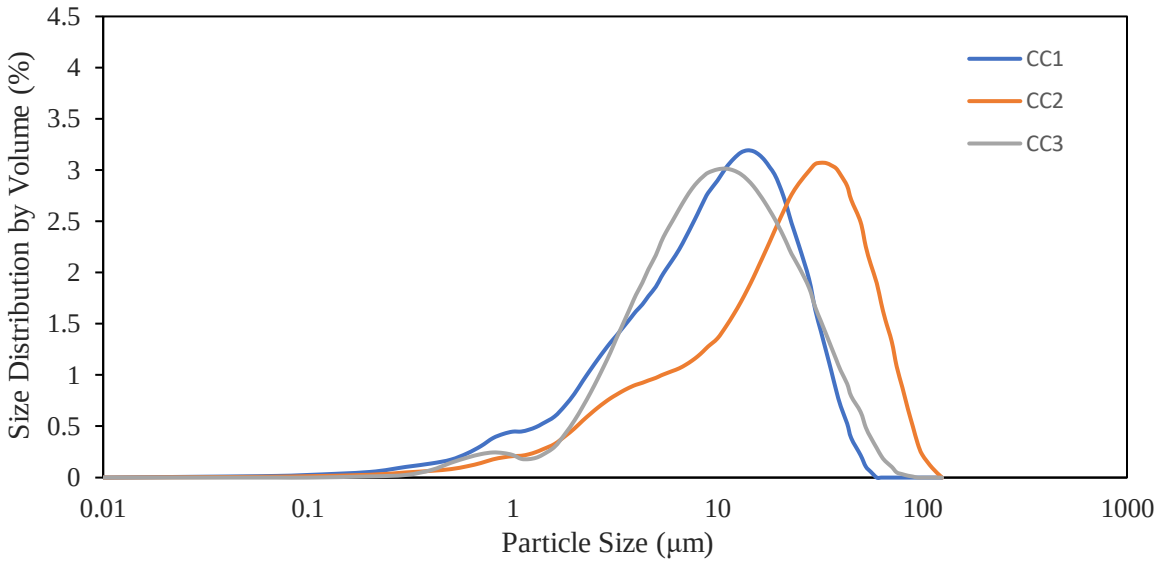

Figure 4.3. Particle size distribution for CC1 (d_{50} 9.35 μm), CC2 (d_{50} 20.76 μm), and CC3 (d_{50} 9.66 μm).

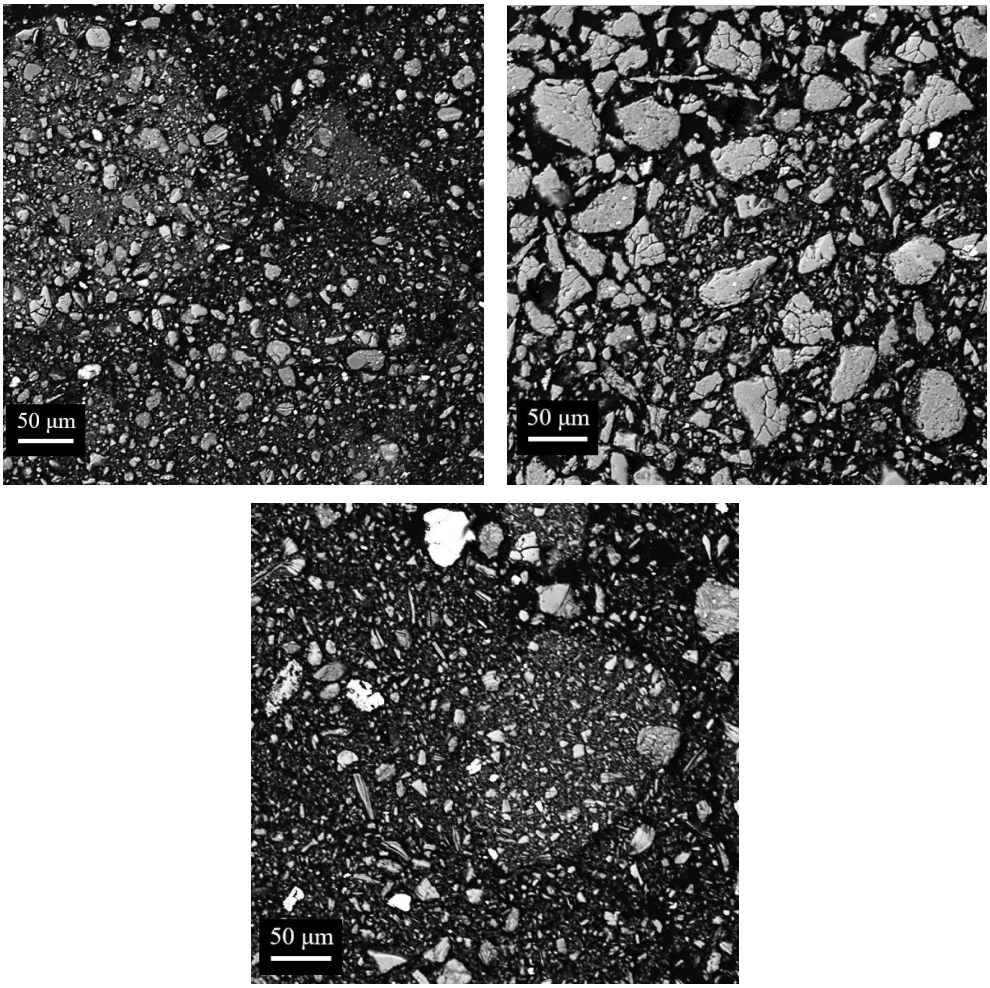

Figure 4.4. SEM images of CC1 (top left), CC2 (top right), and CC3 (bottom).

4.2.2 Natural Pozzolans

Three different natural pozzolans were used in this study and labeled as NP1, NP2, and NP3. These NPs were obtained based on three different types of volcanic ashes, such as obsidian, pumice, and tuff. NP1 (obsidian) was obtained from the Western United States. NP2 (pumice) was obtained from the Western United States. NP3 (tuff) was obtained from the Western United States. The chemical composition of the NPs is given in Table 4.4 while the physical properties can be seen in Table 4.8. The data was provided by Penn State University as part of the FHWA EAR-693JJ31950019 project.

Table 4.4. Chemical composition of NPs.

Common name	Chemical Abbreviation	NP1	NP2	NP3
		Wt., %		
Total Carbon		0.07	0.07	0.13
Sodium Oxide	Na_2O or N	3.61	2.39	2.83
Magnesium Oxide	MgO or M	0.15	0.28	1.0
Aluminum Oxide	Al_2O_3 or A	12.13	11.5	12.83
Silicon Dioxide	SiO_2 or S	71.89	72.39	70.35
Phosphorus Oxide	P_2O_5	0.0	0.03	0.05
Sulfur Trioxide	SO_3 or $	0.06	0.0	0.08
Potassium Oxide	K_2O or K	4.73	5.23	4.07
Calcium Oxide	CaO or C	0.72	0.84	1.91
Titanium Oxide	TiO_2	0.0	0.1	0.19
Iron Oxide	Fe_2O_3 or F	0.82	1.34	2.0
Equivalent Alkalis	Na_2O_{eq}	6.72	5.83	5.51
Loss on Ignition	LOI	4.83	4.21	3.18
Moisture Content		1.24	2.24	2.42

Table 4.5. Physical properties of NPs

Properties	NP1	NP2	NP3
Fineness (%)	2	5	0
7-Day Strength Activity Index (%)	94	88	92
28-Day Strength Activity Index (%)	106	106	107
Water requirement (%)	103.3	103.3	103.3
Autoclave expansion or contraction	0.00	-0.01	-0.01
Specific Gravity (g/cc)	2.40	2.42	2.50

As seen in Table 4.4, NPs had an elevated content of SiO_2 and were comparable among all three NPs. The Al_2O_3 and Fe_2O_3 content were low in comparison to the other NNPs since the SiO_2 content of the NPs were high. Moreover, the sum of SiO_2, Al_2O_3, and Fe_2O_3 for NP1, NP2, and NP3 was over 70% (84.84%, 85.23%, and 85.2% respectively) as ASMT C618-19 requires for class N calcined clays. Additionally, every NP had a significant amount of equivalent alkalis and LOI. The significant quantity of alkalis found in NPs could potentially lead to problems of alkali-silica reaction as there is a potential of leaching alkalis. The moisture content for NP2 and

NP3 was close to the 3% limit given in ASTM C618-19 whereas NP1 had a lower moisture content.

NPs had a low fineness, water requirement, and specific gravity in contrast to the other NNPs. The SAI at both 7 and 28 days was the highest amongst all NNPs. This elevated SAI found in NPs could potentially lead to a higher reactivity with a given cement.

Table 4.6. Mineralogical composition of NPs.

NNP	Crystalline phases, %	Amorphous phase, %
NP1	-	100
NP2	-	100
NP3	Quartz (SiO_2) – 10.5, albite ($AlNaO_8Si_3$) – 42.4	47.1

Both NP1 and NP2 were entirely amorphous while NP3 had some crystalline phases present. The crystalline phases present found in NP3 were quartz and albite.

The particle size distribution for NPs is displayed in Figure 4.5. From this figure, it can be assumed that NP1 had the coarser grains, followed by NP3 and then NP1. This is also validated by the d_{50} of NP1 (11.64 μm) when compared to NP2 (6.81 μm) and NP3 (8.76 μm). The broad peaks of NP1 and NP3 may indicate a non-uniformity of the grains. As for the sharp peak seen in NP2, this could indicate a uniform gradation. Both of these statements were confirmed when evaluating the SEM images of all NPS (See Figure 4.6). NP1 grains appeared to be coarse with some finer grains agglomerated. NP2 grains on the other hand appeared smooth and well uniformed. Lastly, NP3 grains showed some porosity on the surface and the non-uniformity previously mentioned.

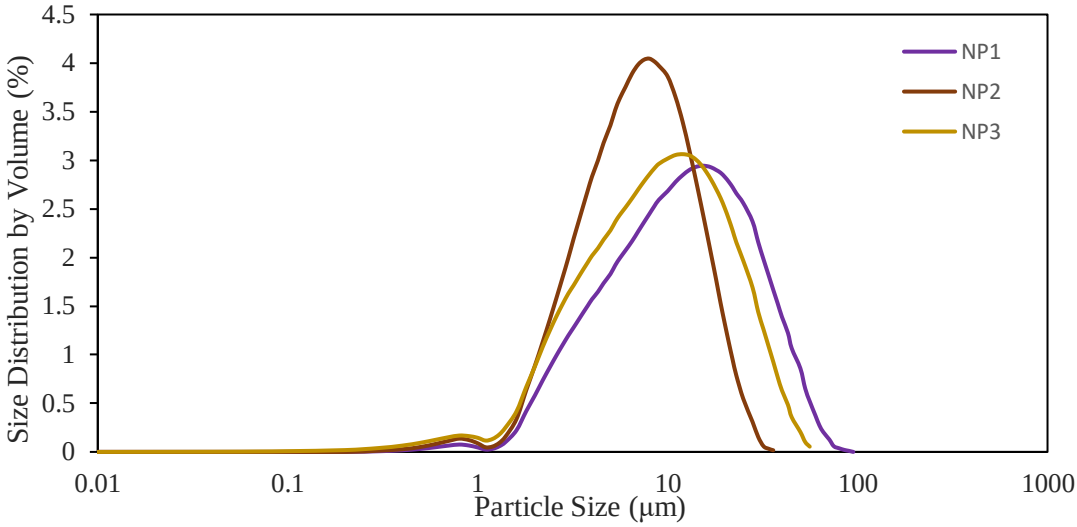

Figure 4.5. Particle size distribution for NP1 (d_{50} 11.64 μm), NP2 (d_{50} 6.81 μm), and NP3 (d_{50} 8.76 μm).

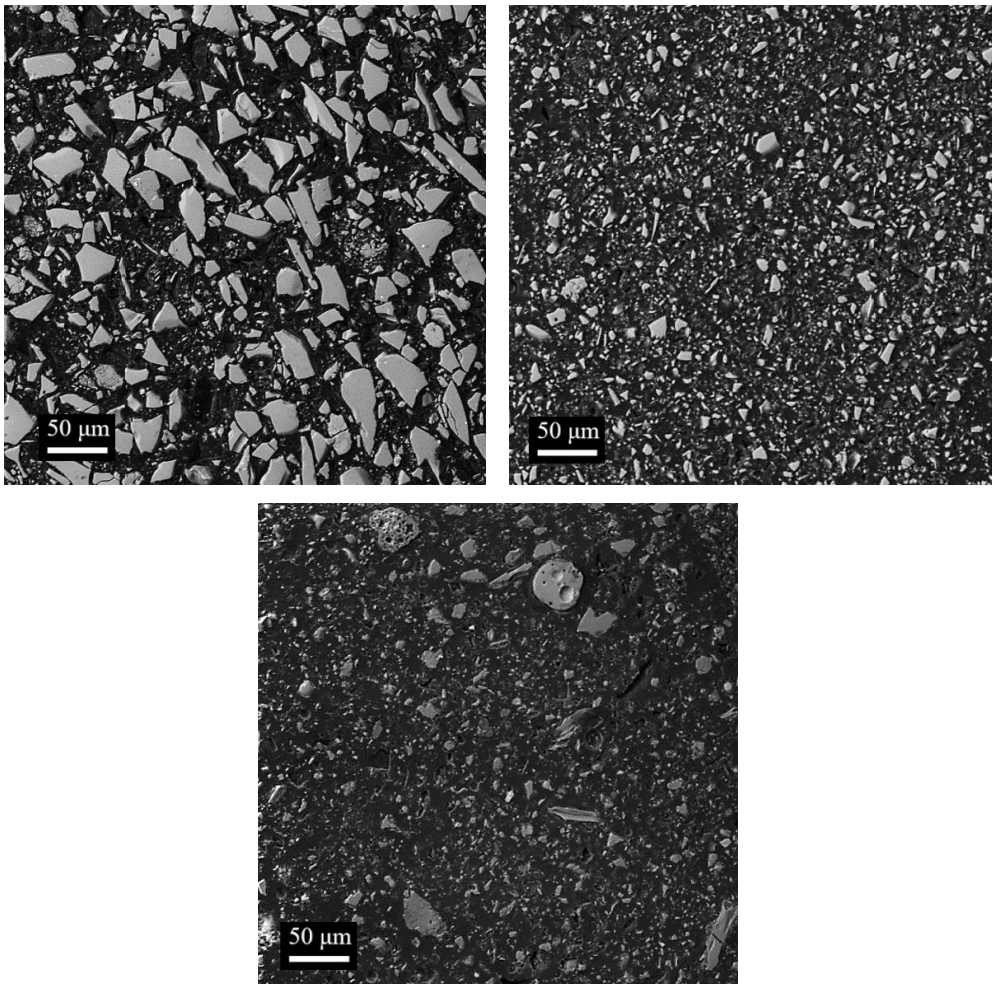

Figure 4.6. SEM images of NP1 (top left), NP2 (top right), and NP3 (bottom).

4.2.3 Fluidized Bed Combustion Ashes

Two different FBCs were selected for this study and were labeled as FBC1 and FBC2. These FBCs were obtained from anthracite coal power plants and were selected based on low and high SO_3 content. The two sources of FBCs were milled to meet the fineness in ASTM C618-19 (<34%). Both FBC1 and FBC2 were obtained from the Northeastern United States. The chemical composition of the FBCs is given in Table 4.7 while the physical properties can be seen in Table 4.8. The data was provided by Penn State University as part of the FHWA EAR-693JJ31950019 project.

Table 4.7. Chemical composition of FBCs.

		FBC1	FBC2
Common name	**Chemical Abbreviation**	**Wt., %**	
Total Carbon		5.82	2.91
Sodium Oxide	Na_2O or N	0.4	0.29
Magnesium Oxide	MgO or M	0.82	1.26
Aluminum Oxide	Al_2O_3 or A	21.47	16.96
Silicon Dioxide	SiO_2 or S	52.89	42.97
Phosphorus Oxide	P_2O_5	0.17	0.18
Sulfur Trioxide	SO_3 or $	1.21	7.98
Potassium Oxide	K_2O or K	3.3	2.21
Calcium Oxide	CaO or C	4.29	14.36
Titanium Oxide	TiO_2	1.66	1.06
Iron Oxide	Fe_2O_3 or F	7.03	8.64
Equivalent Alkalis	Na_2O_{eq}	2.57	1.74
Loss on Ignition	LOI	5.99	3.44
Moisture Content		0.31	0.32

Table 4.8. Physical properties of FBCs.

Properties	FBC1	FBC2
Fineness (%)	32	33
7-Day Strength Activity Index (%)	88	86
28-Day Strength Activity Index (%)	86	91
Water requirement (%)	107.4	107.4
Autoclave expansion or contraction	-0.03	-0.03
Specific Gravity (g/cc)	2.68	2.67

Based on the chemical composition and physical properties provided in Table 4.7 and Table 4.8, FBC1 conforms to the requirements given in ASTM C618-19 for Class F Fly Ash. While FBC2 meets most of the chemical and physical requirements, its elevated SO_3 content is higher than what the specification demands (< 5%).

Table 4.7 shows that FBC1 had the lowest SO_3 content (1.21%) while FBC2 had the highest (7.98%). The elevated presence of SO_3 in FBC2 could lead to abnormal setting behaviors such as retardation in setting time, false set, and flash set when used as supplementary cementitious material and expansion due to ettringite formation. Moreover, the sum of SiO_2, Al_2O_3, and Fe_2O_3 for FBC1 and FBC2 was over 50% (81.39% and 68.57% respectively) which is comparable to traditional fly ashes. Additionally, both FBCs had a significant content of total alkalis, CaO, and Fe_2O_3. The considerable amount of CaO in FBCs could potentially lead to an increase in hydraulic reactivity in cementitious systems when compared to CCs and NPs. FBCs also have an elevated LOI which could lead to carbonation issues and higher dosages of admixtures (more in particular for FBC1). A potential reason for the elevated LOI could be the amount of unburned carbon found in FBCs.

As for the physical properties (see Table 4.8), FBCs had a high fineness and water requirement which could lead to a decrease in the fresh properties of the cementitious systems. Both FBCs had comparable SAI at 7 and 28 days and similar specific gravities.

Table 4.9. Mineralogical composition of FBCs.

NNP	Crystalline phases, %	Amorphous phase, %
FBC1	Muscovite ($Al_3KO_{11}Si_3$) – 27.3, anhydrate ($CaSO_4$) – 2, quartz (SiO_2) – 24.6, (Fe_2O_3) – 3.1, anatase (TiO_2) – 1.3	41.7
FBC2	Muscovite ($Al_2KO_{11}Si_4H_2O$) – 6.2, anhydrate ($CaSO_4$) – 11.1, quartz (SiO_2) – 18.5, hematite (Fe_2O_3) – 4.4, anatase (TiO_2) – 1.9	57.9

From Table 4.9, it can be seen that FBCs contained crystalline phases such as muscovite, quartz, and anatase at different percentages. The elevated SO_3 and Fe_2O_3 content previously reported could be explained by the considerable amount of anhydrate and hematite (respectively)

found. FBC2 had a higher amorphous content than FBC1 which could lead to a higher hydraulic reactivity.

From Figure 4.7 it can be seen that the particle size distribution for both FBCs was fairly similar to one another. FBC1 appeared to have an average coarser grain as indicated by its d_{50} (24.02 μm) but FBC2 had a coarser size distribution from 1 to 20 μm. Both curves had a broad shape, implying a non-uniform gradation, which correlates to the SEM images of the materials (See Figure 4.8). The size of the grains for both FBCs appeared porous, and either fine or significantly coarser (some as coarse as 100 μm). The size of the grains may directly impact the water requirement of the materials, a coarser grain will require more water to hydrate and as mentioned previously, the water requirement for the FBCs was high (See Table 4.8).

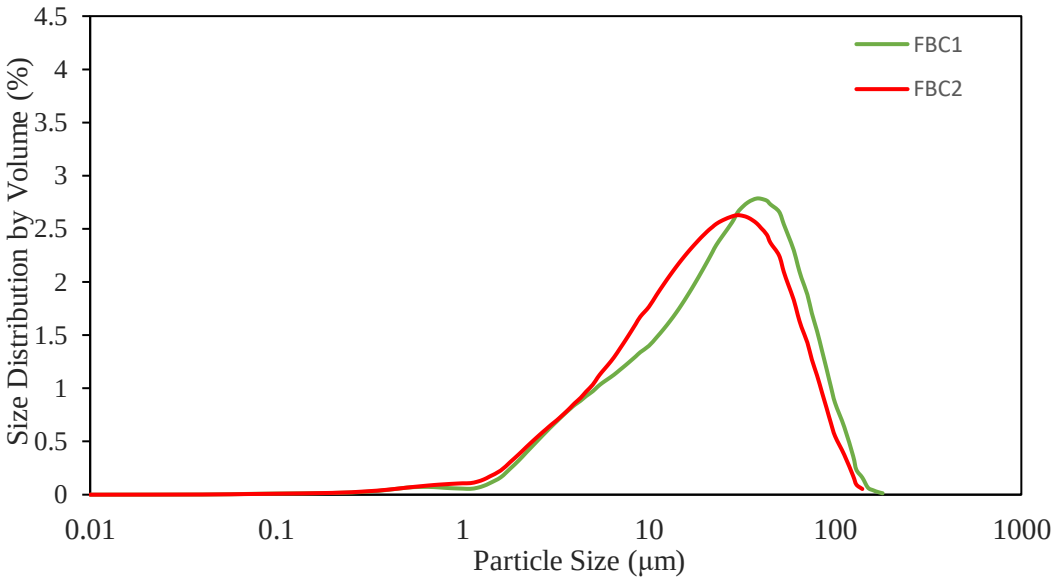

Figure 4.7. Particle size distribution for FBC1 (d_{50} 24.02 μm) and FBC2 (d_{50} 20.54 μm).

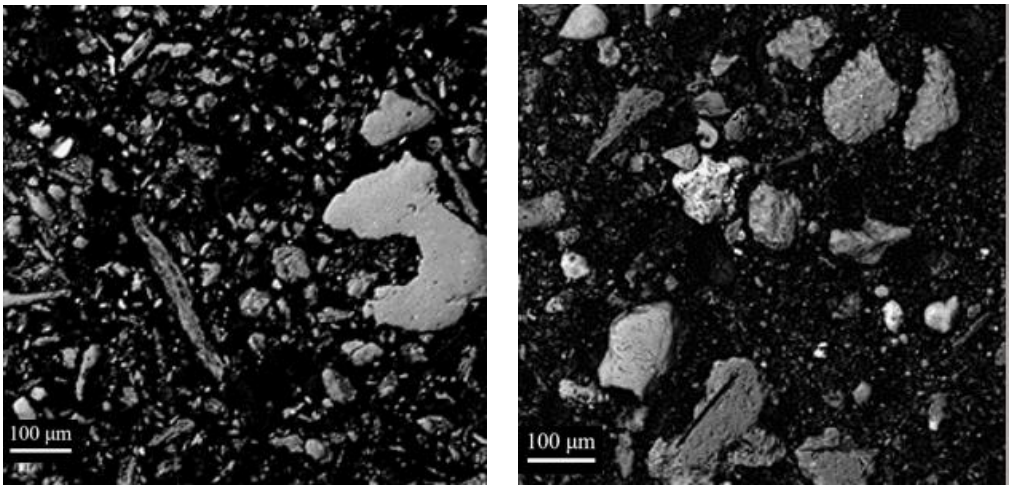

Figure 4.8. SEM images of FBC1 (left), and FBC2 (right).

4.2.4 Ground Bottom Ashes

Three different GBAs were selected for this study and labeled as GBA1, GBA2, and GBA3. These GBAs were obtained from coal-fueled electric generation stations (that already produce fly ashes) and were selected based on low, medium, and high CaO content. Similar to the FBCs, GBAs were milled to meet the fineness requirements in ASTM 618-19. The chemical composition of the GBAs is given in Table 4.10 while the physical properties can be seen in Table 4.11. The data was provided by Penn State University as part of the FHWA EAR-693JJ31950019 project.

Table 4.10. Chemical composition of GBAs.

		GBA1	GBA2	GBA3
Common name	**Chemical Abbreviation**		**Wt., %**	
Total Carbon		0.69	0.72	0.77
Sodium Oxide	Na_2O or N	0.73	0.32	1.02
Magnesium Oxide	MgO or M	0.94	2.51	4.6
Aluminum Oxide	Al_2O_3 or A	20.07	17.89	16.62
Silicon Dioxide	SiO_2 or S	47.57	56.98	42.9
Phosphorus Oxide	P_2O_5	0.09	0.05	0.55
Sulfur Trioxide	SO_3 or $	0.08	1.23	0.38
Potassium Oxide	K_2O or K	1.94	0.99	0.41
Calcium Oxide	CaO or C	2.82	11.48	22.96
Titanium Oxide	TiO_2	0.99	1.14	1.18
Iron Oxide	Fe_2O_3 or F	24.12	5.84	7.46
Equivalent Alkalis	Na_2O_{eq}	2	0.97	1.29
Loss on Ignition	LOI	0.2	1.45	1.29
Moisture Content		0.31	0.94	0.42

Table 4.11. Physical properties of GBAs.

Properties	GBA1	GBA2	GBA3
Fineness (%)	0	0	0
7-Day Strength Activity Index (%)	88	86	89
28-Day Strength Activity Index (%)	87	82	96
Water requirement (%)	100.6	100.6	100.6
Autoclave expansion or contraction	-0.02	-0.02	0.00
Specific Gravity (g/cc)	2.89	2.69	3.00

Based on the chemical composition and physical properties provided in Table 4.7 and Table 4.8, GBA1 and GBA2 conform to the requirements given in ASTM C618-19 for Class F Fly Ash. GBA3 on the other hand conforms to the requirements for Class C Fly Ash.

It can be seen in Table 4.10 that GBA1 had the lowest CaO content (2.82%), GBA2 had the medium amount (11.48%), and GBA3 had the highest amount (22.96%). As mentioned previously, the amount of CaO was decided to be used as the main factor when selecting each GBA. This is because typically, high-calcium fly ashes tend to be more reactive as most of the CaO found is in the form of reactive crystalline compounds. GBA2 had the highest quantity of

aluminosilicates whereas GBA3 had the lowest. Adding to this, the sum of SiO_2, Al_2O_3, and Fe_2O_3 for GBA1, GBA2, and GBA3 was over 50% (91.78%, 80.71%, and 66.98% respectively) which is comparable to traditional fly ashes. Furthermore, every GBA had a significant content of equivalent alkalis and Fe_2O_3, especially in GBA1. The Fe_2O_3 content present in GBA1, albeit high, is within the range of expected values for class F Fly Ash. In contrast, GBA1 had the lowest LOI and moisture content. In fact, GBA2 and GBA3 also had low LOI and moisture content.

Table 4.11 shows that GBAs had a low water requirement in comparison to the other NNPs. This is consistent with the low moisture content discussed in the last paragraph. A low water requirement may lead to a lower amount of water used in a mixture design or a reduction in the usage of water reducing agents. GBA1 and GBA2 had a low SAI (but still met the minimum requirement of 75%) at 28 days while GBA3 had the highest. It is also worth noting that GBAs appeared to have a medium to high specific gravity.

Table 4.12. Mineralogical composition of GBAs.

NNP	Crystalline phases, %	Amorphous phase, %
GBA1	Quartz (SiO_2) – 1.3, mullite ($Al_{2.34}Si_{0.66}O_{4.83}$) – 8.4, hematite ($Fe_2O_3$) – 5.4, magnetite ($Fe_3O_4$) – 7.8	77.1
GBA2	Quartz (SiO_2) – 13.1, albite ($AlNaO_8Si_3$) – 3.3, anorthite ($Na_{0.15}Al_{1.85}Ca_{0.85}Si_{2.15}O_8$) – 16.4.	67.2
GBA3	Quartz (SiO_2) – 2.3, akermanite ($Al_{0.92}Ca_2Mg_{0.54}O_7Si_{1.54}$) – 7.4, anorthite ($Na_{0.36}Al_{1.64}Ca_{0.64}Si_{2.36}O_8$) – 17.4, diopside ($Ca_{0.8}Mg_{1.2}O_6Si_2$) – 18.9, augite ($CaMgO_6Si_2$) – 3.4	50.6

Table 4.12 shows the mineralogical composition of the GBAs. GBA1 had the highest amorphous content (77.1%), followed by GBA2 (67.2%) and then GBA3 (50.6%). All GBAs had quartz at different percentages. Furthermore, some of the crystalline phases found in GBA1 were hematite and magnetite, which could potentially explain the significant amount of Fe_2O_3 present. GBA2 had similar crystalline phases present as GBA3 such as anorthite and albite.

The particle size distribution for GBAs was comparatively similar to one another. GBA1 appeared to have the average coarser grain as indicated by its d_{50} (11.40 μm), followed by GBA3 (12.79 μm), and then by GBA2 (11.83 μm). Unlike the other NNPs, GBAs have a sharp peak,

which suggests a uniform gradation. This can be observed in the SEM images of the GBAs (See Figure 4.10). In these figures, the size of the grains for both all GBAs appeared to be fine. As mentioned earlier, the size of the grains may directly impact the water requirement of the materials. In this case, the finer grains seen in GBAs contribute to a decrease in water requirement in comparison to the other NNPs.

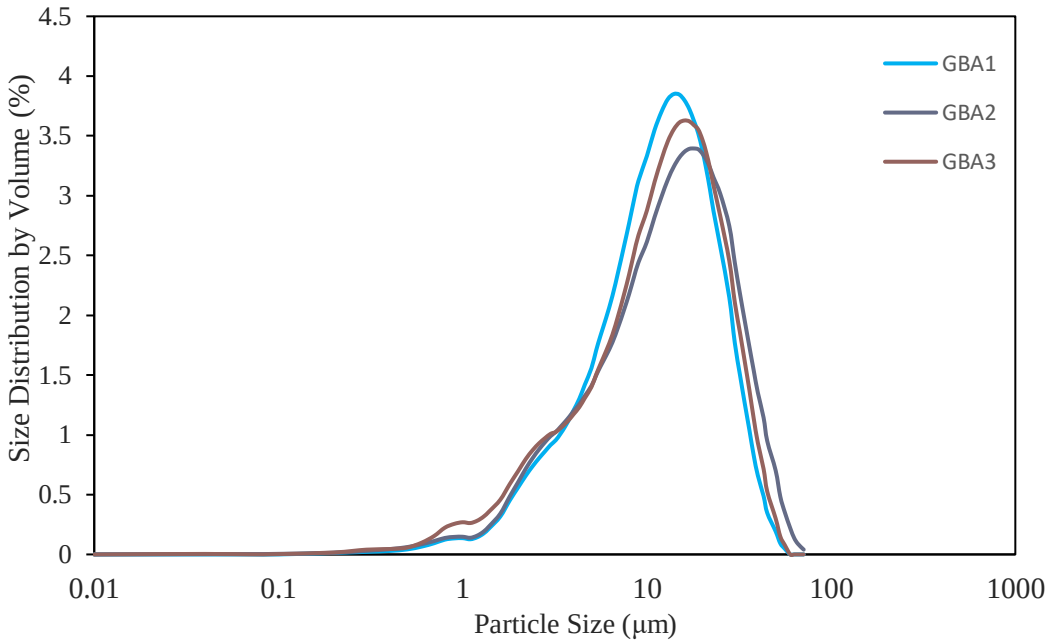

Figure 4.9. Particle size distribution for GBA1 (d_{50} 11.40 μm), GBA2 (d_{50} 12.79 μm), and GBA3 (d_{50} 11.83 μm).

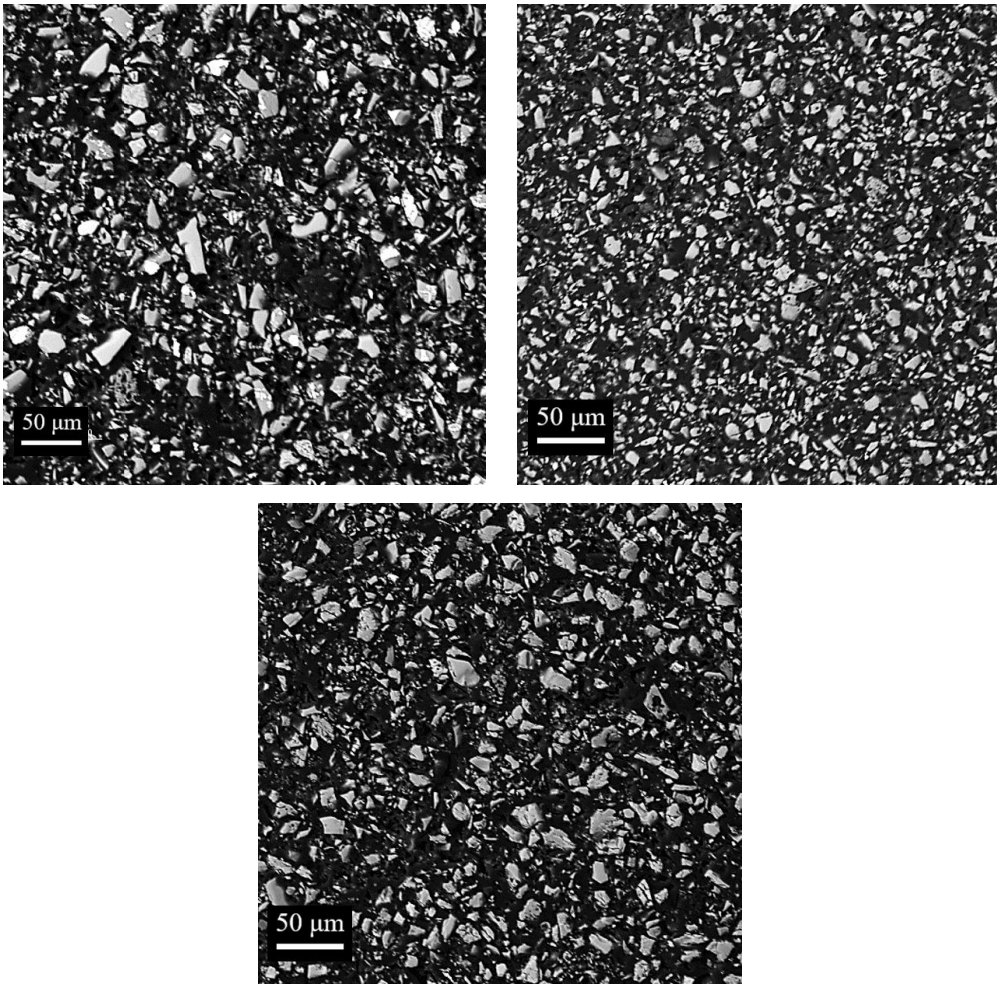

Figure 4.10. SEM images of GBA1 (top left), GBA2 (top right), and GBA3 (bottom).

4.2.5 Cement

The cement used was a commercial-grade Type I portland cement, meeting the requirements of ASTM C150-20 [83]. Two different batches of cement supplied by Buzzi Unicern were used as the first batch was depleted midway through the study. The first batch of cement was used for all mortar mixtures excluding drying shrinkage specimens up to 30% replacement level (except for CC1 material which was only used with the second batch) and concrete samples containing CC2 and NP3. On the other hand, the second batch was used for all mixtures at a 35% replacement level, including drying shrinkage specimens and concrete samples containing FBC1 and GBA3. The chemical and phase compositions are summarized in Table 4.13 and the physical properties are shown in Table 4.14.

Table 4.13. Chemical and phase composition of the first and second batch of cement.

		First Batch	Second Batch
Common name	**Chemical Abbreviation**	**Wt., %**	
Silicon Dioxide	SiO_2 or S	19.08	19.75
Aluminum Oxide	Al_2O_3 or A	5.27	5.10
Iron Oxide	Fe_2O_3 or F	2.70	3.06
Calcium Oxide	CaO or C	63.30	62.44
Magnesium Oxide	MgO or M	2.65	2.27
Sulfur Trioxide	SO_3 or $	3.16	3.36
Loss on Ignition	LOI	2.73	2.48
Alite	$3CaOSiO_2$ or C_3S	61.32	54.20
Belite	$2CaOSiO_2$ or C_2S	5.78	14.00
Tricalcium Aluminate	$3CaOAl_2O_3$ or C_3A	8.95	8.09
Calcium Aluminoferrite	$4CaOAl_2O_3Fe_2O_3$ or C_4AF	7.82	9.03
Equivalent Alkalis	Na_2O_{eq}	0.65	0.38

Table 4.14. Physical properties of the first and second batch of cement.

Properties	**First Batch**	**Second Batch**
Blain specific surface area (cm^2/kg)	3972	4015
Specific gravity	3.15	3.15

4.2.6 Aggregates

A size No. 23 natural siliceous sand conforming to section 900 of Indiana Department of Transportation (INDOT) specifications was used as fine aggregate. INDOT No. 8 crushed limestone conforming to section 900 was used as a coarse aggregate in this study. The physical properties of both aggregates are summarized in Table 4.15. To verify the gradation requirements and to observe the ranges in a particular sieve, aggregate gradation was performed. As seen in Figure 4.11, the fine and coarse aggregate meet the requirements for sizes No.23 and No. 8 respectively. It should be noted that the fine aggregate used appeared to be on the coarser side of the ranges for each sieve. This could potentially affect the workability of a given mixture; therefore, a considerate thought must be given to the amount of fine aggregate needed.

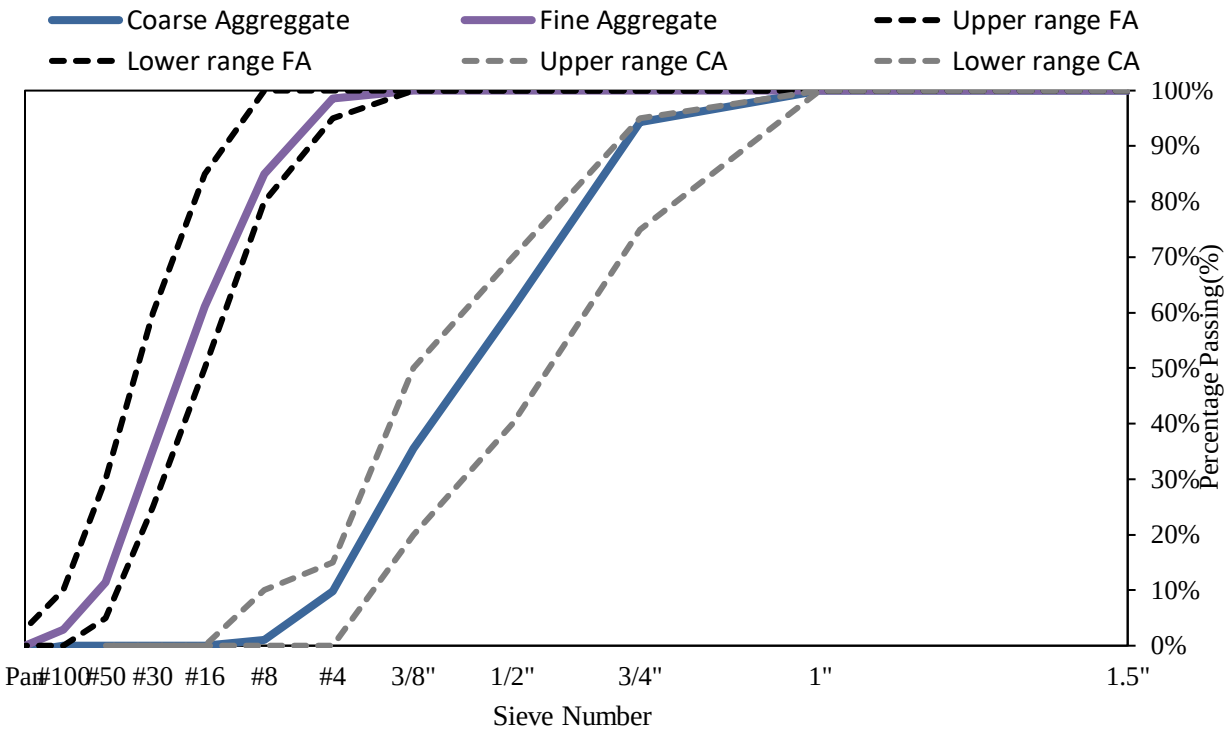

Figure 4.11. Gradation of fine and coarse aggregate.

Table 4.15. Physical properties of fine and coarse aggregate.

Aggregate	Saturated Surface-Dry (SSD) Specific Gravity	Absorption (%)
Fine Aggregate	2.74	1.97
Coarse Aggregate	2.61	2.28

4.2.7 Admixtures

MasterGlenium 7700 superplasticizer (SP) was used only for mortar mixtures containing various replacement levels of CC1, CC3 FBC1 materials to address the issues of reduced workability resulting from the use of these NNPs. This SP met the requirements of the ASTM C494-19 [85] for type F, high-range water-reducing agents, and was included on the Indiana Department of Transportation (INDOT) list of approved materials meeting the requirements of section 900 of INDOT's standard specifications [86] for portland cement concrete admixtures.

Water reducing agent (WRA) and air entraining agent (AEA) were used for all concrete mixtures. The WRA used was WRDA 82, a medium-range water reducer admixture conforming

to ASTM C494-19 type A and D admixtures. The AEA used was DARAVAIR 1400 conforming to ASTM C260-10 [92]. Both of these admixtures are under the qualified products of INDOT section 900 materials for portland cement concrete approved admixtures.

5. SELECTED FRESH AND HARDENED PROPERTIES OF MORTARS CONTAINING NNPS

5.1 Introduction

The main components of mortar are cement, water, and fine aggregate. In some instances, SCMs are used to increase mechanical properties and to improve durability and sustainability. Mortar is mostly used to bond masonry units together or to provide structural capacity to different structures. Results derived from mortars containing NNPs will be compared to the results obtained from a control mixture, which contained the ordinary portland cement (OPC) as the only binder.

This chapter describes results obtained from a series of mortars, containing variable levels of NNPs, subjected to various tests to determine their fresh, mechanical, and durability properties. The primary objective of this part of the study was to assess how the properties of interest were influenced by the type of NNPs, their physical and chemical characteristics, and the amount of NNP used to replace the cement. The secondary objective was to use data obtained from mortars to identify the subset of NNPs, one from each of the four groups presented in Chapter 4, that showed the lowest levels of reactivity and performance, and use them as materials of choice for the preparation of concrete mixtures to be tested in the second part of the study. Since, due to a large number of materials being evaluated, it was not practical to test all of them in concrete mixtures, the selection of the worst-performing NNPs was assumed to provide lower bound values of expected concrete properties.

Mortars were prepared using three levels of replacement of cement with NNPs (25%, 30%, and 35% by total weight of cementitious materials). These replacement percentages were selected based on the available literature, accounting for both, their potential impact on performance and the sustainability issues. The experiments performed on the mortars included measurement of fresh (slump, spread, fresh air content, setting time) and hardened (compressive strength and drying shrinkage) properties.

5.2 Materials

5.2.1 Materials and Mortar Mixtures Designs

All eleven NNPs, fine aggregate, cement, and water were utilized in the preparation of mixtures used for the determination of both, fresh and hardened properties of mortars. The only exception was a set of mortars used for measurements of drying shrinkage. In this case, only four (CC2, NP3, FBC1, and GBA3) NNPs were used as these were the materials selected to prepare concrete mixtures. Since, due to time and budget contains, it was not possible to evaluate the shrinkage of concretes directly, the values of shrinkage obtained from mortar specimens were used as a surrogate indicator of this particular property.

The batch proportions for mixtures used to evaluate the fresh and hardened properties of mortars are summarized in Table 5.1. It should be noted that for the penetrometer resistance tests the proportions given in Table 5.1 were multiplied by a factor of 1.7 (except for SP content shown in Table 5.2) in order to produce a sufficient volume of mixture needed for this test. All mortars were prepared at the constant value of the water-cementitious material (w/cm) ratio of 0.42 and a constant ratio of sand to cement (S/C) of 1.7. Due to their low workability, mixtures prepared with CC1, CC3, and FBC1 materials required the addition of the superplasticizer in the quantities shown in Table 5.2.

The specimens used for evaluation of the drying shrinkage were prepared using two sets of mortars, each having different mixture proportions. The proportions of the first set (see Table 5.3) followed the recipe provided in the ASTM C596-18 [84] with the amount of the mixing water adjusted to produce a constant flow of 110 ± 5%. The proportions of the second set of mortars (See Table 5.4) were kept constant, including the use of a single value of w/cm = 0.44. Although this approach resulted in variation of the slump and flow values, it allowed for a more direct comparison of results obtained from mortars to those obtained from concretes as the latter were also prepared using w/cm of 0.44.

Table 5.1. Batch proportions (SSD basis) for mixtures used to evaluate the fresh and hardened properties of mortars with and without NNPs.

Mixture	Replacement level (%)	Cement (g)	SCM (g)	Water (g)	Fine Aggregate (g)
OPC	-	1350	-	612.21	2295
11 NNPs	25	1012.5	337.5	612.21	2295
	30	945	405	612.21	2295
	35	877.5	472.5	612.21	2295

Table 5.2. The amounts of SP added to mixtures used to evaluate the fresh and hardened properties of mortars with NNPs.

Mixture	Replacement level (%)	SP (mL) for fresh properties and compressive strength cubes	SP (mL) for penetration test cylinders
CC1	25	11.6	40
	30	12.5	50
	35	15.5	-
CC3	25	6.5	Too unworkable to conduct test
	30	7	37.3
	35	8	45.3
FBC1	35	-	34.7

Table 5.3. ASTM C596-18 batch proportions (SSD basis) for constant flow (110 ± 5%) mortar mixtures used to evaluate the drying shrinkage of mortars with and without NNPs (25% replacement of cement).

Mixture	Cement (g)	SCM (g)	Fine Aggregate (g)	Water (g)	w/cm	Flow (%)
Reference	750	-	1500	314.5	0.38	108
GBA3	562.5	187.5	1500	322	0.39	106
CC2	562.5	187.5	1500	337	0.41	105
NP3	562.5	187.5	1500	344.5	0.42	110
FBC1	562.5	187.5	1500	367	0.45	108

Table 5.4. Batch proportions (SSD basis) for constant (0.44) w/cm values mortar mixtures used to evaluate the drying shrinkage of mortars with and without NNPs (25% replacement of cement).

Mixture	Cement (g)	SCM (g)	Fine Aggregate (g)	Water (g)	w/cm
Reference	750	-	1500	330	0.44
CC2, NP3, GBA3, FBC1	562.5	187.5	1500	330	0.44

5.3 Experimental Methods

5.3.1 Slump, Spread, and Fresh Air Content

ASTM C1810-20 [87] was followed to measure the slump, spread, and air content of mortars with different NNPs. Once the mixing process of mortar for each replacement level of a particular NNP was completed, the slump of the resulting mixture was determined by filling the mortar-slump mold (with an aid of a plastic funnel (ring)). The slump mold was filled with mortar using two layers of equal volume and tamping each layer 15 times. Excess mortar was removed from the top of the cone with a trowel and, subsequently, the cone was lifted up in one steady motion. The cone was then turned upside down and placed next to the slumped mortar, with the tamping rod laying across the bottom surface of the cone. Shortly after, the slump was recorded by measuring the distance from the bottom of the tamping rod to the top center of the slumped mortar using a ruler.

After the slump was recorded, a caliper was used to measure the horizontal spread of the mortar at two locations 90 degrees apart, and the average spread was recorded as a result of this test.

To measure the fresh air content of the mixed mortar, a brass cup of 400 mL was used. Mortar was placed inside the cup in three layers, and each layer was tampered 20 times. Once the cup was filled, the sides were lightly tapped at 5 different locations using a rubber mallet. After screeding the surface to remove the excess mortar, two additional passes were made across the cup in two directions at right angles to each other (horizontally and vertically). Lastly, the weight of the filled cup was determined. Eq. 5-1 was used to calculate the fresh air content of the mortar. A sample calculation of the air content is provided in Appendix A.

$$Air\ Content = \frac{Vol.of\ mortar\ in\ the\ batch - Abs.\ vol\ of\ all\ materials\ batched}{Volume\ of\ mortar} * 100\% \quad \text{Eq. 5-1}$$

5.3.2 Setting Time

The setting time of the various mixes was determined by using ASTM C403-16 [88]. Three specimens were casted in containers measuring 6 x 6 (D x L) inches. The mortar was placed in the containers in a single layer, in which the surface of the mortar was 0.5 inches below the top edge of the container and rodded 29 times. After the rodding, the mortar was consolidated by tapping the sides with the tamping rod. To prevent evaporation of moisture, the specimens were covered with water-impermeable plastic until the start of the penetration test. Before starting the test, the bleeding water from the surface of the mortar was removed. The initial penetration of 1 inch was made 3 hours after the cement was mixed with water and the resistance required to make this penetration was recorded. Subsequent penetrations of 1 inch were made apart every half an hour until the last penetration resistance equaled or exceeded 4000 psi (at least 6 penetrations were made for every specimen). Each penetration was 1 inch apart from the side of the container, and 0.5 inches apart in between measurements. Eq. 5-2 was used to determine the initial and final setting time of the mortar mixtures. A sample calculation can be seen in Appendix A.

$$Log(time) = \frac{Log(Penetration\ Resistance) - a}{b} \quad \text{Eq. 5-2}$$

Where: a and b = regression constants

5.3.3 Compressive Strength

Cubes measuring 2 x 2 x 2 (B x W x L) inches were tested in accordance with ASTM C109-20 [89]. For each age to be tested, 3 samples were made. The specimens were cast in two layers, and each layer was rodded 32 times. After removing the excess mortar from the top surface, the specimens were finished using a trowel. Soon after finishing the surface of the specimens, they were placed in a moist room with plastic covering the top surface to prevent dripping water to fall into the specimens. After 24 hours, the specimens were demolded and placed back into the moist room to cure until the age of 7 and 28 days. The load was applied to

the surfaces that were in contact with the bottom surfaces in the molds to avoid potential errors coming from the finished surface. Eq. 5-3 was used to calculate the compressive strength of the mortar cubes.

$$f_{cm} = \frac{P_{max}}{A} \quad \text{Eq. 5-3}$$

Where: f_{cm}= Compressive strength, P_{max} = Maximum load and A = Area

5.3.4 Drying Shrinkage

To study the drying shrinkage of mixtures containing NNPs, ASTM C596-18 was followed. The specimens. measuring 1 x 1 x 11.25 (B x W x L), were batched on 3 different days (4 beams per day) as suggested by the ASTM C596-18 standard. According to this specification, the amount of mixing water needed should be sufficient to produce a flow of 110 +/- 5%. Table 5.3 shows the measured flow values determined in conformance with the test method for the flow of hydraulic cement mortar (ASTM C1437-20 [90]). Instead, a fixed w/cm of 0.44 was used to effectively compare them to the concrete mixes (which also had a w/cm of 0.44). Additionally, another set of 12 beams was prepared using mixture designs shown in Table 5.4 . When preparing the new set of beams, instead of using the amount of mixing water needed to produce a flow of 110 +/- 5%, the w/cm of all mortars, including the reference one, was fixed to 0.44 in order to replicate the w/cm values used in concrete mixtures.

For both procedures, once the specimens were cast, they were moist cured in the molds for 24 hours. After 24 hours, the beams were demolded, and the standard suggests curing them in lime saturated water for 2 days. Alternatively, the beams were cured in lime saturated water for 6 days to give the mixtures with NNPs a better opportunity to develop strength. The specimens were then removed from the lime saturated water and an initial length comparator measurement was taken. Following the initial measurement, the specimens were placed in air storage at a temperature of 23 °C. Length comparator measurements of each specimen were taken at 4, 11, 18, and 25 days of air storage.

5.4 Results and Discussion

5.4.1 Effects of NNPs on the Fresh and Mechanical Performance of Mortar

The slump and spread of mortar containing all NNPs can be seen in Figure 5.1 and Figure 5.2 respectively. Table 5.5 shows the values for both slump and spread. As it can be seen in Figure 5.1 a), the mortars with CCs had a lower slump at every replacement percentage than the reference mixture. It should be noted that due to the poor workability that mixtures containing CC1 and CC3 demonstrated, superplasticizer had to be used at every replacement percentage for CC1 mixtures and 30 and 35% replacement of mortar with CC3. The superplasticizer was added to target the slump of the only CC mixture that did not need superplasticizer, CC2. As the replacement percentage increased, there was a decrease in slump for all mortars containing CCs without considering the use of SP. The low workability presented in CC samples was in agreeance with the water requirement results. As seen in Table 4.1, the water requirement was relatively high (in the case of the CC1 mixture, it was higher than the maximum amount allowed) meaning that low workability was expected. The spread of mortars containing CCs was also lower at every replacement percentage when compared to the OPC mixture. Furthermore, there was an increase in the spread for mortar with CC1 after 30% replacement and CC3 after 25% replacement. This increase can be attributed to the usage of SP.

Figure 5.1 b), shows that mortars containing FBCs also had a lower slump than the reference mixture at every replacement percentage. In this case, both FBC mixtures had a similar slump to one another as the replacement percentage increased (the largest difference being 0.6 inches at 25% replacement) but mortar with FBC2 consistently had a higher slump than mortar with FBC1. Nonetheless, for both 30% and 35% replacement, there was a significant decrease in slump for FBCs mixtures when compared to OPC mixtures. This can be attributed to both the water requirement and particle size distribution of FBCs. The water requirement was shown to be moderately high (See Table 4.8) and both FBCs had an elevated d_{50} as shown in Figure 4.7. A larger grain will require more water to hydrate, resulting in lower workability. With regards to the spread, FBC mixtures had a lower (yet still comparable) spread to OPC at every replacement percentage. Mortar containing FBC2 had a higher spread than mortar with FBC1 for 25 and 30% replacement. From 30 to 35% replacement, FBC1 mixture had 0.5 inches increase in spread meaning that it had a higher spread than the FBC2 mixture at 35% replacement (See Table 5.5).

The slump of NPs appears in Figure 5.1 c). From this figure, all mortars containing NPs had a lower slump at every replacement percentage when compared to the reference mixture. NP3 and NP2 mixtures had a significantly lower slump than mortar with NP1 at almost every replacement percentage (with the exception of the increase in slump for NP2 mixture at 35% replacement). Additionally, NP3 and NP2 mixtures had slump values close to one another except at 35% replacement. This was a result of the water requirement and particle size distribution as all mortars containing NPs have similar results. The spread of NP mixtures was also lower than the reference mixture at every replacement percentage. In this case, all mortars with NPs had a similar spread value when compared to one another and follow the same trend as what was seen for the slump results.

From Figure 5.1 d), mortars containing GBAs had a lower slump at every replacement percentage than the reference mixture. Unlike the other mortars containing NNPs, GBA mixtures had slumps comparable to the reference mixture at every replacement percentage (the lowest slump being 2.95 inches for GBA1 at 30% replacement). While mortar with GBA1 had the highest slump at both 25 and 35% replacement, GBA2 and GBA3 mixtures had similar slumps to one another in every case. A trend that was noted amongst the GBAs mixtures, was that they had an increase of slump at 35% replacement. Moreover, mortars containing GBAs had a comparable spread to the reference mixture at every replacement percentage. GBA3 mixtures had the highest spread followed closely by GBA1 and GBA2 mixtures. The reason for their high workability can be attributed to the water requirement summarized in Table 4.11. and the particle size distribution as seen in Figure 4.9. GBAs had the lowest water requirement amongst NPs while also having a uniform particle size distribution, thus aiding them to obtain satisfactory workability.

When comparing the mixtures NNPs amongst each other, it was clear that mixtures with GBAs performed the best as the slump did not significantly decrease from 25 to 35% replacement. On the other hand, mortars containing CCs, FBCs, and NPs respectively had the lower slumps. In each NNP group, it can be noted that mixtures with NNPs perform similarly to one another at almost every replacement percentage, except for NP2 mixtures at 35% replacement in NPs. The optimum replacement percentage (from 25, 30, and 35% replacement) to produce the highest slump for all 11 mortars with NNPs was 25%. Mortar with GBAs had the most comparable spread to OPC followed by FBCs mixtures. On the contrary, mortar containing

CCs (without the usage of SP) and NPs had a significantly lower spread since the minimum spread was at around 3 inches. The poor slump and spread showed at 30 and 35% replacement for mixtures containing CCs, FBCs, and NPs could lead to potential problems with workability such as mixing, consolidating, and compacting (in the form of honeycombing) more in particular at 35% replacement.

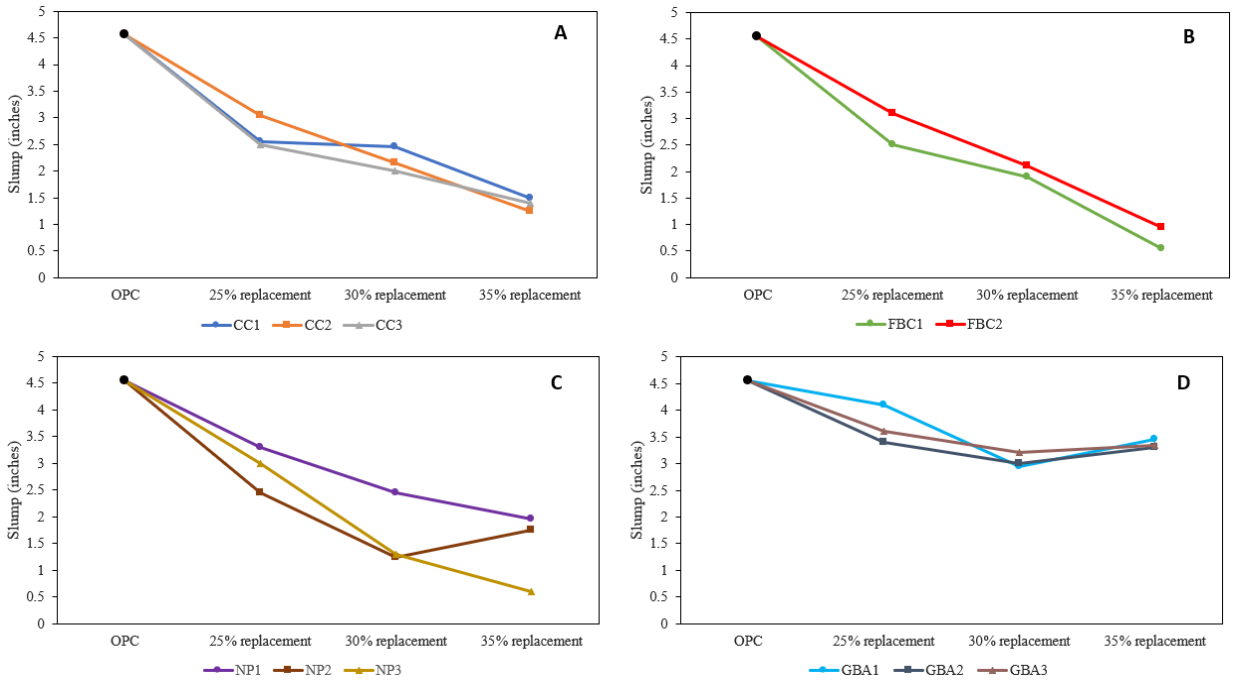

Figure 5.1. Slump of mortar of all eleven NNPs with 25, 30, and 35% replacement. a) Calcined Clays b) Fluidized Bed Combustion c) Natural Pozzolans d) Ground Bottom Ashes.

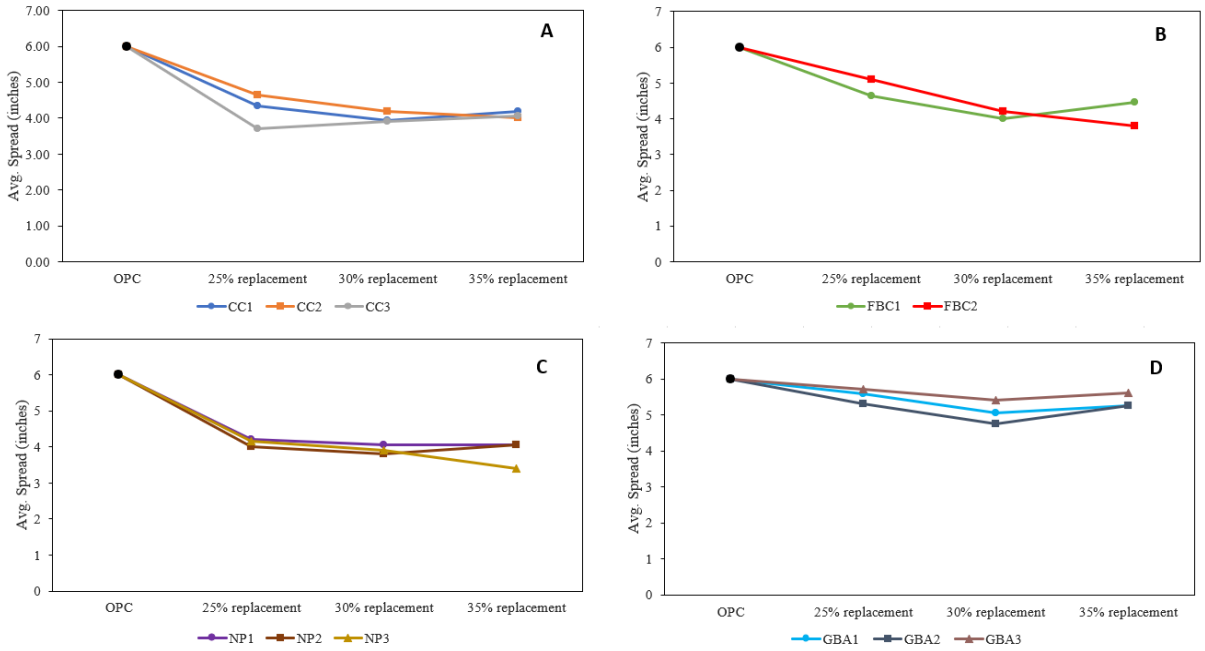

Figure 5.2. Avg. Spread of mortar of all eleven NNPs at 25, 30, and 35% replacement. a) Calcined Clays b) Fluidized Bed Combustion c) Natural Pozzolans d) Ground Bottom Ashes.

Table 5.5. Slump of mortar of all eleven NNPs at 25, 30, and 35% replacement.

	25% replacement		30% replacement		35% replacement	
Mixture	Slump (inches)	Spread (inches)	Slump (inches)	Spread (inches)	Slump (inches)	Spread (inches)
Reference	4.55	6.00	-		-	
CC1	2.55	4.35	2.45	3.95	1.50	4.20
CC2	3.05	4.65	2.15	4.20	1.25	4.00
CC3	2.50	3.70	2.00	3.90	1.40	4.05
FBC1	2.50	4.65	1.90	4.00	0.55	4.45
FBC2	3.10	5.10	2.10	4.20	0.95	3.80
NP1	3.30	4.20	2.45	4.05	1.95	4.05
NP2	2.45	4.00	1.25	3.80	1.75	4.05
NP3	3.00	4.15	1.3	3.90	0.6	3.40
GBA1	4.10	5.60	2.95	5.05	3.45	5.25
GBA2	3.40	5.30	3.00	4.75	3.30	5.25
GBA3	3.60	5.70	3.20	5.40	3.35	5.60

The fresh air content and unit weight of all eleven mortar mixtures containing NNPs can be seen in Figure 5.3 and Table 5.6. No correlation was found in the increase or decrease of fresh air content at different replacement percentages. A correlation was found between fresh air content and the unit weight (see Figure 5.3) of all mortars, indicating that the calculated fresh air content was accurate. From Figure 5.3 a), mortars containing CCs had unit weights similar to one another with a broad range in air content. CC1 mixtures demonstrated a higher air content whereas CC3 specimens showed the lowest air content. It can be seen in Figure 5.3 b), that FBC samples had comparable air content to one another (between 2.19 - 2.23%) regardless of the replacement percentage. Much like the mixtures containing CCs, Figure 5.3 c) shows that NP specimens had unit weights similar to one another but had a narrow range in air content. Mortar with NP2 had the highest air content, followed by NP3 specimens which had similar air content at every replacement percentage, and then followed by NP1 samples. Mixtures with GBAs presented a similar behavior to FBC specimens since they had a comparable air content to one another regardless of the replacement percentage, as shown in Figure 5.3 d).

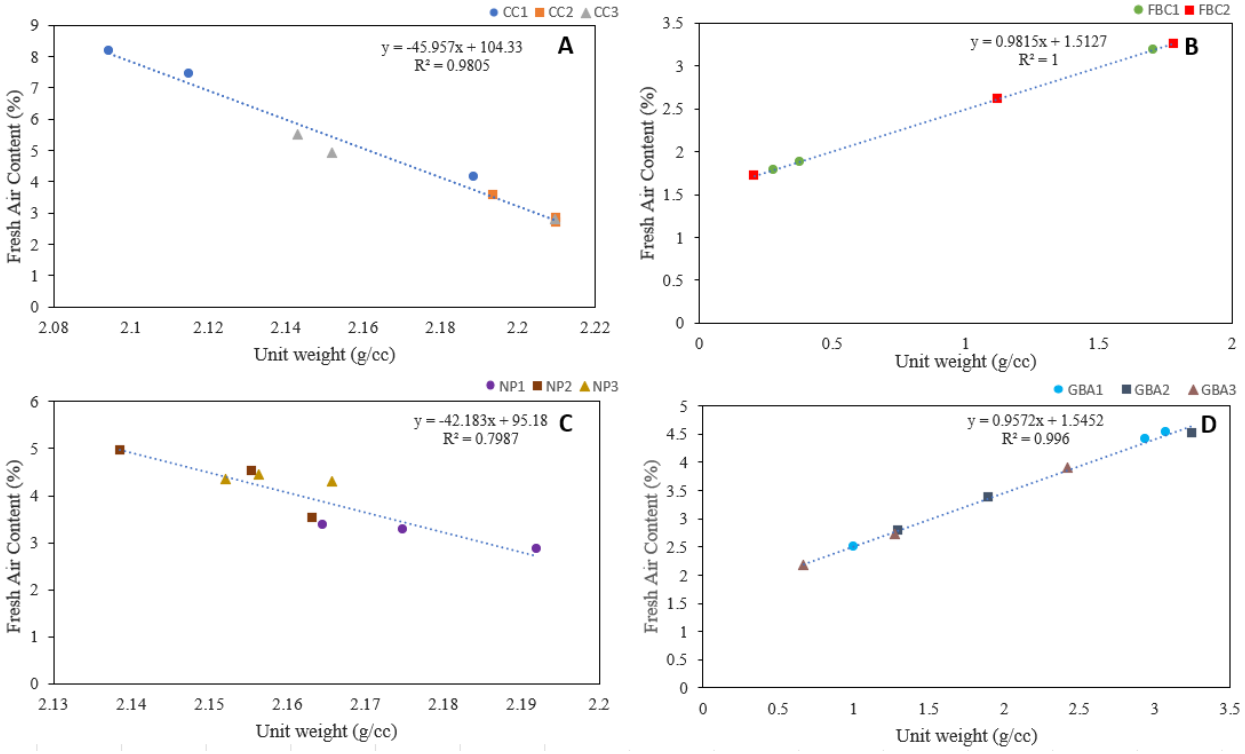

Figure 5.3. Fresh air content and unit weight of mortar of all eleven NNPs with 25, 30, and 35% replacement. a) Calcined Clays b) Fluidized Bed Combustion c) Natural Pozzolans d) Ground Bottom Ashes.

Table 5.6. Fresh air content and unit weight of all eleven mortar mixtures containing NNPs at 25, 30, and 35% replacement.

	25% replacement		30% replacement		35% replacement	
Mixture	Fresh Air Content (%)	Unit Weight (g/cc)	Fresh Air Content (%)	Unit Weight (g/cc)	Initial set (mins)	Unit Weight (g/cc)
Reference	0.22	2.26	-		-	
CC1	6.04	2.12	2.67	2.19	6.77	2.09
CC2	1.35	2.21	2.08	2.19	1.19	2.21
CC3	1.31	2.21	4.08	2.14	3.48	2.15
FBC1	2.23	0.38	2.23	0.28	2.19	1.71
FBC2	2.23	0.21	2.21	1.12	2.19	1.78
NP1	1.38	2.19	1.81	2.17	1.93	2.16
NP2	3.08	2.16	3.51	2.14	2.07	2.16
NP3	2.85	2.16	2.99	2.16	2.89	2.15
GBA1	2.18	2.93	2.18	3.07	2.22	1.00
GBA2	2.21	1.29	2.19	1.90	2.16	3.25
GBA3	2.24	0.67	2.20	2.42	2.23	1.28

The initial and final set of the mixtures containing NNPs can be found in Figure 5.4 - Figure 5.7 and in Table 5.7. From Figure 5.4, it can be noted that all CCs mixtures at the different replacement levels decreased the setting time when compared to the reference mixture. CC1 samples had a prominent low setting time (lowest amongst CCs and all other NPs) which decreased as the replacement level increased. However, it should be noted that the setting time for 35% was not performed as CC1 specimens presented workability issues. Mortar with CC2 had the highest setting time amongst CCs specimens and was comparable to OPC specimens at both 30 and 35% replacement. CC3 samples moderately reduced the time at both 25 and 25% replacement. Nonetheless, mixtures containing CC3 at 30% replacement had a comparable setting time to the CC1 mixtures. No clear trend was observed when increasing the replacement level. The retardation in setting time for mortars with CCs can be attributed to the high-water demand that has been previously discussed. The elevated water demand potentially made the binder phase denser, thus a lower setting time might be expected.

Mixtures containing FBCs either accelerated or delayed the setting time of the cementitious system when compared to the reference mix, as seen in Figure 5.5. FBC1 specimens accelerated the setting time at every replacement percentage. It was observed that at 30 and 35% replacement, FBC1 samples set faster than at 25% replacement. When compared to the reference mixture, FBC1 mixtures at 25% replacement had a similar setting time, 30% replacement had a comparable setting time and there was a clear acceleration of setting time at 35% replacement. As for mortar with FBC2, there was evident retardation of setting time at every replacement percentage. Furthermore, as the replacement percentage increased, the setting time also increased. The substantial delay in setting time for mortar containing FBC2 can be attributed to the high sulfate content of the material that was observed in Table 4.7.

From Figure 5.6, all mixtures with NPs had a lower setting time than the reference mixture at every replacement percentage. NP1 specimens had the highest setting time while mortar with NP2 had the lowest setting amongst NPs. For NP1 samples, as the replacement percentage increased, an accelerated setting time was noted. As the replacement level increased the setting time also increased. In fact, the final setting time increased to 350 minutes at a 35% replacement percentage, making it comparable to the reference mixture's final setting time (365 mins). NP2 specimens accelerated the setting time as the replacement percentage increased. Amongst mixtures with NPs, NP2 at 35% replacement had the fastest setting time. On the other hand, NP3 samples had a decrease in setting time from 25 to 30% replacement but an increase from 30 to 35% replacement which still surpassed the setting time at 25% replacement. Adding to this, the initial set for NP3 specimens at every replacement percentage was similar to one another (see Table 5.7).

The setting time of mixtures with GBAs can be seen in Figure 5.7. GBA specimens exhibit a faster setting time than the reference mixture at almost every replacement percentage, except for samples with GBA1 at 25% replacement. Mortar with GBA1 had a faster setting time as the replacement percentage increased. Of all mixtures with GBAs, GBA1 samples not only had the slowest setting time at 25% percent as previously mentioned, but they also had the fastest setting time at 35% replacement. For mixtures with GBA2s, there was an increase between 25 to 30% replacement but there was a decrease between 30 to 35% replacement. In addition, GBA2 specimens had a similar initial and final setting time at every replacement percentage. While mortar containing GBA3 had a faster setting time than the reference mixture at 25% replacement,

30%, and 35% replacement had an increase in setting time so much so that at 35%, GBA3 samples had a similar setting time to the reference mixture.

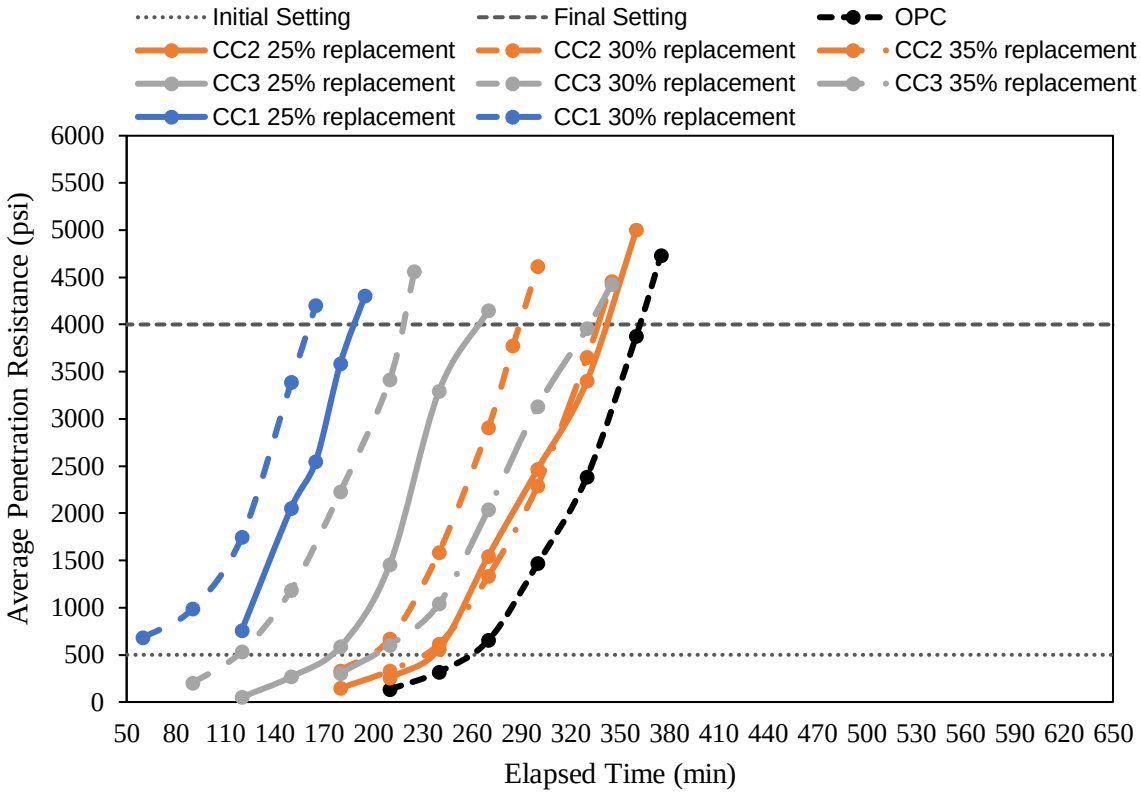

Figure 5.4. Setting time of CCs at 25, 30, and 35% replacement.

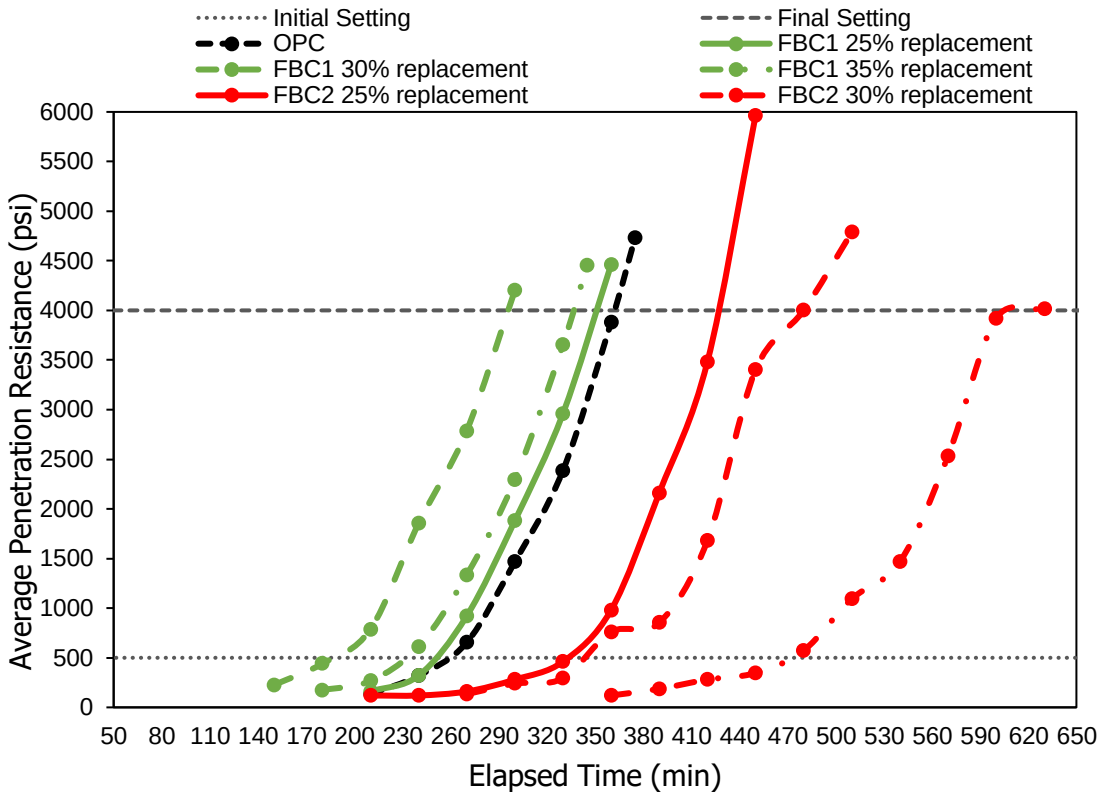

Figure 5.5. Setting time of FBCs at 25, 30, and 35% replacement.

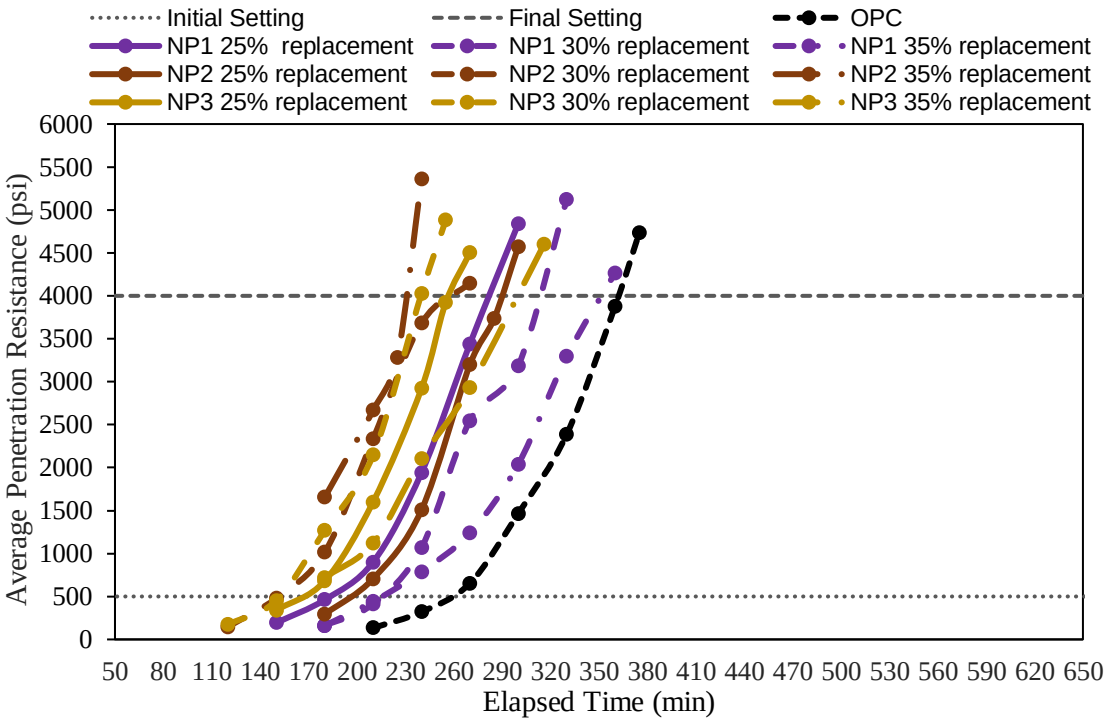

Figure 5.6. Setting time of NPs at 25, 30, and 35% replacement.

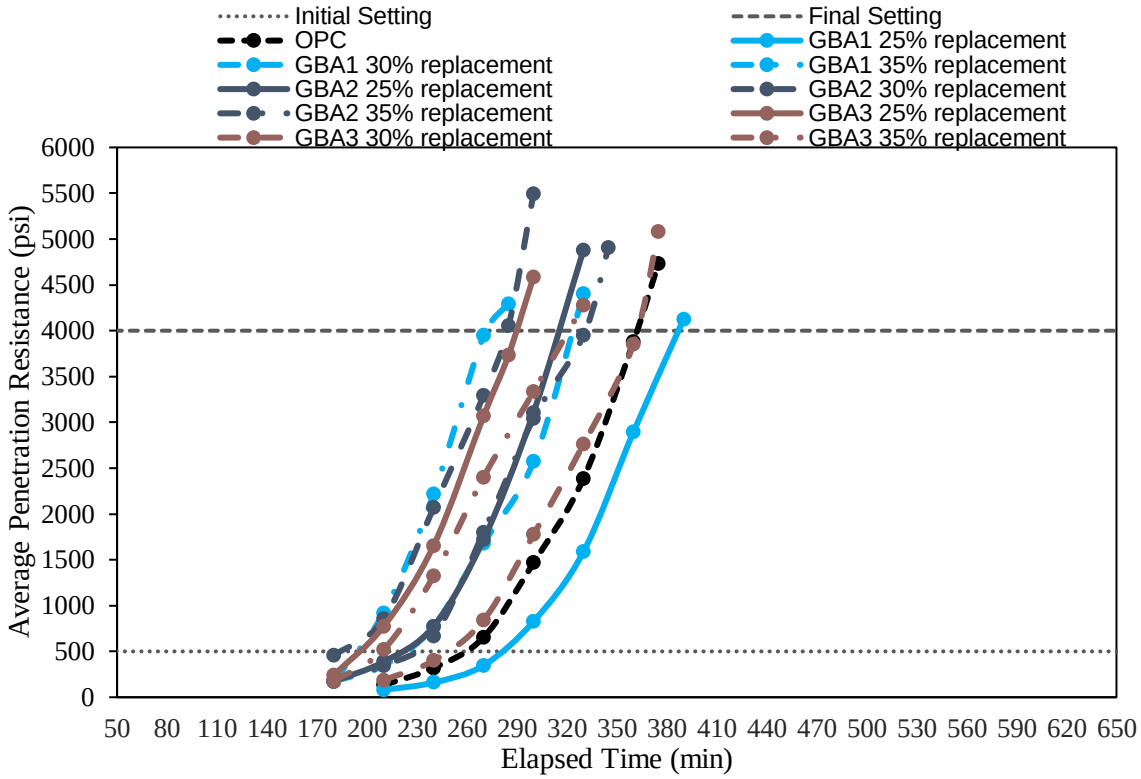

Figure 5.7. Setting time of GBAs at 25, 30, and 35% replacement.

Table 5.7. Initial and final set of all eleven mortar mixtures containing NNPs at 25, 30, and 35% replacement.

	25% replacement		30% replacement		35% replacement	
Mixture	Initial set (mins)	Final Set (mins)	Initial set (mins)	Final Set (mins)	Initial set (mins)	Final Set (mins)
Reference	258	360	-		-	
CC1	105	187	56	172		
CC2	232	336	195	289	227	336
CC3	171	260	117	217	200	327
FBC1	251	246	183	295	227	337
FBC2	344	488	343	485	456	622
NP1	187	286	215	307	222	347
NP2	197	288	154	245	134	230
NP3	167	259	151	240	134	299
GBA1	280	383	221	323	201	271
GBA2	219	317	184	281	220	326
GBA3	199	286	247	356	210	310

The average compressive strength at 7 and 28 days for 25, 30, and 35% replacement can be seen in Figure 5.8, and Figure 5.9 as well as in Table 5.8. Figure 5.10 shows the average compressive strength difference between 7 and 28 days at all replacement percentages. Except for mortar with CC2 at 30 % replacement, CC specimens had higher compressive strength than the reference mixture at 7 days. For the most part, as the replacement percentage increased, the compressive strength decreased. Adding to this, mortar with CC1 and CC3 had similar results to one another while CC2 specimens had the lowest compressive strength for each replacement percentage at 7 days. At 28 days, mixtures containing CCs performed similarly (CC2 at 30 and 35% replacement) or better than the reference mixture. It was observed that CC3 samples had an increase in compressive strength after 25% replacement whereas CC1 and CC2 samples decreased in compressive strength. The difference in compressive strength between 7 and 28 days was mainly lower than the reference mixture (besides mixtures with CC2 at 25% and CC3 at 30% replacement), perhaps indicating a faster plateau in compressive strength.

For mortar with NPs, it can be seen at 7 days they had a lower, yet comparable, compressive strength than the reference mixture. NP mortars also exhibited similar compressive strength to one another and also at every replacement percentage when compared at 7 days. Once they reached 28 days, NP specimens were still comparable to one another but mortar with NP2 had the highest compressive strength, followed by NP1 and NP3 mixtures respectively. A decrease in compressive strength was observed when increasing the replacement percentage of specimens with NPs. Figure 5.10 shows that NP1 and NP2 specimens had a substantial increase in compressive strength for almost all replacement percentages. On the other hand, NP3 specimens had a similar increase in compressive strength to the reference mixture.

At 7 days, FBC1 specimens had a significantly lower compressive strength at every replacement percentage than the reference mixture, while mixtures with FBC2 has a similar compressive strength at 25% replacement. The trend observed for FBC specimens at this age was the decrease in compressive strength as the replacement percentage increased. Mortar with FBC1 and FBC2 had a similar compressive strength to one another at both 30 and 35% replacement. Figure 5.9, showed an increase in compressive strength at 28 days. FBC1 mortar now had a comparable compressive strength at every replacement percentage while mixtures containing FBC2 had a higher compressive strength. Furthermore, mortar with FBC1 had an increase in compressive strength at each replacement percentage whereas FBC2 specimens only had an increase at 35% replacement. This significant increase between 7 and 28 days can be seen in Figure 5.10, in which mixtures with FBCs had a greater compressive strength increase than the reference mixture.

Mortar-containing GBAs had a significantly lower compressive strength than the reference mixture at 7 days. Not only that but mixtures with GBAs had similar compressive strength to one another at all replacement percentages but GBA3 samples had the lowest compressive strength. At 28 days, there was a substantial increase from 7 days, as seen in Figure 5.10. When comparing the increase of specimens with GBAs to the reference mixture, GBA samples at almost every replacement percentage had an increase of twice the size of the reference mixture. This meant that mortar containing GBAs started performing similar to or better than the reference mixture. GBA2 specimens had the highest compressive strength, followed by mixtures with GBA1 while GBA3 samples had a compressive strength similar to all

replacement percentages while still having the lowest compressive strength amongst all mortar with GBAs.

When comparing mortars with NNPs at 7 days, it was evident that CC specimens had the highest compressive strength (even higher than the reference mixture). Mortars with CCs were then followed by NPs, FBC, and GBA specimens respectively which had lower compressive strength than the reference mixture. Both mixtures with FBCs and GBAs had a significantly lower compressive strength than the other mixtures containing NNPs. A trend that can be noted for most mortars containing NNPs was that as the percentage replacement increased, the compressive strength decreased. In other words, 25% replacement produced the highest compressive strength for almost all mixtures with NNPs at 7 days. At 28 days, all mixtures with NNPs performed similarly or better than the reference mixture. As well at 7 days, CCs mortar mixtures had the highest compressive strength amongst mixtures containing NNPs at 28 days. NPs, FBCs, and GBAs mortar had a substantial increase in compressive strength from 7 to 28 days – more specifically FBCs and GBAs mortar. Overall, the best performing mixture containing NNP in terms of compressive strength was CC3 and the lowest was FBC1.

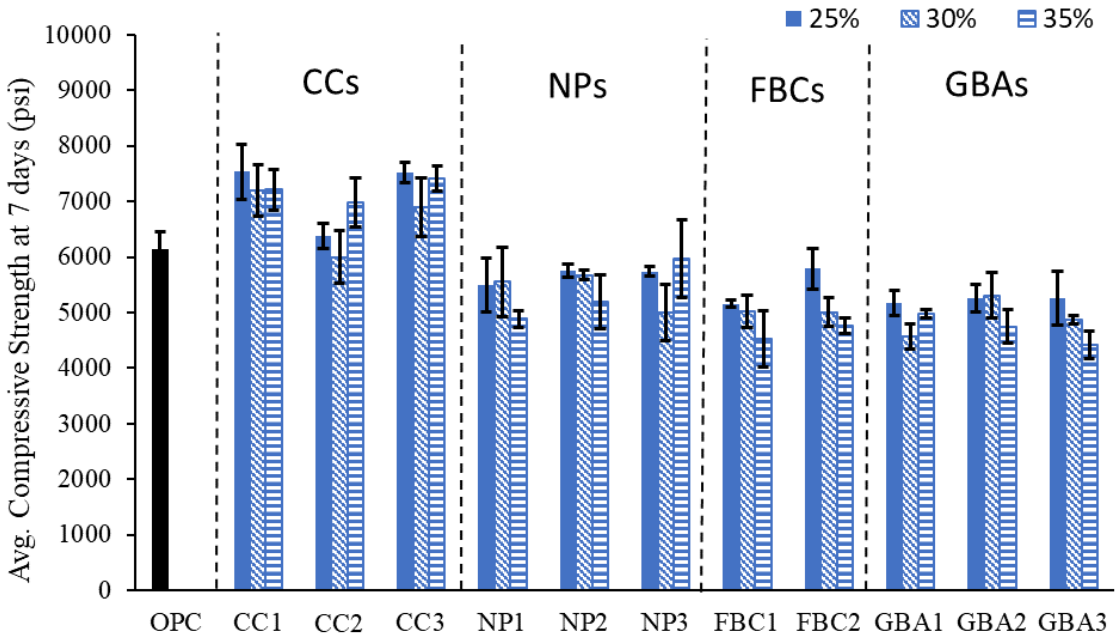

Figure 5.8. Avg. compressive strength of all mortar cubes containing NNPs at 7 days for 25, 30, and 35% replacement.

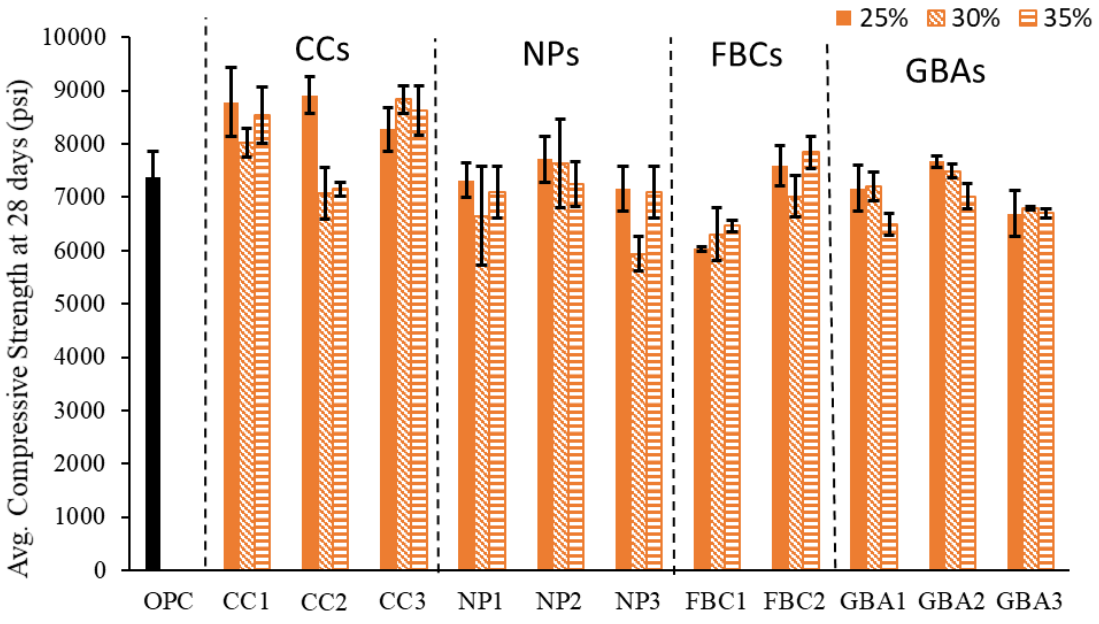

Figure 5.9. Avg. compressive strength of all mortar cubes containing NNPs at 28 days for 25, 30, and 35% replacement.

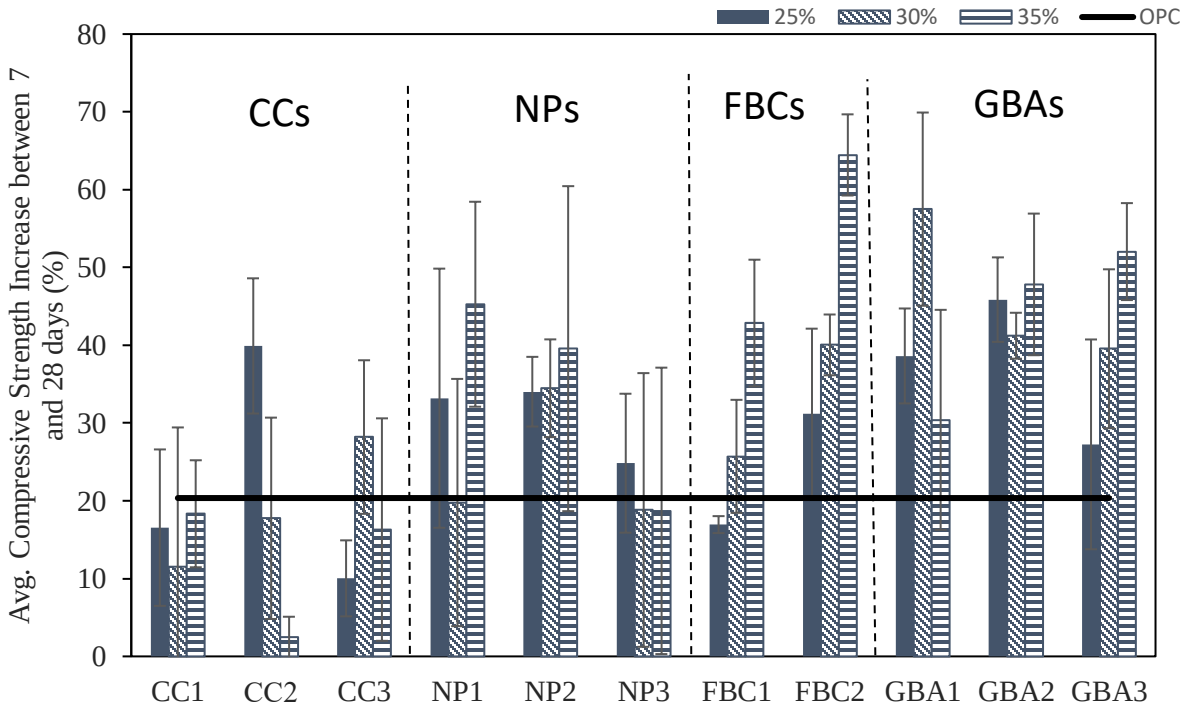

Figure 5.10. Avg. compressive strength increase between 7 and 28 days for 25, 30, and 35% replacement.

Table 5.8. Avg. compressive strength of all mortar cubes containing NNPs at 7 and 28 days for 25, 30, and 35% replacement.

	Avg. compressive strength - 25% replacement		Avg. compressive strength - 30% replacement		Avg. compressive strength - 35% replacement	
Mixture	7 days	28 days	7 days	28 days	7 days	28 days
Reference	6130	7380	-		-	
CC1	7530	8780	7190	8020	7210	8540
CC2	6370	8910	6000	7070	6980	7150
CC3	7520	8270	6900	8840	7410	8620
FBC1	5160	6030	5020	6310	4520	6460
FBC2	5790	7590	5010	7020	4770	7840
NP1	5490	7320	5550	6650	4890	7100
NP2	5750	7710	5670	7630	5190	7250
NP3	5740	7170	5000	5940	5980	7090
GBA1	5170	7170	4570	7200	4980	6500
GBA2	5260	7670	5310	7400	4750	7020
GBA3	5260	6690	4870	6800	4410	6700

5.4.2 Effects of NNPs on the Drying Shrinkage Performance of Mortar

The drying shrinkage test results for plain mortar and mortar with all four NNPs prepared to meet the ASTM C596-18 target flow of 110 +/- 5% used in this study are summarized in Figure 5.11 and Table 5.9. It should be noted that to maintain the constant target value of the flow, the w/cm values of mortars varied in the range from 0.38 to 0.45, depending on the composition of the mixture. After 4 days of air storage, the specimens with GBA3 and FBC1 materials exhibited shrinkage values similar to the shrinkage values of reference specimens. At the same age, the shrinkage of specimens with NP3 was the highest whereas the shrinkage of the specimens with CC2 was in-between the values for the NP3 and reference specimens. The subsequent measurements, performed after 11, 18, and 25 days of air storage indicate that all specimens continued to shrink at relatively constant rates. After 25 days of air storage, the shrinkage of the GBA3 and reference mortars was the lowest (and practically the same for both types of mortar) whereas the shrinkage of the NP3 mortar was the highest. The values of

shrinkage for the CC2 and FBC1 mortars were also practically the same and located between those of NP3 and GBA3/reference mortars. One possible reason why GBA3 mortars had a much lower shrinkage than the rest of the specimens containing NNPs at 25 days of air storage was that GBA3 mortars had the lowest w/cm. On the other hand, FBC1 specimens which contained the highest w/cm performed similarly to the GBA3 specimens. This could be attributed to the coarser particle size of FBC1 materials.

The results of drying shrinkage measurements for mortars prepared at a constant w/cm of 0.44 are shown in Figure 5.12 and Table 5.10. As it was seen, fixing the value of the w/cm did not significantly change the values, or the order, of the observed shrinkage. After 4 days of air storage, GBA3 had the lowest shrinkage among all materials. At the next measurement (performed after 11 days of air storage), the reference specimen had the lowest shrinkage, and GBA3 specimens had the highest increase in-between measurements, performing similar to CC2 and FBC1 specimens. Similar to what was observed for mortars prepared at constant flow, NP3 mortar had an overall highest shrinkage. Between all NNP specimens at both 18 and 25 days of air storage, mortar containing GBA3 had the lowest shrinkage measurement (closely followed by FBC1 mortar) while mortar with NP3 had the highest. When using the same w/cm, the shrinkage of GBA3 and FBC1 specimens showed a trend similar to that of the reference specimen. In contrast, for specimens prepared to meet the constant value of flow (and thus having different w/cm values) this was only observed for the GBA3 specimens. This was because specimens with GBA3 material had an increase of w/cm value (from 0.39 to 0.44) while FBC1 specimens had a decrease in w/cm value (from 0.45 to 0.44). Mortar with CC2 had the highest increase in shrinkage at 25 days of air storage with an increase of w/cm (from 0.41 to 0.44), but it was still not the worst-performing NNP, partially because it had the second coarsest particle size. Lastly, mortars with NP3 material continued to display the highest shrinkage with the lowest increase of w/cm (from 0.42 to 0.44). Overall, the shrinkage trends for all the specimens prepared at constant w/cm were similar to the shrinkage trends of specimens prepared at different w/cm. Furthermore, the magnitude of shrinkage of all mortars with NNPs was comparable to the values of shrinkage observes in specimens containing OPC only.

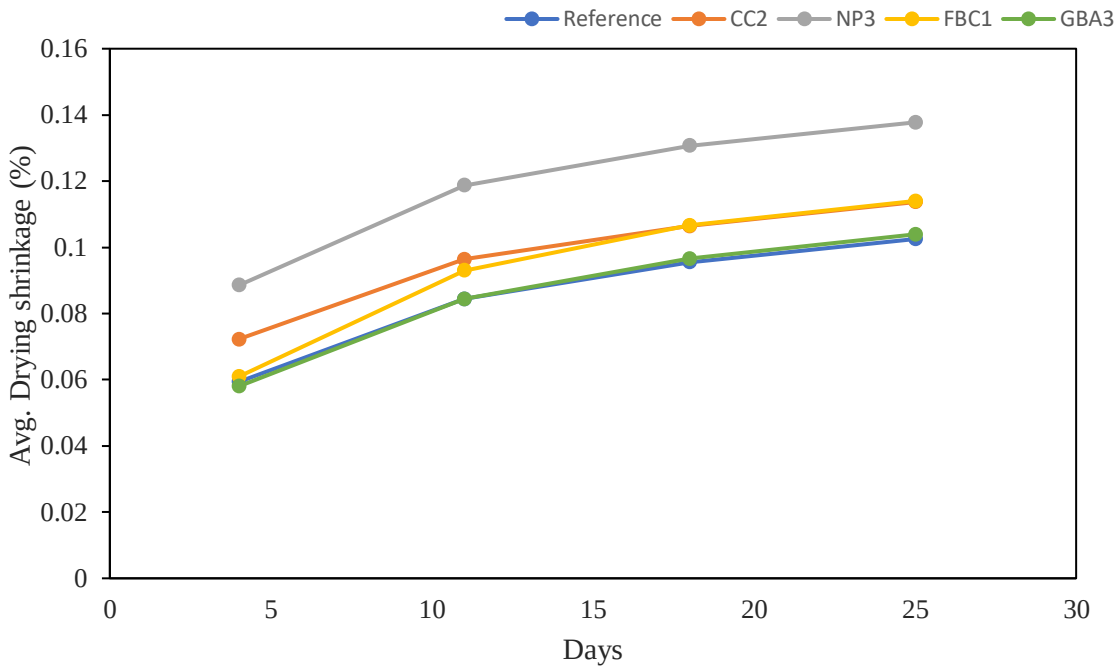

Figure 5.11. Avg. Drying shrinkage of reference, CC2, NP3, FBC1, and GBA3 with a constant flow of 110 +/- 5% - 25% replacement.

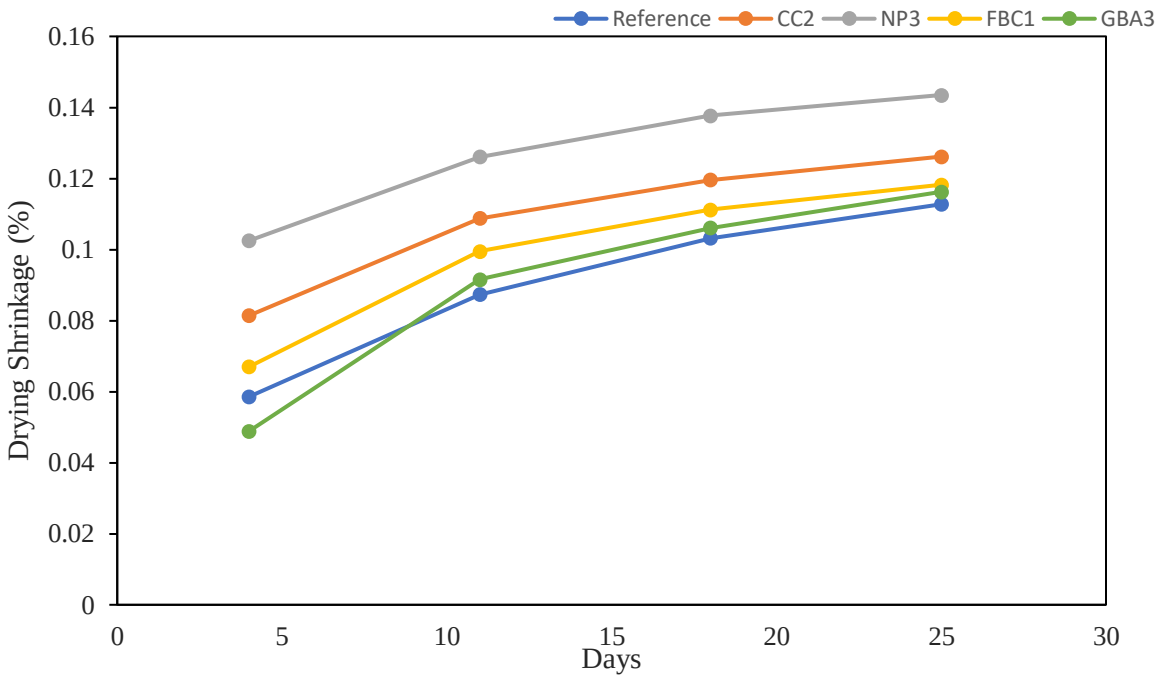

Figure 5.12. Avg. Drying shrinkage of reference, CC2, NP3, FBC1, and GBA3 with a w/cm 0.44 – 25% replacement.

Table 5.9. Avg. Drying shrinkage results for specimens with a target flow of 110 +/- 5%.

Specimen	w/cm	Flow (%)	4d (%)	11d (%)	18d (%)	25d (%)
Avg. Reference	0.38	108	0.059	0.084	0.095	0.10
Avg. GBA3	0.39	106	0.058	0.085	0.097	0.104
Avg. CC2	0.41	105	0.072	0.096	0.106	0.113
Avg. FBC1	0.45	110	0.061	0.093	0.106	0.114
Avg. NP3	0.42	108	0.089	0.119	0.131	0.138

Table 5.10. Avg. Drying shrinkage results for specimens with 0.44 w/cm.

Specimen	4d (%)	11d (%)	18d (%)	25d (%)
Avg. Reference	0.057	0.086	0.10	0.11
Avg. GBA3	0.048	0.092	0.106	0.114
Avg. FBC1	0.067	0.010	0.111	0.118
Avg. CC2	0.081	0.108	0.120	0.127
Avg. NP3	0.102	0.127	0.131	0.144

5.5 Conclusions

Based on the results presented in this chapter, the following conclusions can be drawn:

- When used at the 25% replacement levels, all NNPs produced mortars with performance characteristics comparable to, or better than, those observed in the OPC mortars.
- With the increase of the replacement level from 25% to 30% and to 35%, the values of slump, spread, and compressive strength of mortar containing NNPs decreased. This implies that the 25% replacement level may be optimum for these materials with respect to the properties tested.
- With the exception of mortars with CC1 (at all replacement levels) and with CC2 at 35% replacement level, mortars with all other NNPs have either comparable or significantly higher increases in compressive strength from 7 to 28 days in comparison to OPC mortars.
- Excluding FBC1 (at all replacement levels) and GBA1 at 25% replacement level, all other NNPs decreased the setting time of mortars. Mortars with CCs and NPs had the fastest

setting time whereas the setting times of all GBA-containing mortars were similar and comparable to the setting time of the reference mixture.

- The values of the compressive strength and drying shrinkage for CC mortars compared well with those obtained for the OPC mortars. However, mortar mixtures containing CCs experienced workability problems and faster setting times that the OPC mortars at all replacement levels.
- The strengths of mortars with NPs were comparable to the strengths of the reference mortars. However, when compared to the OPC mortars, the mortars containing NPs experienced higher drying shrinkage, reduction of slump (at replacement levels higher than 25%), and faster setting time.
- When compared to control mortars, mixtures containing FBCs experienced workability issues (at replacement levels beyond 25%) and a reduction in 7 days compressive strengths (the 28 days strength values were similar to those of the OPC mortars). Adding to this, depending on the type of FBC used, the mixtures containing FBCs could either increase or decrease the setting time of a given mixture.
- The fresh properties and the values of both, the compressive strength at 28d, and the drying shrinkage of mortars containing GBAs were comparable to the results obtained from the reference mixture. The significant increase in compressive strength between 7 and 28 days indicates a somewhat delayed pozzolanic reactivity process.
- Based on the results of all experiments presented in this chapter, the "best-performing" materials from each of the four groups of NNPs were CC3, NP2, FBC2, and GBA1. The "worst-performing" NNPs were CC2, NP3, FBC1, and GBA3.

6. MECHANICAL AND DURABILITY PROPERTIES OF CONCRETE CONTAINING NNPS

6.1 Introduction

As previously discussed, in section 5.1, the NNPs that showed the lowest levels of reactivity performance when used in the mortar mixtures tests were selected to prepare the concrete mixtures. These included the following NNPs: CC2, NP3, FBC1, and GBA3. This approach was adopted under the assumption that achieving adequate concrete characteristics with lowest-quality materials will all but assure satisfactory performance of concretes with higher-quality materials. In addition, this approach could also help to predict general trends for better quality NNPs.

When preparing the concrete mixtures, the level of cement replacement with NNPs was held constant at 25% (by the total weight of cementitious materials). This is due to the fact that, based on literature review, the vast majority of traditional SCMs are being used with maximum replacement levels of 20 – 25%. The experiments that were performed on concrete mixtures included slump, fresh air content, compressive strength, flexural strength, rate of water absorption, determination of the formation factor, and scaling resistance. These tests mainly characterize fresh, mechanical, durability, and transport properties. The understanding of these properties is critical since the results of some of these tests are required by different agencies and they also aid in the prediction of the overall performance of concrete.

6.2 Materials

6.2.1 Materials and Concrete Mix Design

The worst performing NNP of each group (CC2, NP3, FBC1, and GBA3), fine aggregate, coarse aggregate, cement, and water were used for the concrete mix designs (CMDs) For more information regarding these materials, refer to Chapter 4.

The CMDs used for the fresh and mechanical properties of concrete containing NNPs are summarized from Table 6.1 to Table 6.5. The CMDs were developed based on section 502 of the 2020 INDOT specifications [91] with a slight adjustment to the maximum replacement

percentage of fly ash (an increase from 20% to 25%). It should be noted that due to poor workability demonstrated by FBC1 during trial mixtures, a higher fine aggregate to total aggregate ration had to be used (FA/tot. agg.). The w/cm was selected to be 0.44 to help with the workability of each material and reduce the amount of admixtures used. The FA/tot. agg. varied from 0.40 (for CC2, NP3, and GBA3) to 0.45 (for FBC1). All mixtures needed the use of WRA and AEA to meet the target slump (2 +/- 1 inch) and air content (6.5 +/- 1.5 %).

Table 6.1. CMD for OPC specimens per yd^3 (SSD Basis).

Material	**S.G.**	**QTY**	**Volume (ft^3)**
Cement	3.15	564 lb	2.87
Coarse Aggregate	2.61	1833 lb	11.25
Fine Aggregate	2.74	1222 lb	7.15
Water	1.00	248 lb	3.97
Air			1.76
WRA (per 100 lbs of cementitious)		4.78 fl oz	
AEA (per 100 lbs of cementitious)		0.81 fl oz	

Table 6.2. CMD for CC2 specimens per yd^3 (SSD Basis).

Material	**S.G.**	**QTY**	**Volume (ft^3)**
Cement	3.15	423 lb	2.15
CC2	2.75	141 lb	0.82
Coarse Aggregate	2.61	1820 lb	11.17
Fine Aggregate	2.74	1218 lb	7.12
Water	1.00	248 lb	3.97
Air			1.76
WRA (per 100 lbs of cementitious)		9.86 fl oz	
AEA (per 100 lbs of cementitious)		0.97 fl oz	

Table 6.3. CMD for NP3 specimens per yd^3 (SSD Basis).

Material	**S.G.**	**QTY**	**Volume (ft^3)**
Cement	3.15	423 lb	2.15
NP3	2.50	141 lb	0.90
Coarse Aggregate	2.61	1810 lb	11.11
Fine Aggregate	2.74	1214 lb	7.10
Water	1.00	248 lb	3.97
Air			1.76
WRA (per 100 lbs of cementitious)		7.59 fl oz	
AEA (per 100 lbs of cementitious)		0.97 fl oz	

Table 6.4. CMD for FBC1 specimens per yd^3 (SSD Basis).

Material	**S.G.**	**QTY**	**Volume (ft^3)**
Cement	3.15	423 lb	2.15
FBC1	2.68		0.84
Coarse Aggregate	2.61	1802 lb	11.06
Fine Aggregate	2.74	1223 lb	7.15
Water	1.00	248 lb	3.97
Air			1.76
WRA (per 100 lbs of cementitious)		18.30 fl oz	
AEA (per 100 lbs of cementitious)		1.68 fl oz	

Table 6.5. CMD for GBA3 specimens per yd^3 (SSD Basis).

Material	**S.G.**	**QTY**	**Volume (ft^3)**
Cement	3.15	423 lb	2.15
GBA3	3.00	141 lb	0.75
Coarse Aggregate	2.61	1828 lb	11.22
Fine Aggregate	2.74	1221 lb	7.14
Water	1.00	248 lb	3.97
Air			1.76
WRA (per 100 lbs of cementitious)		1.42 fl oz	
AEA (per 100 lbs of cementitious)		1.13 fl oz	

6.3 Experimental Methods

6.3.1 Slump

ASTM C143-20 [93] was followed to measure the slump of the different mixtures. Before the concrete finished mixing, the slump cone was dampened and placed on a slump base by clamping it to the sides. Once the concrete finished mixing, the mold was filled in an even distribution by using a scoop in three equal layers. Using a rod, each layer was rodded 25 times uniformly. For the second and third layers, the rod only penetrated through the layer being rodded and an extra inch into the layer below. An excess of concrete was kept at the top of the last layer before rodding and subsequently, the excess was screeded off. The excess concrete surrounding the base was removed before raising the slump cone in 5 +/- 2 seconds. The slump cone was then turned upside down next to the slumped concrete, with the tamping rod laying across the bottom surface of the cone. Shortly after, the slump was recorded by measuring the bottom of the tamping rod to the top center of the slumped concrete using a ruler. The whole process was done in less than 2:30 minutes.

6.3.2 Air Content

ASTM C231-17 [94]was followed to obtain the fresh air content of concrete. Before the concrete finished mixing, the measuring bowl was dampened and placed on a flat surface. Once the concrete finished mixing, the measuring bowl was filled in an even distribution in three equal layers. Using a rod, each layer was rodded 25 times uniformly. For the second and third layers, the rod only penetrated through the layer being rodded and an extra inch into the layer below. After each layer was rodded, the sides were tapped 10 – 15 times using a mallet. An excess of concrete was kept at the top of the last layer before rodding and subsequently, the excess was screeded off. The excess was carefully removed to avoid overfilling by sliding a strike-off plate with a sawing motion until completely leveled at the top. Subsequently, the air meter was placed on the top of the measuring bowl and tightly clamped to the sides. Water was added to the concrete by opening the petcocks holes (with a valve), injecting water until water emerged from the opposite petcock, and closing the petcocks holes. Air was then pumped until the gauge hand

was at the initial pressure line. Following this, the pressure was stabilized, and the air was released and recorded.

6.3.3 Compressive Strength

Twelve cylindrical concrete specimens measuring 4 x 8 (D x L) inches of each material were tested following ASTM C39-21 [95]. The specimens were cast in plastic molds and covered with a cap for 24 hours. After 24 hours, the specimens were removed from the molds and then immersed in lime saturated water until the age of 7, 28, 56, and 90 days to be tested. Caps were used at the top and bottom surfaces of the cylinders to achieve a plane surface. Average compressive strength was calculated using Eq. 6-1 (the average of the three specimens, rounded to the nearest 10 psi was used).

$$f_{cm} = \frac{4P_{max}}{\pi D^2} \qquad \text{Eq. 6-1}$$

Where: f_{cm}= Compressive strength, P_{max}= maximum force, and D = Diameter.

6.3.4 Flexural Strength

Flexural strength test with third-point loading was performed on three concrete beams of each material per ASTM C78-21 [96]. The concrete beams had a dimension of 4 x 4 x 14 (B x W x L) inches. The beams remained in the molds for 24 hours before being demolded. After demolding, the beams were then placed in lime saturated water until an age of 28 days to be tested. The beams were placed on top of the support block at a distance equal to the span length (12 inches). The specimens were tested using leather shims on the contract surface to eliminate any gaps between the machine and specimen. The average modulus of rupture was calculated using Eq. 6-2 and taking the average of the three specimens, rounded to the nearest 5 psi.

$$R = \frac{PL}{HD^2} \qquad \text{Eq. 6-2}$$

Where: R = Modulus of rupture, L= span length, H= Width, and D= Depth

6.3.5 Rate of Water Absorption

Three cylindrical concrete specimens measuring 4 x 2 (D x L) of each material were tested in accordance with ASTM C1585-20 [97]. The three specimens were cut from one molded cylinder with dimensions of 4 x 8 (D x L) that was cured in lime saturated water until the age of 28 days. The three specimens were vacuum-saturated following ASTM C1202-19, then placed in an oven at a temperature of 50 °C and relative humidity of 80% for 3 days. After the three days, each specimen was placed separately in a sealed container at a temperature of 23 °C for 15 days before sealing and starting the absorption test. Figure 6.1 shows the setup of the test.

The initial absorption and rate of absorption are measured during the first 6 hours while the secondary absorption and rate of absorption are measured for the next 7 days. For both initial and secondary absorption, the data between the first measurement and the last must follow a linear relationship (a correlation coefficient of 0.98 or higher).

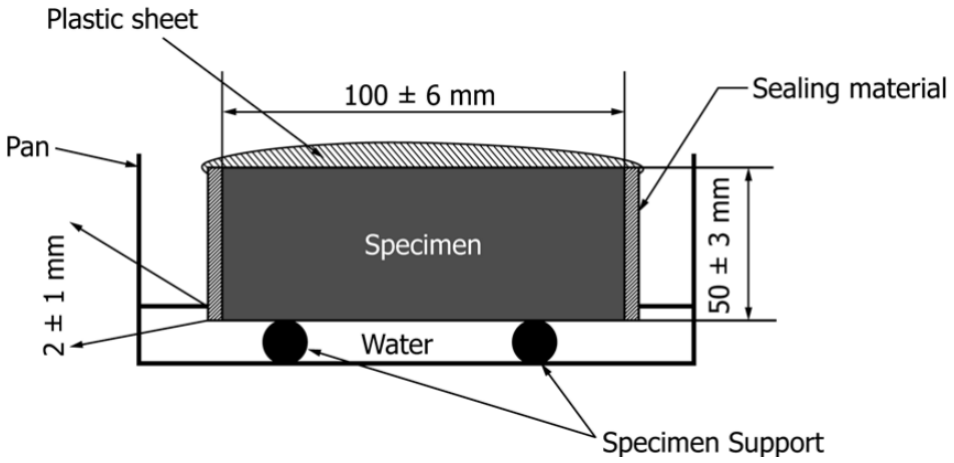

Figure 6.1. Set up for the absorption test, reproduced from the ASTM C1585-20.

DIN 52617 test method was also performed to compare the results to those obtained using ASTM C1585-20 [98]. The only difference between DIN 52617 and ASTM C1585-20 is the procedure for conditioning. Instead of placing the specimens in an oven at a temperature of 50 °C and relative humidity of 80% for 3 days, the specimens were placed in an oven at 60 °C until a daily mass change of less than 0.2% was achieved. The same specimens used for ASTM C1585-20 were used for DIN 52617.

6.3.6 Formation Factor

Formation factor is the ratio of concrete resistivity to a simulated pore solution. This transport property is able to measure the transport through the pore system of concrete. A higher formation indicates a lower porosity or pore connectivity, therefore in terms of durability performance, a higher formation factor is preferred.

To perform the formation factor test, three concrete specimens measuring 4 x 8 (D x L) from each material were cast and conditioned using option A from AASHTO TP119-21 [99]. Option A requires samples to be immersed in a calcium hydroxide-saturated, simulated pore solution at a temperature of 23 °C. The sample's bulk resistivity was measured at an age of 14, 21, 28, 56, and 91 days. The formation factor was calculated using the equation given in AASHTO PP84 [100] (See Eq. 6-3) and the results of the three specimens were averaged.

$$F_{app} = \frac{\rho}{\rho_o} \qquad \text{Eq. 6-3}$$

Where: F_{app}= Formation Factor, ρ= Bulk body (Ωm), ρ_o = Resistivity of the pore solution (Ωm).

6.3.7 Scaling Resistance

To perform scaling resistance test, ASTM C672-12 [101] requires that specimens should have a surface area of 72 inches^2 and at least 3 inches in depth. Two slabs of each material were cast, measuring 3 x 8 x 11 (B x W x L). The slabs conformed to the standards specification for surface area, having 88 inches^2, and a minimum depth of 3 inches. During the fabrication process, special attention was given to the finishing of the specimens. The concrete was leveled after several passes of a wood strike-off board, and after the concrete finished bleeding, three more passes using the wood strike-off board were given. After finishing, the slabs were placed under a polyethylene sheet for 24 hours. Following the 24 hours, the slabs were cured in lime saturated water until an age of 14 days and subsequently stored in air at a temperature of 23°C and relative humidity of 50% for 14 days.

At an age of 28 days, a dike was placed around the perimeter of the finished surface of the slab to contain the deicing solution that the finished surface will be exposed to for the duration of the experiment. The finished surface was exposed to a 4% (i.e. 4g/100 mL) solution of calcium chloride in a controlled chamber. The chamber was programmed to have a temperature of -18 °C for 16 to 18 hours and then it would raise the temperature to 23 °C for 6 to 8 hours to complete

one cycle. At the end of every 5 cycles, the slabs were removed from the chamber to flush off the surface flakes and/or aggregates. The flakes and/or aggregates were dried and weighted to obtain the mass loss of the slabs, and a picture of the dried expose surface was taken. After the picture was taken, calcium chloride solution was added to the slabs. The scaling test was performed for 50 cycles.

To evaluate the condition of the surface of each slab can be found in Table 6.6, which was provided in ASTM C672-12 was used. Furthermore, the mass loss obtained from the flakes and/or aggregates was used to estimate the scaling resistance of the slabs to the maximum limit (0.8 kg/m^2 after 50 cycles) given by the Ontario Ministry of Transportation (MTO).

Table 6.6. Visual rating of the condition of the surface as per ASTM C672-12.

Rating	Condition of Surface
0	No scaling
1	Very slight scaling (3 mm [1/8 in] depth, max, no coarse aggregate visible)
2	Slight to moderate scaling
3	Moderate scaling (some coarse aggregate visible)
4	Moderate to severe scaling
5	Severe scaling (coarse aggregate visible over the entire surface)

6.4 Results and Discussion

6.4.1 Effects of NNPs on the Mechanical Performance of Concrete

The 7-, 28-, 56-, and 90-days compressive strength results for concretes with all four NNPs used in this study are summarized in Figure 6.2 and Table 6.7. It can be seen that at 7 days mixes with CC2, NP3, and FBC1 materials had a compressive strength that was either comparable to or higher than, the compressive strength of the reference mix. The only mixture with a 7- day compressive strength lower than that of the reference mixture was the one containing GBA3 material. At 28 days, CC2 and NP3 had a significantly higher compressive strength than the reference mix while FBC1 and GBA3 had compressive strength similar to that of the reference mix. At 56 days, all but one (GBA3) NNP mixtures had higher compressive strength than the reference mix. Finally, at 90 days, all NNP mixtures had higher compressive strength than the

reference mix. The relative changes in the values of compressive strength over time had a similar trend for mixtures with CC2, NP3, and GBA3. On the other hand, the trend observed for the mixture with FBC1 is similar to that observed for the reference (i.e. OPC only) mixture.

While the reference mixture had a higher air content than the NNP mixtures, even if the air content were to be lowered to a value closer to the mixtures with NNPs, the compressive strength of all NNP concretes would still be either higher or comparable to the reference mixture. This is because as a general rule, with a 1 percent increase in the air content the compressive strength decreases by about 5 percent. It is also worth noting that, when looking at the percentage increase of the NNP specimens between 28 and 90 days, CC2 and FBC1 mixtures had a similar low increase, concrete with NP3 had a considerable increase, and GBA3 specimens had the highest. As mentioned earlier, GBA3 specimens had the lowest compressive strength at 7 days amongst all specimens but at 90 days that is no longer the case. This confirms that mixtures with GBA3 needed more time to develop more strength and that the strength development happens relatively quickly since it meets and exceeds the compressive strength of the reference mixture at different ages. These results follow the same trend of mortar (a significant increase after 7 days) and correlate to the compressive strength shown by each group.

Overall, the compressive strength of mixtures containing NNPs was either higher than or comparable to, the compressive strength of the reference mixture. At 90 days, the highest strength was observed in mixtures with the CC2 material whereas the lowest was observed in mixtures with FBC1 material.

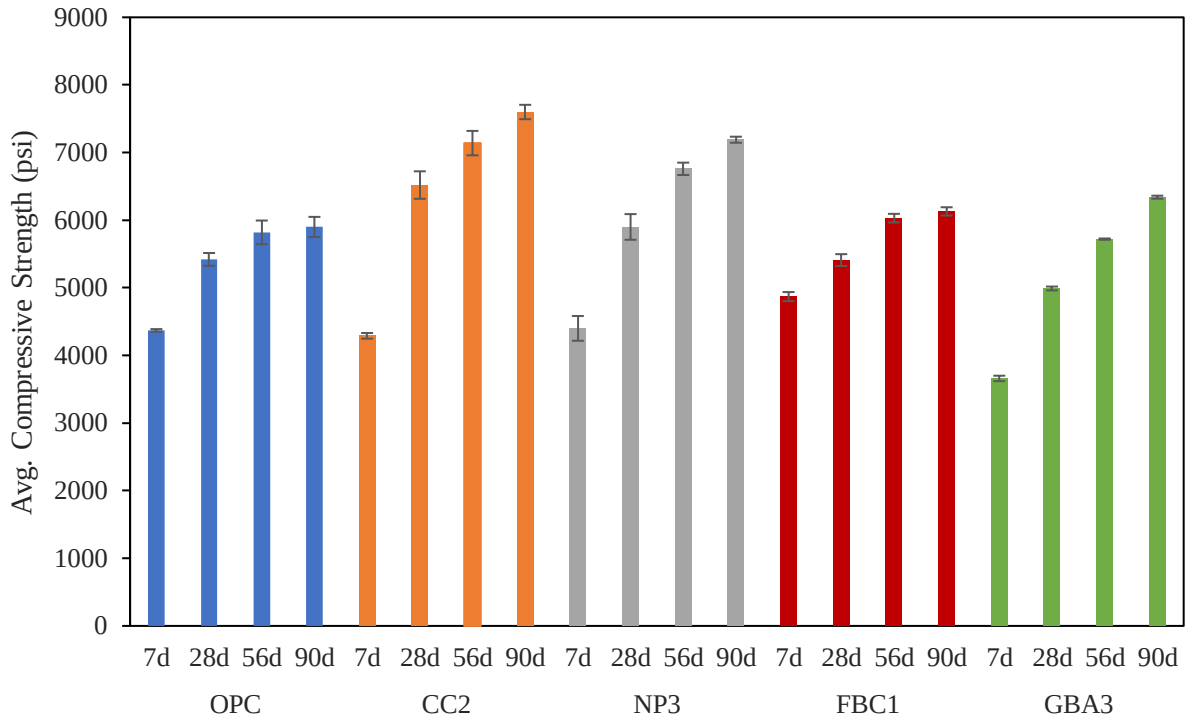

Figure 6.2. Average values of compressive strength for all concretes at different ages – (25% weight replacement of cement by NNPs).

Table 6.7. Average values of compressive strength for all concretes (25% weight replacement of cement by NNPs).

Mixture	Slump (in.)	Air Content (%)	Avg. Comp. Strength at 28 days (psi)	Avg. Comp. Strength at 90 days (psi)	% increase between 28 and 90 days avg. comp. strength (%)
Reference	2.25	7.7	5420	5900	8.86
CC2	1.00	6.2	6520	7600	16.56
NP3	1.00	5.4	5900	7190	21.86
FBC1	3.00	5.8	5410	6130	13.31
GBA3	1.75	5.7	4990	6340	27.05

The 28-day flexural strength results for plain concrete and concretes with all four NNPs used in this study are summarized in Figure 6.3 and Table 6.8. It can be seen that specimens with three of the four NNPs used in the study developed flexural strength either comparable to or

higher, than the flexural strength of the reference mixture. The only mixture with flexural strength slightly lower than the reference concrete was the one containing CC2 material. In contrast, the mixture with the highest flexural strength was the one containing GBA3 material, closely followed by mixtures with NP3, and FBC1 materials. Just as the compressive strength that was previously obtained for cylinders, the flexural strength of beams with SCMs is close to that of the reference mixture. One possible explanation as to why the flexural strength results do not follow a trend similar to that of compressive strength results could be due to the difference in air content among the specimens. Furthermore, the average flexural strength of the five specimens lay within 15 - 22% of the average compressive strength obtained from the cylinders. Literature has shown that flexural strength is about 10 – 20% of compressive strength if a similar size and volume of coarse aggregate is used [102]. Therefore, the flexural strength results indicated a comparatively well performance to the percent of compressive strength at 28 days.

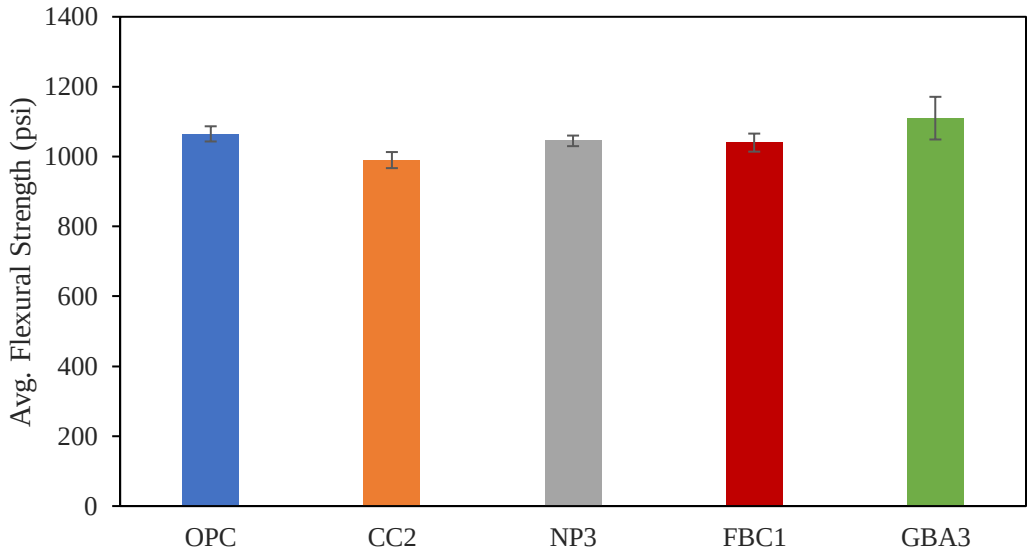

Figure 6.3. Average values of flexural strength for all concretes at 28days – (25% weight replacement of cement by NNPs).

Table 6.8. Average values of flexural strength for all concretes (25% weight replacement of cement by NNPs).

Mixture	Slump (in.)	Air Content (%)	Avg. Flexural Strength at 28 days (psi)	% of the avg. comp. strength at 28 days (psi)
Reference	2.25	7.1	1065	19.65
CC2	1.50	7.5	990	15.18
NP3	1.50	7.5	1045	17.80
FBC1	1.00	5.1	1040	19.22
GBA3	1.00	5.4	1110	22.25

6.4.2 Effect of NNPs on the Transport Properties Performance of Concrete

As can be seen from the data presented in Figure 6.4 and Table 6.9, at 14 days mixes with GBA3, NP3, and FBC1 materials had a formation factor comparable to that of the reference mixture. At this age, only specimens with CC2 had a higher formation factor than the reference mix. This trend continues at 21 days for almost all specimens except for NP3 specimens, since its formation factor was higher than the reference specimen. Between 21 and 28 days, there is a noticeable increase in formation factor for CC2 and NP3 mixtures. Also, formation factors for GBA3 and FBC1 mixtures were comparable to each other at this age. The highest increase in the formation factor was seen for CC2, NP3, and GBA3 specimens between 28 and 56 days. At 56 days, all materials except for FBC1 had a higher formation factor than the reference material. At 91 days, the formation factors for CC2, GBA3, and NP3 mixtures were considerably higher than the formation factor of the reference mix whereas the formation factor of the FBC1 mixture was only slightly higher than that of the reference mixtures. Not only that but the formation factor for the reference material plateaued while the other formation factors for all four NNP mixtures kept increasing.

Two limits can also be seen in Figure 6.4. According to the standard, the limit at 500 represents concrete not subjected to freezing and thawing or deicers applications. The limit at 1000 represents concrete subjected to freezing and thawing or deicers applications. There were three NNP mixtures (CC2, NP3, and GBA3) that had a higher formation factor than 1000 at 91

days. On the other hand, FBC1 and the reference specimens were lower. The elevated formation factor shown by CC2, NP3, and GBA3 specimens indicated a slower transport through the pore system.

At the end of the test, mixtures with NP3 material had the highest formation factor amongst all NNPs, followed by mixtures with CC2, GBA3, and FBC1.

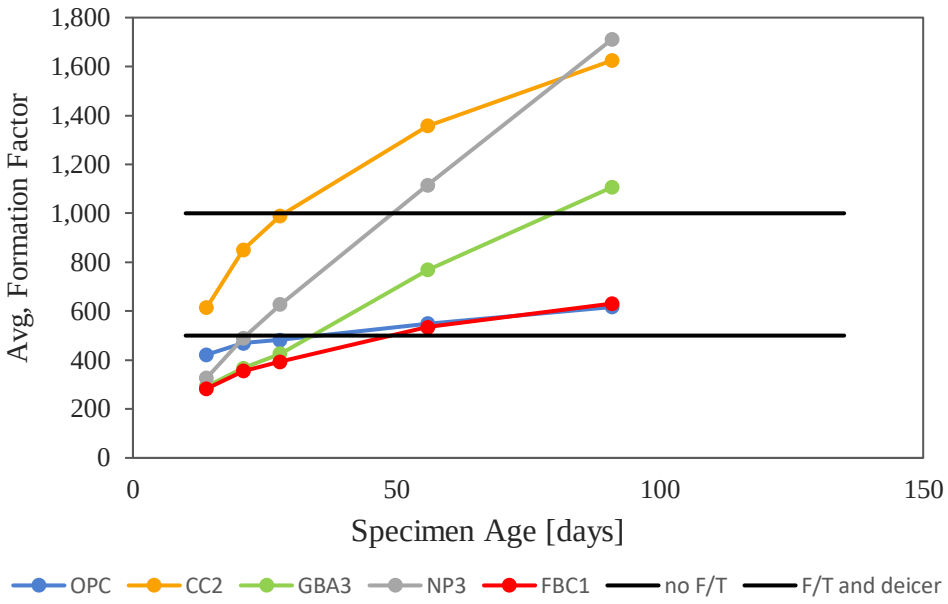

Figure 6.4. Change in the average values of Formation Factor for all concretes as a function of time (25% weight replacement of cement by NNPs).

Table 6.9. Avg. values of formation factor of all concretes (25% weight replacement of cement by NNPs).

Mixture	Age (d)	Avg. Bulk Resistivity (Ωm)	Avg. Formation Factor
Reference	14	53.6	422
	21	59.5	469
	28	61.3	482
	56	69.7	549
	91	78.3	617
CC2	14	78.1	615
	21	108.0	851
	28	125.8	990
	56	172.5	1358
	91	206.4	1625
GBA3	14	37.1	292
	21	46.6	367
	28	54.0	426
	56	97.6	769
	91	140.6	1107
NP3	14	41.6	327
	21	62.3	490
	28	79.7	627
	56	141.7	1115
	91	217.5	1712
FBC1	14	36	283
	21	45.1	355
	28	50.0	394
	56	67.9	535
	91	80.1	631

The results for ASTM C1585-20 and DIN 52617 can be found in Figure 6.5 - Figure 6.8 and Table 6.10 - Table 6.11. It can be seen that the ASTM C1585-20 conditioning method does not do a sufficient job of emptying the pores in the specimens. This is because, when comparing both methods, DIN 58267 has both a higher initial and secondary absorption. For instance, when examining Figure 6.5, all specimens had a ~3 times higher absorption in the first 6 hours of the tests using the conditioning method in DIN 52617 instead of ASTM C1585-20. Adding to this, the R^2 correlation in most cases increased (and sometimes it helped meet the threshold of 0.98) when using the conditioning method in DIN52617 when compared to ASTM C1585-20. This can be seen in Figure 6.9. Since the conditioning method in DIN 52617 emptied the pores more

appropriately, moving forward the results to be discussed will only be those from DIN 52617 (noted as ‘material ii.’ in the graphs and table).

Of the four NNPs used in the study, specimens with CC2, and NP3 material had a lower initial absorption than the reference specimen while the absorptions of specimens with FBC1 and GBA3 materials were higher. When comparing amongst SCMs, specimens with CC2 had the lowest initial absorption while the initial absorption of specimens with FBC1 was the highest (see Figure 6.5). The same trends were observed in the secondary absorption. Mixtures with CC2 and NP3 had a lower secondary absorption than the reference specimen whereas secondary absorptions of mixtures with FBC1 and GBA3 were higher (See Figure 6.6).

As for the initial rate of absorption, of the four NNPs, both CC2 and NP3 specimens had the lowest initial rate of absorption while concrete with GBA3 material had the highest (see Figure 6.7). This is reasonable since as discussed before, the same trend is observed for the initial absorption of the specimens. For the secondary rate of absorption, NP3 material had the lowest secondary rate of absorption and GBA3 material had the highest (see Figure 6.8). Again, this made sense since all mixtures with these materials behaved almost identical when looking at the secondary absorption of the specimens. In short, both initial and secondary rates of absorption helped visualize that the relative changes in the values of initial and secondary absorption over time had a similar trend for all materials.

Overall, CC2 and NP3 were the best performing material among the four NNPs, the performance of mixtures with FBC1 materials were comparable to the performance of the reference material, and the performance of mixtures with GBA3 material was of the lowest quality. Even with the GBA3 material being the lowest performance, it was not too far off the performance of the reference material.

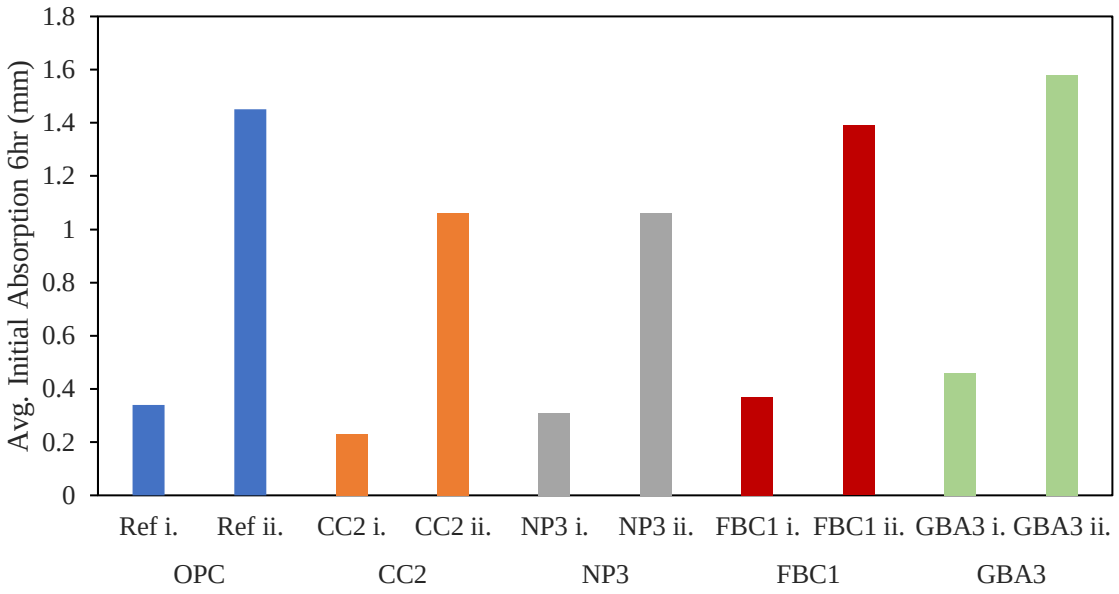

Figure 6.5. Avg. Initial absorption following ASTM C1585-20 (i.) and DIN 52617 (ii.) for all materials – (25% weight replacement of cement by NNPs).

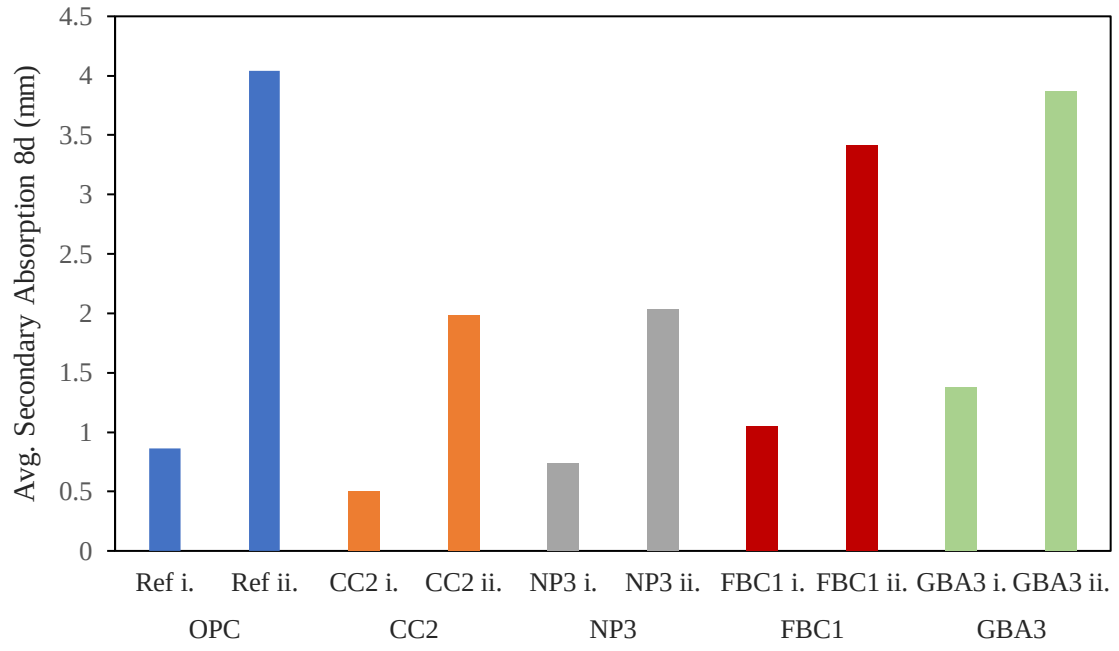

Figure 6.6. Avg. Secondary absorption following ASTM C1585-20 (i.) and DIN 52617 (ii.) for all materials – (25% weight replacement of cement by NNPs).

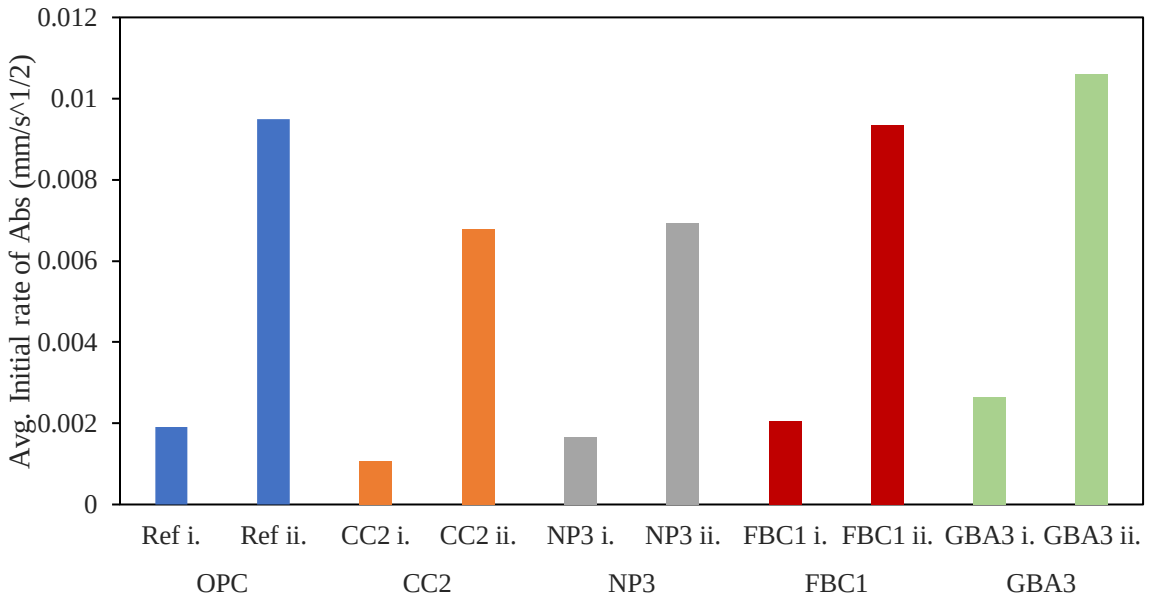

Figure 6.7. Avg. Initial rate of absorption following ASTM C1585-20 (i.) and DIN 52617 (ii.) for all materials – (25% weight replacement of cement by NNPs).

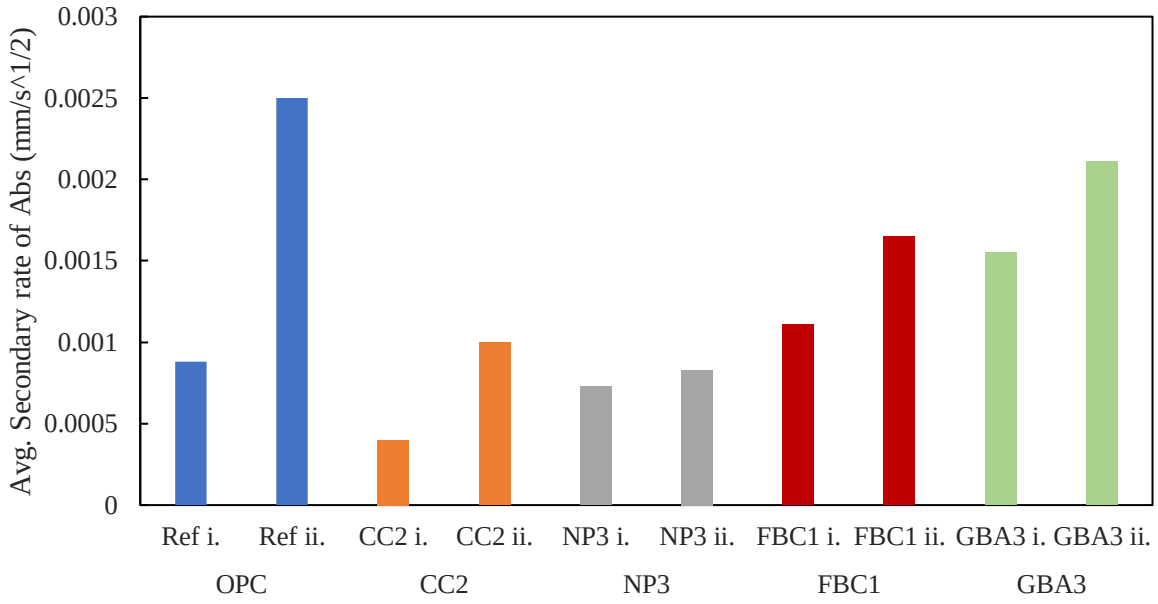

Figure 6.8. Average values of the secondary rate of absorption for concretes conditioned according to the ASTM C1585-20 (i) and DIN 52617-87 (ii) for all materials – (25% weight replacement of cement by NNPs).

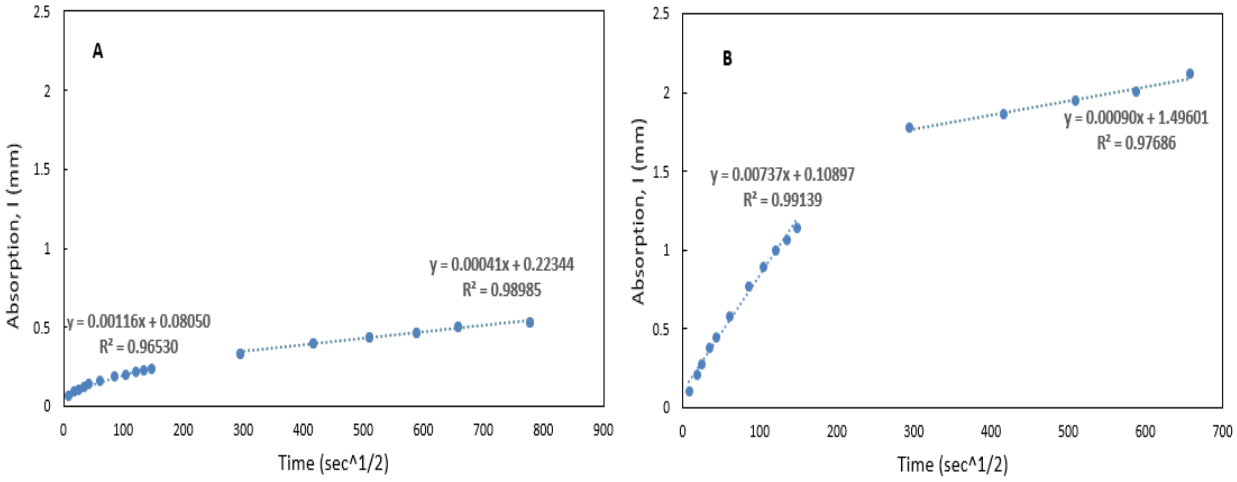

Figure 6.9. Absorption values for a CC2 concrete specimen conditioned according to the ASTM C1585-20 method (A) and absorption values for a CC2 concrete specimen conditioned using the DIN 52617-87 method (B) – (25% weight replacement of cement by NNPs).

Table 6.10. The ASTM C1585-20 rate of absorption results for concrete specimens

Mixture	Avg. Initial Rate of Absorption (x10^-4 mm/s^1/2)	Avg. Initial Absorption (mm)	Avg. Secondary Rate of Absorption (x10^-4 mm/s^1/2)	Avg. Secondary Absorption (mm)	Air Content (%)
Reference i.	19.1	0.34	8.8	0.86	7.6
CC2 i.	10.7	0.23	4.0	0.51	7.8
NP3 i.	16.7	0.31	7.3	0.74	6.0
FBC1 i.	20.6	0.46	9.4	1.01	5.5
GBA3 i.	26.4	0.38	15.5	1.37	5.1

Table 6.11. The DIN 52617-87 rate of absorption results for concrete specimens (25% weight replacement of cement by NNPs).

Mixture	Avg. Initial Rate of Absorption (x10^-4 mm/s^1/2)	Avg. Initial Absorption (mm)	Avg. Secondary Rate of Absorption (x10^-4 mm/s^1/2)	Avg. Secondary Absorption (mm)	Air Content (%)
Reference ii.	94.4	1.45	25.0	4.04	7.6
CC2 ii.	67.9	1.06	10.0	1.98	7.8
NP3 ii.	69.4	1.06	8.3	2.03	6.0
FBC1 ii.	93.6	1.39	16.5	3.41	5.5
GBA3 ii.	106.1	1.58	21.1	3.87	5.1

6.4.3 Effect of NNPs on Scaling Performance of Concrete

Results and visual appearances of the slabs at different FT cycles can be found in Figure 6.10-Table 6.11 and Table 6.12. As can be seen from the data presented in Table 6.12, the total average mass loss observed in the reference mix was only 0.19% and the slabs had an average value of visual rating of 2. Among the groups of samples containing NNPs, slabs with CC2 performed the best (average mass loss of 0.63% and average visual rating of 3). It should be pointed out that CC2-containing mixtures also developed the highest values of compressive strength. The slabs containing FBC1 material were the second-best performing, with an average mass loss of 1.24% and an average visual rating of 4. Slabs with GBA3 behave very similarly, with an average weight loss of 1.42% and an average visual rating of 4.5. The slabs containing NP3 performed worst, experiencing high (~3%) mass loss and severe scaling (average visual rating of 5). That high degree of scaling was already visible after the first 15 FT cycles. That behavior does not correlate well with the strength of the same mixtures as (when compared at 28 days) NP3 mixtures were stronger than (or comparable) to FBC1, GBA3, and reference mixtures.

Figure 6.12 illustrates the trend of the slabs over time after each cycle. Slabs with the NNPs (except for GBA3) experience higher mass loss during the first 15 FT cycles than during the remaining 35 FT cycles. Out of the four materials, it can be observed that CC2 specimens had similar behavior to the reference slabs since, after the first 15 FT cycles, the mass loss plateaued for both materials. After the first 15 FT cycles, FBC1 slabs showed a decrease in the rate of mass loss over time but the rate remained constant as there was an increase in the mass

loss until 50 FT cycles. For the GBA3 slabs, after the first 5 FT cycles, the rate of mass loss over time was constant until 50 FT cycles. It appears that GBA3 slabs had a lower rate of mass loss than FBC1 slabs. From the trend of both materials, FBC1 slabs might surpass the total mass loss of GBA3 slabs after additional FT cycles. Lastly, the NP3 slabs experienced the most mass loss after the first 10 FT cycles and onwards. The rate of mass loss started to decrease over time, more specifically at 20 FT cycles, but the slabs still lost a considerable amount of mass during the following FT cycles.

To have a greater assessment if these NNPs could potentially be implemented, the total mass loss was compared against the MTO maximum limit of mass loss at 50 FT cycles (See Figure 6.13). All four NNPs did not meet the threshold of the MTO maximum limit (0.8 kg/m^2). In fact, the only NNP close to meeting the limit was CC2 with 1.14 kg/m^2 mass loss at 50 FT cycles. The other NNPs were further away from the MTO limit. Both FBC1 and GBA3 had ~3 times the MTO limit while NP3 had ~7 times the MTO limit at 50 cycles.

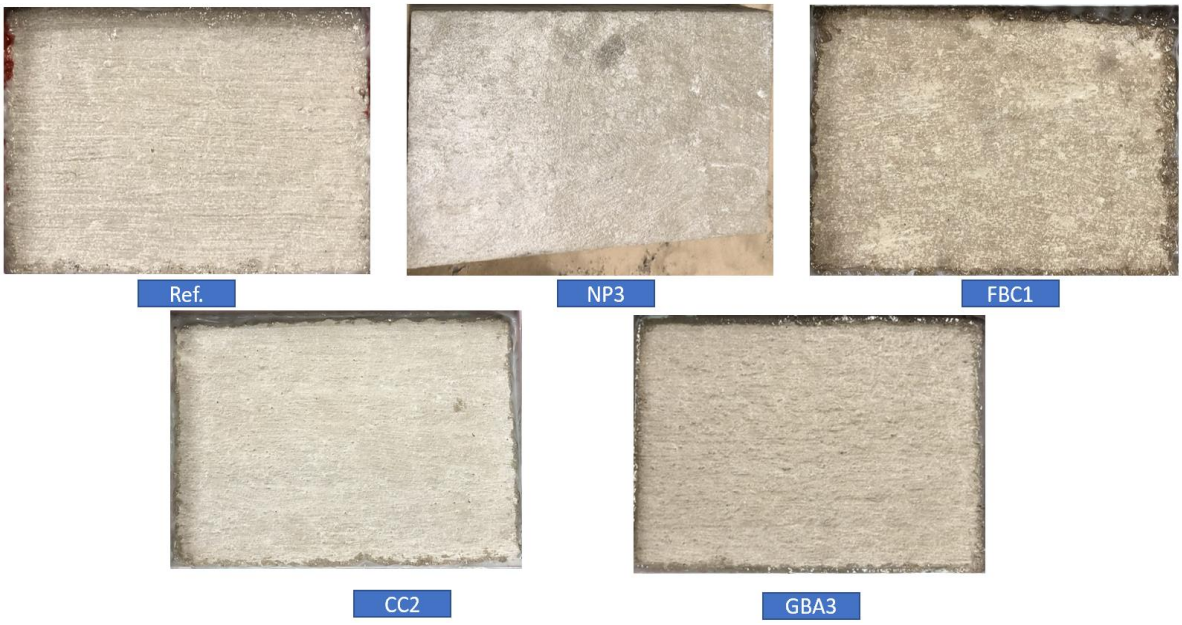

Figure 6.10. Visual appearance of the surfaces of the slabs before initiation of the scaling test (i.e. at zero FT cycles) – 25% weight replacement of cement by NNPs.

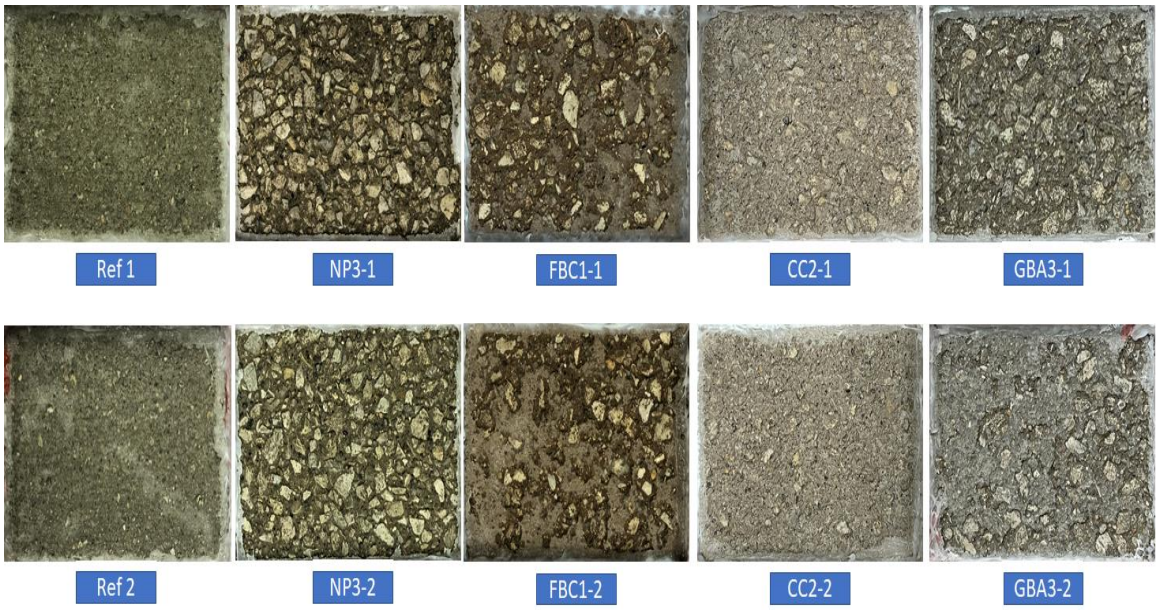

Figure 6.11. The visual appearance of the scaling slabs after 50 FT cycles (25% weight replacement of cement by NNPs).

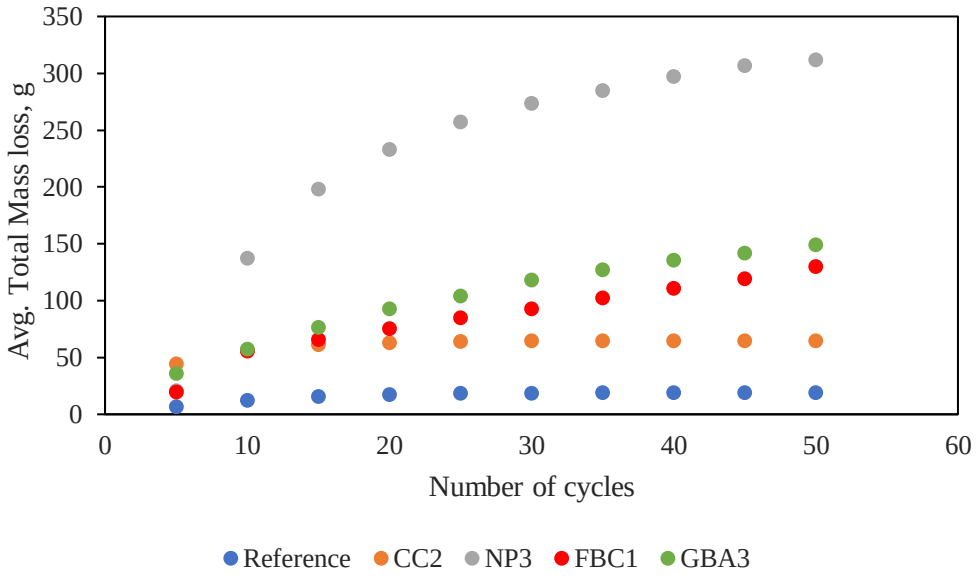

Figure 6.12. Total mass loss for the worst-performing slab of each concrete at different number of cycles – (25% weight replacement of cement by NNPs).

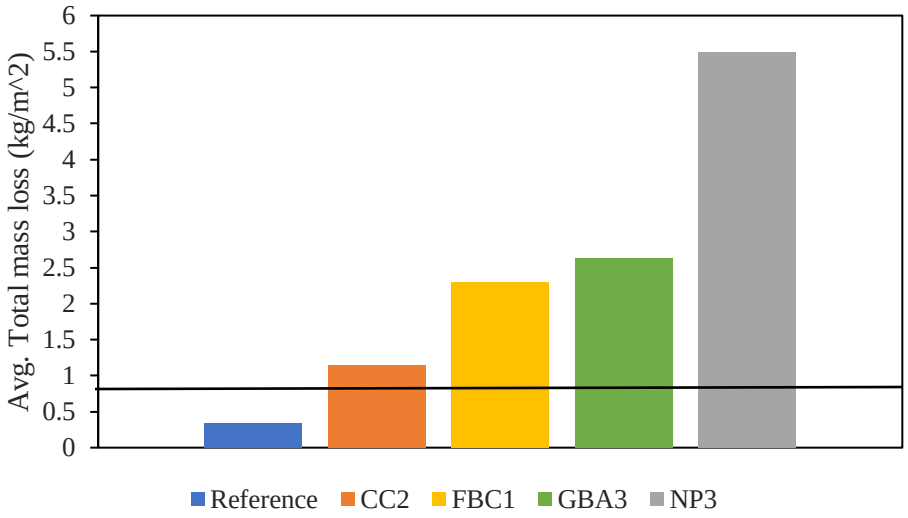

Figure 6.13. Total mass loss after 50 FT cycles for the worst-performing slab of each concrete (25% weight replacement of cement by NNPs). The horizontal line represents the MTO threshold limit (0.8 kg/m^2) of mass loss after 50 FT cycles.

Table 6.12. Average values of scaling test results (mass losses and visual rating) after 50 FT cycles. 25% weight replacement of cement by NNPs.

Mixture	Slump (in.)	Air Content (%)	Avg. Mass Loss (kg/m^2)	Avg. Mass Loss (%)	Avg. Visual Rating
Reference	1.50	6.4	0.34	0.19	2
CC2	1.75	7.4	1.14	0.63	3
NP3	1.00	6.1	5.49	2.97	5
FBC1	1.00	5.5	2.29	1.24	4
GBA3	1.75	5.8	2.63	1.42	4.5

6.5 Conclusions

Based on the results presented in this chapter, the following conclusions can be drawn:

- The properties of all concrete specimens containing NNPs described in this chapter were either comparable or improved when compared to the properties of the OPC-only concrete. The only exception was the scaling resistance. In this case, concretes with NNPs performed worse than the OPC concretes. It should be noted, however, that an inferior (compared to

OPC mixtures) scaling resistance of concretes with traditional pozzolans, such as fly ash or slag cement, has been widely reported in the past and thus this phenomenon is not unique to NNPs used in this study,

- When tested after 28 days of curing, all NNP concretes described in this section achieved compressive strengths comparable to the strength of the reference (OPC-only) concrete. However, when tested after 56 and 90 days of curing, all NNPs concreted achieved compressive strengths that were higher than that of the OPC concretes.
- The percent increase in compressive strength between 28 and 90 days was also significantly higher for all NNP concretes than for the OPC concrete. The observed late-age strength increases were particularly high for NP3 and GBA3 mixes.
- The 28 days flexural strength of all NNP concretes were comparable and were roughly the same as the flexural strength of the OPC concrete.
- The 91-day values of the formation factor for concretes with three of the four NNPs used (NP3, CC2, and GBA3) were higher than the formation factor of the reference concrete. These trends correlate well with trends observed for the results of the secondary water absorption as concretes with CC2 and NP3 materials were found to be best performing in both tests while concretes with the FBC1 and GBA3 materials showed a similarly decreased rate of performance in both tests.
- Based on the secondary absorption and formation factor results, concretes containing CC2, NP3, FBC1, and GBA3 demonstrated to have either a lower or comparable pore degree of pore connectivity to that of the plain concrete
- All slabs with NNPs described in this chapter showed signs of significant surface deterioration after 50 cycles of freezing and thawing. Longer curing in lime saturated water could potentially improve the scaling resistance of concretes containing these materials.
- Based on the results of all experiments performed in this chapter, the ranking from ‘best’ to ‘worst’ performing NNPs is as follows CC2>NP3>GBA3> FBC1.

7. GENERAL FINDINGS AND CONCLUSIONS

Finding alternative sources of supplementary cementitious materials (SCMs) is critical with respect to addressing potential supply shortage of traditional pozzolanic materials, such as fly ash and slag cement, and reducing the CO_2 emissions caused by the concrete industry. The first part of this study focused on the evaluation of the influence of 11 different natural and non-traditional pozzolans (NNPs) on both, fresh and hardened properties of mortars. The mortar mixes were prepared using either the ordinary portland cement (OPC), for reference mortar, or a binary binder system in which part of the cement was replaced with varying levels (25%, 30%, or 35% by weight of total cementitious materials) of cement replacement by each of the 11 NNPs.

The NNPs which, when compared to other materials of the same type, showed the lowest reactivity, and thus reduced level of performance in the mortar's study were subsequently selected to be used in the concrete study (at the 25% cement replacement level). The selected materials included the following: CC2, NP3, FBC1, and GBA3. In making this selection, it was assumed that the chosen materials represent the "worst-case scenario with respect to the ability to produce concrete with acceptable performance characteristics in both, fresh and hardened states. However, if concrete with satisfactory properties could be produced using these types of materials, it will imply that NNPs which performed better in the mortar tests could be used to produce concreters with truly excellent characteristics.

The general findings of this study could be summarized as follows:

- Nine out of the eleven NNPs used in the study were found to conform to the requirements of the ASTM C618-19, which is the standard specification for fly ash and raw or calcined natural pozzolans for use in concrete.
- When used at the 25% replacement levels, all NNPs produced mortars with performance characteristics comparable to, or better than, those observed in the OPC mortars. These findings imply that 25% is, at least with respect to properties evaluated in this study, close to the optimum replacement level for these types of materials.
- The "best-performing" NNPs, in terms of reactivity and both fresh and hardened properties of mortars, were CC3, NP2, FBC2, and GBA1. In contrast, the "worst-performing" materials were CC2, NP3, FBC1, and GBA3.

- Despite showing the lowest levels of performance in mortar systems, when used at 25% replacement levels, all four of these NNPs (i.e. CC2, NP3, FBC1, and GBA3) produced concretes with properties comparable to, or better, than those of the OPC-only concretes.
- All types of NNPs contributed to the improvement of properties of mortars and concretes, especially at later ages.
- Considering all properties of mortars and concretes, of the four groups of materials tested CCs were found to be the best performing group (with the exception of the workability of mortars with CC1), followed by, respectively, NPs, GBAs, and FBCs

APPENDIX

Sample Calculations:

- The calculation for the air content of CC2 25% replacement (mortar)
    - Determination of Density:

$$D = \frac{M - C}{V_c} = \frac{1605.8\ g - 720.4\ g}{400\ mL} = 2.2135 \frac{g}{mL}$$

Where:

D= Density, g/mL,

M= mass of mortar and cup, g,

C= mass of empty cup, g,

V_c= measure volume of the cup, mL

    - Determination of total mass batched:

$$W1 = C + P + S + W = 1012.5g + 337.5g + 2295g + 567g = 4212g$$

Where:

W1= total mass of materials batched, g,

C= cement, g,

P= SCM, g,

S= sand, g,

W= water, g,

    - Determination of volume of mortar batched:

$$\text{volume of mortar in the batch} = \frac{W1}{D} = \frac{4212\ g}{2.2135 \frac{g}{mL}} = 1902.869mL$$

    - Determination of absolute volume of all materials batched

$$absolute\ volume\ of\ all\ materials\ batched$$

$$= \frac{C}{S.G\ of\ cement} + \frac{P}{S.G.\ of\ P} + \frac{S}{S.G.ofS} + \frac{W}{S.G.of\ W}$$

$$= \frac{1012.5\ g}{3.15} + \frac{337.5g}{2.75} + \frac{2295g}{2.74} + \frac{567g}{1} = 1848.747\ mL$$

- Determination of air content:

$$Air\ Content = \frac{Volume\ of\ mortar - Abs.\ volume\ of\ all\ materials}{Volume\ of\ mortar} * 100\%$$

$$= \frac{1902.869mL\ - 1848.747\ mL}{1902.869mL} * 100 = \mathbf{2.84}\%$$

- Setting time of GBA3 20% replacement (mortar), using Eq. 5-2:

$$Log(time) = \frac{Log(Penetration\ Resistance) - a}{b} = initial\ set = 10^{(\log(500)-(-10.454))/5.7211}$$

$$= 199\ min$$

Where:

penetration resistance = 500 (4000 for final set)

a= -10.454 (y-intercept of Figure A-1)

b= 5.7211 (slope of Figure A-1)

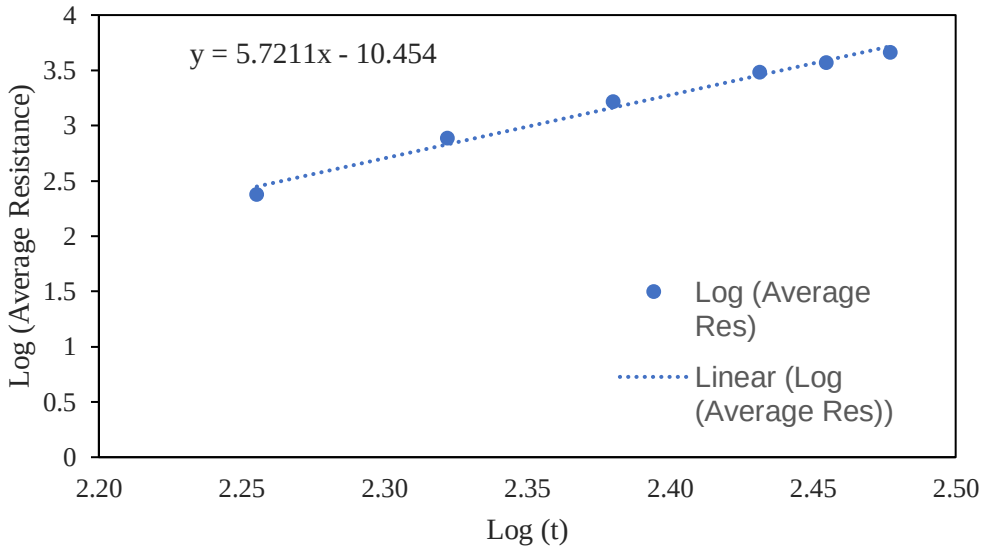

Figure A-1. Log. Resistance of GBA3 at 25% replacement level at different Log. Time.

REFERENCES

[1] "CEMBUREAU Activity Report 2020," 2020.

[2] "Cement – Analysis - IEA." https://www.iea.org/reports/cement

[3] C. Chen, G. Habert, Y. Bouzidi, and A. Jullien, "Environmental impact of cement production: detail of the different processes and cement plant variability evaluation," *Journal of Cleaner Production*, vol. 18, no. 5, pp. 478–485, Mar. 2010, doi: 10.1016/J.JCLEPRO.2009.12.014.

[4] R. M. Andrew, "Global CO2 emissions from cement production, 1928–2017," *Earth System Science Data*, vol. 10, no. 4, pp. 2213–2239, Dec. 2018, doi: 10.5194/essd-10-2213-2018.

[5] M. S. Imbabi, C. Carrigan, and S. McKenna, "Trends and developments in green cement and concrete technology," *International Journal of Sustainable Built Environment*, vol. 1, no. 2, pp. 194–216, Dec. 2012, doi: 10.1016/J.IJSBE.2013.05.001.

[6] A. Favier, C. de Wolf, K. Scrivener, and G. Habert, "A sustainable future for the European Cement and Concrete Industry," 2018, doi: 10.3929/ETHZ-B-000301843.

[7] K. M. Rahla, R. Mateus, and L. Bragança, "Comparative sustainability assessment of binary blended concretes using Supplementary Cementitious Materials (SCMs) and Ordinary Portland Cement (OPC)," *Journal of Cleaner Production*, vol. 220, pp. 445–459, May 2019, doi: 10.1016/J.JCLEPRO.2019.02.010.

[8] K. H. Yang, Y. B. Jung, M. S. Cho, and S. H. Tae, "Effect of supplementary cementitious materials on reduction of CO2 emissions from concrete," *Journal of Cleaner Production*, vol. 103, pp. 774–783, Sep. 2015, doi: 10.1016/J.JCLEPRO.2014.03.018.

[9] S. A. Miller, "Supplementary cementitious materials to mitigate greenhouse gas emissions from concrete: can there be too much of a good thing?," *Journal of Cleaner Production*, vol. 178, pp. 587–598, Mar. 2018, doi: 10.1016/J.JCLEPRO.2018.01.008.

[10] "The GCCA 2050 Cement and Concrete Industry Roadmap for Net Zero Concrete." https://gccassociation.org/concretefuture/

[11] "Roadmap to Carbon Neutrality." https://www.cement.org/sustainability/roadmap-to-carbon-neutrality

[12] “ASTM C618-19 - Standard Specification for Coal Fly Ash and Raw or Calcined Natural Pozzolan for Use in Concrete,” *ASTM Int.*, 2019, doi: 10.1520/C0618-19.

[13] American Road & Transportation Builders Association, “Production and use of coal combustion products in the U.S.; Market forecast through 2033,” 2015.

[14] American Coal Ash Association, “Fly Ash Use in Concrete Increases Slightly As Overall Coal Ash Recycling Rate Declines,” 2020.

[15] K. Scrivener, V. John, and E. Gartner, “United Nations Environment Programme Eco-efficient Cements: Potential Economically Viable Solutions for a Low-CO2 Cement-based Materials Industry.,” *https://wedocs.unep.org/20.500.11822/25281*.

[16] T. R. Naik and B. W. Ramme, “High Early Strength Concrete Containing Large Quantities of Fly Ash”.

[17] “Effect of Silica Fume on Workability and Compressive Strength of OPC Concrete,” *Journal of Environmental Nanotechnology*, vol. 3, no. 3, pp. 32–35, Sep. 2014, doi: 10.13074/JENT.2014.09.143086.

[18] J. Ahmad *et al.*, “Coconut Husk Ash (CHA), Palm Oil Fuel Ash (POFA), Wood Waste Ash (WWA), Sugar Cane Bagasse Ash (SCBA), Corn Cob Ash (CCA)”, doi: 10.1088/1757-899X/640/1/012071.

[19] W. M. Hale, S. F. Freyne, T. D. Bush, and B. W. Russell, “Properties of concrete mixtures containing slag cement and fly ash for use in transportation structures,” *Construction and Building Materials*, vol. 22, no. 9, pp. 1990–2000, Sep. 2008, doi: 10.1016/J.CONBUILDMAT.2007.07.004.

[20] G. A. Rao, “Investigations on the performance of silica fume-incorporated cement pastes and mortars,” *Cement and Concrete Research*, vol. 33, no. 11, pp. 1765–1770, Nov. 2003, doi: 10.1016/S0008-8846(03)00171-6.

[21] P. Choi, J. H. Yeon, and K. K. Yun, “Air-void structure, strength, and permeability of wet-mix shotcrete before and after shotcreting operation: The influences of silica fume and air-entraining agent,” *Cement and Concrete Composites*, vol. 70, pp. 69–77, Jul. 2016, doi: 10.1016/J.CEMCONCOMP.2016.03.012.

[22] Z. Liu, S. El-Tawil, W. Hansen, and F. Wang, “Effect of slag cement on the properties of ultra-high performance concrete,” *Construction and Building Materials*, vol. 190, pp. 830–837, Nov. 2018, doi: 10.1016/J.CONBUILDMAT.2018.09.173.

[23] G. A. Rao, “Investigations on the performance of silica fume-incorporated cement pastes and mortars,” *Cement and Concrete Research*, vol. 33, no. 11, pp. 1765–1770, Nov. 2003, doi: 10.1016/S0008-8846(03)00171-6.

[24] R. Siddique and N. Chahal, “Use of silicon and ferrosilicon industry by-products (silica fume) in cement paste and mortar,” *Resources, Conservation and Recycling*, vol. 55, no. 8, pp. 739–744, Jun. 2011, doi: 10.1016/J.RESCONREC.2011.03.004.

[25] D. Ravina and P. K. Mehta, “Properties of fresh concrete containing large amounts of fly ash,” *Cement and Concrete Research*, vol. 16, no. 2, pp. 227–238, Mar. 1986, doi: 10.1016/0008-8846(86)90139-0.

[26] Y. K. Cho, S. H. Jung, and Y. C. Choi, “Effects of chemical composition of fly ash on compressive strength of fly ash cement mortar,” *Construction and Building Materials*, vol. 204, pp. 255–264, Apr. 2019, doi: 10.1016/J.CONBUILDMAT.2019.01.208.

[27] A. A. Ramezanianpour and V. M. Malhotra, “Effect of curing on the compressive strength, resistance to chloride-ion penetration and porosity of concretes incorporating slag, fly ash or silica fume,” *Cement and Concrete Composites*, vol. 17, no. 2, pp. 125–133, Jan. 1995, doi: 10.1016/0958-9465(95)00005-W.

[28] R. Duval and E. H. Kadri, “Influence of Silica Fume on the Workability and the Compressive Strength of High-Performance Concretes,” *Cement and Concrete Research*, vol. 28, no. 4, pp. 533–547, Apr. 1998, doi: 10.1016/S0008-8846(98)00010-6.

[29] M. Potha Raju, M. Shobha, and K. Rambabu, “Flexural strength of fly ash concrete under elevated temperatures,” *Magazine of Concrete Research*, vol. 56, no. 2, pp. 83–88, May 2004, doi: 10.1680/MACR.2004.56.2.83/ASSET/IMAGES/SMALL/MACR56-083-F5.GIF.

[30] R. Siddique, “Utilization of silica fume in concrete: Review of hardened properties,” *Resources, Conservation and Recycling*, vol. 55, no. 11, pp. 923–932, Sep. 2011, doi: 10.1016/J.RESCONREC.2011.06.012.

[31] S. Bhanja and B. Sengupta, “Influence of silica fume on the tensile strength of concrete,” *Cement and Concrete Research*, vol. 35, no. 4, pp. 743–747, Apr. 2005, doi: 10.1016/J.CEMCONRES.2004.05.024.

[32] A. J. Jeya arthi, M. Hemavathy, and M. Gouthampriya, “Partial Replacement Of Cement By Ground Granulated Blast-Furnace Slag In Concrete,” *J Arch.Egyptol*, vol. 17, no. 7, pp. 10021–10029, Nov. 2020.

[33] Ph. D. P. Kumar Mehta and Ph. D. Paulo J. M. Monteiro, *Concrete: Microstructure, Properties, and Materials*. McGraw-Hill Education, 2014. Accessed: Apr. 04, 2022. [Online]. Available: https://www.accessengineeringlibrary.com/content/book/9780071797870

[34] Jr. P. Kumar Mehta and Ben C. Gerwick, “Cracking-Corrosion Interaction in Concrete Exposed to Marine Environment,” *Concrete International*, vol. 4, no. 10.

[35] M. H. Shehata and M. D. A. Thomas, “The effect of fly ash composition on the expansion of concrete due to alkali–silica reaction,” *Cement and Concrete Research*, vol. 30, no. 7, pp. 1063–1072, Jul. 2000, doi: 10.1016/S0008-8846(00)00283-0.

[36] A. K. Saha, M. N. N. Khan, P. K. Sarker, F. A. Shaikh, and A. Pramanik, “The ASR mechanism of reactive aggregates in concrete and its mitigation by fly ash: A critical review,” *Construction and Building Materials*, vol. 171, pp. 743–758, May 2018, doi: 10.1016/J.CONBUILDMAT.2018.03.183.

[37] W. Aquino, D. A. Lange, and J. Olek, “The influence of metakaolin and silica fume on the chemistry of alkali–silica reaction products,” *Cement and Concrete Composites*, vol. 23, no. 6, pp. 485–493, Dec. 2001, doi: 10.1016/S0958-9465(00)00096-2.

[38] J. Duchesne and M. A. Bérubé, “The effectiveness of supplementary cementing materials in suppressing expansion due to ASR: Another look at the reaction mechanisms part 1: Concrete expansion and portlandite depletion,” *Cement and Concrete Research*, vol. 24, no. 1, pp. 73–82, Jan. 1994, doi: 10.1016/0008-8846(94)90084-1.

[39] C. M. Aldea, F. Young, K. Wang, and S. P. Shah, “Effects of curing conditions on properties of concrete using slag replacement,” *Cement and Concrete Research*, vol. 30, no. 3, pp. 465–472, 2000, doi: 10.1016/S0008-8846(00)00200-3.

[40] T. Naik, B. Ramme, R. N. Kraus, and R. Siddique, “Long-term performance of high-volume fly ash concrete pavements,” *ACI Materials Journal*, vol. 100, pp. 150–155, Mar. 2003.

[41] M. I. Khan and R. Siddique, “Utilization of silica fume in concrete: Review of durability properties,” *Resources, Conservation and Recycling*, vol. 57, pp. 30–35, Dec. 2011, doi: 10.1016/J.RESCONREC.2011.09.016.

[42] S. S. S. Tarun R. Naik And Bruce W. Ramme, “Mechanical Properties and Durability of Concrete Made with Blended Fly Ash,” *ACI Materials Journal*, vol. 95, no. 4, doi: 10.14359/388.

[43] R. Bleszynski, R. D. Hooton, M. D. A. , Thomas, and C. Rogers, “Durability of ternary blend concrete with silica fume and blast-furnace slag: laboratory and outdoor exposure site studies,” *ACI Materials Journal*, vol. 99, no. 5.

[44] R. Grim and H. Kodama, “clay mineral | Britannica.” https://www.britannica.com/science/clay-mineral/additional-info#contributors

[45] T. Danner, H. Justnes, G. Norden, and T. Østnor, “Feasibility of calcined marl as an alternative pozzolanic material,” *RILEM Bookseries*, vol. 10, pp. 67–73, 2015, doi: 10.1007/978-94-017-9939-3_9.

[46] M. Maier, N. Beuntner, and K. C. Thienel, “Mineralogical characterization and reactivity test of common clays suitable as supplementary cementitious material,” *Applied Clay Science*, vol. 202, p. 105990, Mar. 2021, doi: 10.1016/J.CLAY.2021.105990.

[47] R. Sposito, M. Maier, N. Beuntner, and K. C. Thienel, “Physical and mineralogical properties of calcined common clays as SCM and their impact on flow resistance and demand for superplasticizer,” *Cement and Concrete Research*, vol. 154, p. 106743, Apr. 2022, doi: 10.1016/J.CEMCONRES.2022.106743.

[48] R. S. Almenares, L. M. Vizcaíno, S. Damas, A. Mathieu, A. Alujas, and F. Martirena, “Industrial calcination of kaolinitic clays to make reactive pozzolans,” *Case Studies in Construction Materials*, vol. 6, pp. 225–232, Jun. 2017, doi: 10.1016/J.CSCM.2017.03.005.

[49] K. Jafari and F. Rajabipour, “Performance of Impure Calcined Clay as a Pozzolan in Concrete:,” *https://doi.org/10.1177/0361198120953140*, vol. 2675, no. 2, pp. 98–107, Nov. 2020, doi: 10.1177/0361198120953140.

[50] M. Antoni, J. Rossen, F. Martirena, and K. Scrivener, “Cement substitution by a combination of metakaolin and limestone,” *Cement and Concrete Research*, vol. 42, no. 12, pp. 1579–1589, Dec. 2012, doi: 10.1016/J.CEMCONRES.2012.09.006.

[51] K. Scrivener, F. Martirena, S. Bishnoi, and S. Maity, “Calcined clay limestone cements (LC3),” *Cement and Concrete Research*, vol. 114, pp. 49–56, Dec. 2018, doi: 10.1016/J.CEMCONRES.2017.08.017.

[52] S. Krishnan, D. Gopala Rao, and S. Bishnoi, “Why Low-Grade Calcined Clays Are the Ideal for the Production of Limestone Calcined Clay Cement (LC),” *RILEM Bookseries*, vol. 25, pp. 125–130, 2020, doi: 10.1007/978-981-15-2806-4_14.

[53] S. Krishnan and S. Bishnoi, “Understanding the hydration of dolomite in cementitious systems with reactive aluminosilicates such as calcined clay,” *Cement and Concrete Research*, vol. 108, pp. 116–128, Jun. 2018, doi: 10.1016/J.CEMCONRES.2018.03.010.

[54] B. Sabir, S. Wild, and J. Bai, “Metakaolin and calcined clays as pozzolans for concrete: a review,” *Cement and Concrete Composites*, vol. 23, no. 6, pp. 441–454, Dec. 2001, doi: 10.1016/S0958-9465(00)00092-5.

[55] G. P. Cordoba *et al.*, “Concretes with Calcined Clay and Calcined Shale: Workability, Mechanical, and Transport Properties,” *Journal of Materials in Civil Engineering*, vol. 32, no. 8, p. 04020224, May 2020, doi: 10.1061/(ASCE)MT.1943-5533.0003296.

[56] R. Bucher, P. Diederich, M. Mouret, G. Escadeillas, and M. Cyr, “Self-compacting concrete using flash-metakaolin: design method,” *Materials and Structures 2014 48:6*, vol. 48, no. 6, pp. 1717–1737, Feb. 2014, doi: 10.1617/S11527-014-0267-X.

[57] R. Gmür, K. C. Thienel, and N. Beuntner, “Influence of aging conditions upon the properties of calcined clay and its performance as supplementary cementitious material,” *Cement and Concrete Composites*, vol. 72, pp. 114–124, Sep. 2016, doi: 10.1016/J.CEMCONCOMP.2016.05.020.

[58] A. Joshaghani, M. A. Moeini, and M. Balapour, “Evaluation of incorporating metakaolin to evaluate durability and mechanical properties of concrete,” *Advances in concrete construction*, vol. 5, no. 3, pp. 241–255, Jun. 2017, doi: 10.12989/ACC.2017.5.3.241.

[59] S. E. Schulze and J. Rickert, “Suitability of natural calcined clays as supplementary cementitious material,” *Cement and Concrete Composites*, vol. 95, pp. 92–97, Jan. 2019, doi: 10.1016/J.CEMCONCOMP.2018.07.006.

[60] A. Játiva, E. Ruales, and M. Etxeberria, “Volcanic Ash as a Sustainable Binder Material: An Extensive Review,” *Materials 2021, Vol. 14, Page 1302*, vol. 14, no. 5, p. 1302, Mar. 2021, doi: 10.3390/MA14051302.

[61] R. Snellings, G. Mertens, and J. Elsen, “Supplementary Cementitious Materials,” *Reviews in Mineralogy & Geochemistry*, vol. 74, pp. 211–278, 2012, doi: 10.2138/rmg.2012.74.6.

[62] P. N. Lemougna *et al.*, “Review on the use of volcanic ashes for engineering applications,” *Resources, Conservation and Recycling*, vol. 137, pp. 177–190, Oct. 2018, doi: 10.1016/J.RESCONREC.2018.05.031.

[63] K. Kupwade-Patil *et al.*, “Microstructure of cement paste with natural pozzolanic volcanic ash and Portland cement at different stages of curing,” *Construction and Building Materials*, vol. 113, pp. 423–441, Jun. 2016, doi: 10.1016/J.CONBUILDMAT.2016.03.084.

[64] K. Kupwade-Patil *et al.*, “Impact of Embodied Energy on materials/buildings with partial replacement of ordinary Portland Cement (OPC) by natural Pozzolanic Volcanic Ash,” *Journal of Cleaner Production*, vol. 177, pp. 547–554, Mar. 2018, doi: 10.1016/J.JCLEPRO.2017.12.234.

[65] K. M. Anwar Hossain, “High strength blended cement concrete incorporating volcanic ash: Performance at high temperatures,” *Cement and Concrete Composites*, vol. 28, no. 6, pp. 535–545, Jul. 2006, doi: 10.1016/J.CEMCONCOMP.2006.01.013.

[66] R. Siddique, “Properties of concrete made with volcanic ash,” *Resources, Conservation and Recycling*, vol. 66, pp. 40–44, Sep. 2012, doi: 10.1016/J.RESCONREC.2012.06.010.

[67] H.-J. Feuerborn, “Workshop on Environmental and Health Aspects of Coal Ash Utilization International workshop 23 rd-24 th,” 2005.

[68] M. Zahedi and F. Rajabipour, “Fluidized Bed Combustion (FBC) fly ash and its performance in concrete,” *ACI Materials Journal*, vol. 116, no. 4, pp. 163–172, 2019, doi: 10.14359/51716720.

[69] P. Basu, “Combustion of coal in circulating fluidized-bed boilers: a review,” *Chemical Engineering Science*, vol. 54, no. 22, pp. 5547–5557, Nov. 1999, doi: 10.1016/S0009-2509(99)00285-7.

[70] E. J. Anthony and D. L. Granatstein, “Sulfation phenomena in fluidized bed combustion systems,” *Progress in Energy and Combustion Science*, vol. 27, no. 2, pp. 215–236, Jan. 2001, doi: 10.1016/S0360-1285(00)00021-6.

[71] D. Gazdič, M. Fridrichová, K. Kulísek, and L. Vehovská, “The Potential Use of the FBC Ash for the Preparation of Blended Cements,” *Procedia Engineering*, vol. 180, pp. 1298–1305, 2017, doi: 10.1016/J.PROENG.2017.04.292.

[72] J. Havlica, J. Brandstetr, and I. Odler, “Possibilities of utilizing solid residues from pressured fluidized bed coal combustion (PSBC) for the production of blended cements,” *Cement and Concrete Research*, vol. 28, no. 2, pp. 299–307, 1998, doi: 10.1016/S0008-8846(97)00258-5.

[73] R. Siddique, “Utilization of coal combustion by-products in sustainable construction materials,” *Resources, Conservation and Recycling*, vol. 54, no. 12, pp. 1060–1066, 2010, doi: 10.1016/J.RESCONREC.2010.06.011.

[74] R. Klein, T. Baumann, E. Kahapka, and R. Niessner, “Temperature development in a modern municipal solid waste incineration (MSWI) bottom ash landfill with regard to sustainable waste management,” *Journal of Hazardous Materials*, vol. 83, no. 3, pp. 265–280, May 2001, doi: 10.1016/S0304-3894(01)00188-1.

[75] C. Argiz, M. Á. Sanjuán, and E. Menéndez, “Coal Bottom Ash for Portland Cement Production,” *Advances in Materials Science and Engineering*, vol. 2017, 2017, doi: 10.1155/2017/6068286.

[76] M. Singh and R. Siddique, “Strength properties and micro-structural properties of concrete containing coal bottom ash as partial replacement of fine aggregate,” *Construction and Building Materials*, vol. 50, pp. 246–256, Jan. 2014, doi: 10.1016/J.CONBUILDMAT.2013.09.026.

[77] M. Cheriaf, J. C. Rocha, and J. Péra, “Pozzolanic properties of pulverized coal combustion bottom ash,” *Cement and Concrete Research*, vol. 29, no. 9, pp. 1387–1391, 1999, doi: 10.1016/S0008-8846(99)00098-8.

[78] S. Ali Mangi, M. H. Wan Ibrahim, N. Jamaluddin, M. F. Arshad, P. J. Ramadhansyah, and C. Khairpur Mir, “Effects of Ground Coal Bottom Ash on the Properties of Concrete,” *Journal of Engineering Science and Technology*, vol. 14, no. 1, pp. 338–350, 2019.

[79] C. Jaturapitakkul and R. Cheerarot, “Development of Bottom Ash as Pozzolanic Material,” *Journal of Materials in Civil Engineering*, vol. 15, no. 1, pp. 48–53, Feb. 2003, doi: 10.1061/(ASCE)0899-1561(2003)15:1(48).

[80] S. Oruji, N. A. Brake, L. Nalluri, and R. K. Guduru, “Strength activity and microstructure of blended ultra-fine coal bottom ash-cement mortar,” *Construction and Building Materials*, vol. 153, pp. 317–326, Oct. 2017, doi: 10.1016/J.CONBUILDMAT.2017.07.088.

[81] S. A. Mangi, M. H. Wan Ibrahim, N. Jamaluddin, M. F. Arshad, and S. Shahidan, “Performances of concrete containing coal bottom ash with different fineness as a supplementary cementitious material exposed to seawater,” *Engineering Science and Technology, an International Journal*, vol. 22, no. 3, pp. 929–938, Jun. 2019, doi: 10.1016/J.JESTCH.2019.01.011.

[82] C. F. Ferraris, V. A. Hackley, and A. I. Avilés, “Measurement of particle size distribution in portland cement powder: Analysis of ASTM round robin studies,” *Cement, Concrete and Aggregates*, vol. 26, no. 2, pp. 71–81, 2004, doi: 10.1520/CCA11920.

[83] “ASTM C150-20 - Standard Specification for Portland Cement,” *ASTM Int.*, 2020, doi: 10.1520/C0150_C0150M-20.

[84] “ASTM C596-18 - Standard Test Method for Drying Shrinkage of Mortar Containing Hydraulic Cement,” *ASTM Int.*, 2018, doi: 10.1520/C0596-18.

[85] “ASTM C494-19 - Standard Specification for Chemical Admixtures for Concrete,” *ASTM Int.*, 2019, doi: 10.1520/C0494_C0494M-19.

[86] I. Division of Construction Management, “DIVISION 900 - MATERIALS DETAILS,” 2022.

[87] “ASTM C1810-19 - Standard Guide for Comparing Performance of Concrete-Making Materials Using Mortar Mixtures,” *ASTM Int.*, 2019, doi: 10.1520/ C1810_C1810M-19.

[88] “ASTM C403-16 - Standard Test Method for Time of Setting of Concrete Mixtures by Penetration Resistance,” *ASTM Int.*, 2016, doi: 10.1520/C0403_C0403M-16.

[89] “ASTM C109-20 - Standard Test Method for Compressive Strength of Hydraulic Cement Mortars (Using 2-in. or [50 mm] Cube Specimens),” *ASTM Int.*, 2020, doi: 10.1520/C0109_C0109M-20B.

[90] “ASTM C1437-20 - Standard Test Method for Flow of Hydraulic Cement Mortar,” *ASTM Int.*, 2020, doi: 10.1520/C1437- 20.

[91] I. Division of Construction Management, “DIVISION 500 - CONCRETE PAVEMENT.”

[92] “ASTM C260-10(2016) - Standard Specification for Air-Entraining Admixtures for Concrete,” *ASTM Int.*, 2016, doi: 10.1520/C0260_C0260M-10AR16.

[93] “ASTM C143-20 - Standard Test Method for Slump of Hydraulic-Cement Concrete,” *ASTM Int.*, 2020, doi: 10.1520/C0143_C0143M-20.

[94] “ASTM C231-17 - Standard Test Method for Air Content of Freshly Mixed Concrete by the Pressure Method,” *ASTM Int.*, 2017, doi: 10.1520/C0231_C0231M-17A.

[95] “ASTM C39-21 - Standard Test Method for Compressive Strength of Cylindrical Concrete Specimens,” *ASTM Int.*, 2021, doi: 10.1520/C0039_C0039M-21.

[96] “ASTM C78-21 Standard Test Method for Flexural Strength of Concrete (Using Simple Beam with Third-Point Loading),” *ASTM Int.*, 2021, doi: 10.1520/C0078_C0078M-21.

[97] “ASTM C1585-20 - Standard Test Method for Measurement of Rate of Absorption of Water by HydraulicCement Concretes,” *ASTM Int.*, 2020, doi: 10.1520/C1585-20.

[98] “DIN 52617 - Determination of the Water Absorption Coefficient of Construction Material,” *Deutsches Institut fur Nor-mung*, 1987.

[99] “AASHTO TP 119-21 Standard Method of Test for Electrical Resistivity of a Concrete Cylinder Tested in a Uniaxial Resistance Test,” *AASHTO Int.*, 2021.

[100] “AASHTO PP84-20 - Developing Performance Engineered Concrete Pavement Mixtures,” *AASHTO Int.*, 2020.

[101] “ASTM C672-12 - Standard Test Method for Scaling Resistance of Concrete Surfaces Exposed to Deicing Chemicals,” *ASTM Int.*, 2012, doi: 10.1520/C0672_ C0672M-12.

[102] “CIP 16-Flexural Strength Concrete,” *National Ready Mixed Concrete Association*.